

Historical analysis and future projection of material stock  
dynamics in buildings and roadways

(建築物と道路の物質ストック動態に関する現状分析と  
将来予測)

ZHANG, Ruirui

(張 瑞瑞)

Doctor of Engineering

Graduate School of Environmental Studies, Nagoya University

(名古屋大学大学院環境学研究科 博士 (工学))



## Summary

Infrastructure has historically served as the essential framework for human societies, forging a vital and unbreakable connection between socioeconomic progress, social welfare, and the built environment. As urbanization continues to accelerate, the development and maintenance of infrastructure systems inherently demand significant consumption of materials and energy, leading to substantial carbon emissions and other environmental impacts. This research retrospectively examines the historical material stock (MS) evolution and material composition of roads and buildings in Japan, the two main components of infrastructure in Japan, from a spatiotemporal viewpoint. Subsequently, this research projects future trends in MS for expected road networks and the floor area and MS of serviceable buildings in Japanese Shared Socioeconomic Pathway scenarios (SSPs). Lastly, this research explores the spatial expansion patterns of land use types, including road and construction areas. It predicts the future changes and spatial distribution of these land use types by leveraging the land use and land cover change model.

The first chapter introduces the critical role of MS in infrastructure, especially buildings and roads, in addressing environmental challenges and fostering sustainable urban development. Then, the main research questions are proposed, followed by the research objectives and thesis structure.

The second chapter begins with a review of theoretical foundations: industrial ecology and material flow and stock analysis. It then delves into a literature review that thoroughly examines the state of the art of MS accounting based on the bottom-up approach and the dynamic evaluation of MS through various methods. This discussion sets the stage for highlighting the academic gaps this research aims to fill.

The third chapter examines how various building attributes influence the material intensity (MI) coefficient. MI is vital for quantifying the MS of buildings and other constructed facilities. However, the application of MI in MS accounting faces significant challenges, primarily due to its regional variability. Feature importance is

measured using an innovative random forest (RF) model. An overarching hierarchy of MI was established, and a full hierarchical MI dataset of six selected building materials was predicted by the RF model. The analysis of building features importance on MI is necessary and meaningful for not only the building MS estimation, but also the local MI database setup.

The fourth chapter analyzes the spatiotemporal evolution of roadway MS in Japan and forecasts the anticipated road MS in each prefecture by the year 2050 under Japanese SSPs. Historical data shows that the total road MS exhibited substantial growth. A notable trend was observed where most prefectures experienced significant expansion in their road networks from 1965 to 1995. However, in the last decade, most of these regions saw an average annual growth rate of less than 1%, indicating a slowdown in the expansion of road infrastructure. The forecast results under five SSPs in all prefectures revealed diverse trends. Some regions exhibited varying trends depending on the SSP scenario, while others demonstrated more consistent patterns of increase or decrease.

The fifth chapter aims to gain a spatial understanding of the dynamics and distribution patterns of building MS over time, with three major metropolitan areas in Japan selected as the study area. This chapter first analyzes the evolution of building MS and the material composition of MS. Then it predicts the floor area and MS of serviceable buildings until 2050 under the SSPs, taking into account a significant population reduction. Although the overall building MS has gradually increased until 2020, the trends of all SSPs show that the serviceable building area and MS will decrease.

The sixth chapter explores the potential mechanisms driving infrastructure development within three major metropolitan areas in Japan. This chapter analyzes the historical changes in land use types, including construction areas and roads, in these areas. It uses the patch-generating land use simulation (PLUS) model to predict the future distribution and changes of different land use types by 2050. The random forest classification method is adopted to identify and quantify the contributions of various

driving factors behind the expansion of each land use type. Simulation results of the PLUS model show continued urban expansion and reduction in cropland and wasteland areas, reflecting the consequences of urbanization trends and population decline in Japan's three metropolitan areas.

The seventh chapter concludes the findings of chapters 3, 4, 5, and 6. Implications for urban sustainability of this research are explained. Finally, the limitations and future work of this research are stated.

## Table of contents

<b>Summary</b> .....	1
<b>1. Introduction</b> .....	4
1.1 Background .....	4
1.2 Research problem statement .....	7
1.3 Research objectives .....	8
1.4 Framework of thesis .....	9
<b>2. Theories and state of the art</b> .....	10
2.1 Theoretical foundations .....	10
2.1.1 Industrial ecology and sustainability .....	10
2.1.2 Material flow and stock analysis .....	11
2.2 Literature review and state of the art .....	13
2.2.1 Bottom-up approach in material flow and stock accounting .....	13
2.2.2 The evolution and projection of MS .....	17
2.2.3 Dynamic simulation of future land use types .....	19
2.2.4 Comparative analysis of MS prediction models .....	21
<b>3. Building MS accounting: exploring the role of MI</b> .....	22
3.1 Data and variables .....	22
3.2 Correlation analysis .....	23
3.3 Methodology: RF regressor .....	24
3.3.1 RF model development .....	25
3.3.2 Identification of the building feature importance .....	27
3.3.3 Effects of building features on MI: partial dependence .....	28
3.3.4 RF-based MI estimation .....	28
3.4 Results .....	29
3.4.1 Correlation analysis .....	29
3.4.2 Building feature importance .....	31
3.4.3 Effects of building features on MI .....	34
3.4.4 RF-based MI .....	36
3.5 Discussion .....	38
3.5.1 Comparison with mean values of MI .....	38
3.5.2 Application in material stock and flow analysis .....	40
3.5.3 Rethinking the MI in different regions .....	42
<b>4. Roadway MS accounting: mapping historical patterns and projecting future trends</b> .....	43
4.1 Methodology .....	43
4.1.1 Estimation of road MS in Japan with bottom-up method for 1965-2020 .....	43
4.1.2 Models: ARIMAX, SVR, hybrid ARIMAX-SVR, ANN, RF, and MLR .....	44
4.1.3 Explanatory variables .....	47
4.1.4 Forecast of road MS in Japan by 2050 .....	49
4.1.5 Data sources .....	51
4.2 Results .....	52
4.2.1 Evolution trends and material decomposition of road MS over the past half	

century	52
4.2.2	Spatiotemporal evolution and prefectural differences of road MS in Japan..... 57
4.2.3	Projection of expected road MS by 2050 ..... 58
4.2.4	Future regional differences in the magnitude of road MS discrepancies ..... 66
4.3	Discussion ..... 67
4.3.1	Identifying opportunities for material allocation under climate change..... 67
4.3.2	Road infrastructure management in a highly urbanized and aging society ..... 68
<b>5.</b>	<b>Building MS dynamics: analyzing spatial patterns and forecasting future developments</b>
	70
5.1	Study area ..... 70
5.2	Methodology..... 71
5.2.1	Estimation of historical spatial building MS ..... 71
5.2.2	Projection of serviceable building MS by 2050..... 71
5.2.3	Data sources..... 72
5.2.4	Model fitting for relationship between floor area, population, and building MS 73
5.3	Results ..... 73
5.3.1	Evolution and material composition of building MS ..... 73
5.3.2	Projections of floor area and MS of serviceable buildings under five SSPs ..... 75
5.4	Discussions..... 76
<b>6.</b>	<b>Urban infrastructure evolution: identifying driving mechanisms and assessing land use changes</b> ..... 77
6.1	Methodology..... 78
6.1.1	Models for LULCC simulation ..... 78
6.1.2	Land use change simulation with PLUS model..... 79
6.1.3	Data sources..... 82
6.1.4	Validation of PLUS model ..... 83
6.2	Results ..... 84
6.2.1	Evolution of historical land use change..... 84
6.2.2	Identification of drive factor importance in three metropolitan areas of Japan. 86
6.2.3	Estimating future land use demands..... 87
6.2.4	Future land use projection in 2050 ..... 88
6.3	Discussion ..... 90
<b>7</b>	<b>Conclusions</b> ..... 91
7.1	Summary of the findings ..... 91
7.2	Research implications ..... 93
7.3	Limitations of research and future work..... 95
	<b>Acknowledgements</b> ..... 97
	<b>Figure list</b> ..... 98
	<b>Table list</b> ..... 99
	<b>References</b> ..... 100
	<b>Appendices</b> ..... 113
	Appendix 1. RF-based MI for a) steel; b) brick; c) wood; d) sand; e) gravel (Unit: ton/100 m <sup>2</sup> )

Appendix 2. RF-based MI dataset for all materials (Unit: ton/100 m<sup>2</sup>).....118  
Appendix 3. Results of expected demand for road MS with each SSP scenario for the remaining  
prefectures .....122

# 1. Introduction

## 1.1 Background

The growth in affluence over the past half-century has significantly outpaced the mitigation offered by technological advances, leading to increased resource utilization and pollutant emissions. The profound changes to Earth's life-sustaining systems, driven by human activity, underscore the failures in addressing environmental degradation and the existential threats posed to societies, economies, and natural systems (Wiedmann et al., 2020). Infrastructure has historically served as the essential framework for human societies, forging a vital and unbreakable connection between socioeconomic progress, social welfare, and the built environment. However, they also necessitate substantial material resource consumption and energy use, often resulting in considerable carbon emissions and other environmental impacts. A recent report reveals that 79% of all greenhouse gas emissions and 88% of adaptation costs were contributed by infrastructure, positioning it at the forefront of efforts to meet the objectives of the Paris Agreement and Sustainable Development Goals (UNEP, 2021). The report calls for a revolutionary shift in how governments conceive and manage infrastructure to emphasize its vital part in mitigating and adapting to climate change.

As societies grow and develop, there is an increased demand for infrastructure—such as transportation networks and buildings—that underpins economic activities and supports quality of life. However, the construction, maintenance, and operation of this infrastructure entail substantial material use, ranging from concrete and steel to rare earth elements, which in turn contributes to significant environmental impacts. The extraction of raw materials often leads to habitat destruction, biodiversity loss, and soil degradation, while the manufacturing processes are energy-intensive and result in considerable greenhouse gas emissions. Furthermore, the disposal and degradation of infrastructure at the end of its life cycle generate waste and pollution. Thus, the relationship between society, infrastructure, and material use is a critical focal point for sustainable development initiatives that aim to mitigate environmental impacts while

supporting human well-being.

The buildings and construction sector (including both direct and indirect emissions from buildings and construction) accounted for around 37% of global energy-related CO<sub>2</sub> emissions in 2021 (UNEP, 2022), while the transport sector contributed more than 20% of global CO<sub>2</sub> emissions (IEA, 2019). The material composition of these infrastructures plays a critical role in their overall environmental impact, both in terms of embodied energy and emissions associated with their resource extraction, construction, maintenance, and end-of-life stages (Krausmann et al., 2017). Furthermore, the lifespan and durability of materials used in buildings and road networks directly influence the frequency and scale of maintenance and reconstruction activities, which in turn affect resource consumption and waste generation. As urbanization continues to accelerate, through analyzing the spatiotemporal evolution and patterns of infrastructure's material stock (MS), we can identify the hotspots and trends of material accumulation and consumption, and identify opportunities for material recycling and reuse, thus providing insights for minimizing the carbon footprint of infrastructure development while ensuring its efficiency and resilience.

#### (1) Built environment stock

Built environment stock is the backbone of modern human well-being by offering a range of desired services essential for daily life and societal functioning. It evolves over time, primarily through a series of material production, construction, and demolition activities, leading to substantial environmental impacts such as greenhouse gas (GHG) emissions, extensive land use, and massive construction waste generation (Berrill and Hertwich, 2021; Peng et al., 2021). However, on the other hand, building MS, as an integral part of the built environment, is increasingly regarded not just as a consumer of resources but also as a potential reservoir of secondary resources. In the concept of recycling strategy, materials used in construction are seen not as waste at the end of their life cycle, but as valuable resources that can be reclaimed and reused. Globally, more than half of the total extracted material is transformed and stored in building MS (Fu et al., 2021; Krausmann et al., 2017). This substantial volume of

material embedded in buildings and infrastructure has attracted numerous MS studies to set up foundation for embodied GHG emission reduction (De Wolf et al., 2020; De Wolf et al., 2016), urban mining and further circular economy (Lanau and Liu, 2020; Lederer et al., 2020).

## (2) Road infrastructure stock

Roads are an indispensable infrastructure element, serving as the essential backbone of transportation networks globally. They facilitate the movement of people and goods across vast distances. By offering a means of access to services, employment opportunities, education, and markets, the road system help fulfill fundamental human needs, facilitate economic growth, and allow trade and commerce to flourish (Meijer et al., 2018; Wu et al., 2023; Wudad et al., 2021). However, roads and transport sector are vulnerable to climate change impacts such as changing precipitation patterns, temperature fluctuations, and the increasing frequency and severity of extreme weather events. Such impacts pose significant challenges, as they can increase maintenance costs, impede road safety, and disrupt mobility (Chinowsky et al., 2013; Koetse and Rietveld, 2009; Markolf et al., 2019). Moreover, road construction and maintenance require substantial quantities of materials, such as asphalt, concrete, and steel. The production and utilization of these materials entail considerable environmental impacts throughout their life cycle, including carbon emissions, habitat loss, and the depletion of natural resources (Jullien et al., 2014; Miatto et al., 2021; Yu et al., 2021). Given these environmental concerns and the increasing impacts of climate change, there is a growing need to rethink road design and maintenance. The focus needs to shift toward creating and maintaining roads that are not only resilient to these impacts but also sustainable in the long term. The goal is to ensure that roads continue to serve their vital function in society while minimizing their environmental impact and adapting to the changing climate conditions.

## (3) Simulating spatiotemporal dynamics of infrastructure

Roads and buildings constitute pivotal components of the infrastructure fabric that require careful analysis and planning. In Japan, about 70% of materials are stored in

buildings and roads, with buildings accounting for 43%, followed by roads at 26% (Tanikawa et al., 2015). The spatiotemporal changes in these infrastructural elements are not merely physical transformations but are intrinsically linked to socio-economic dynamics. This interlinkage underlines the necessity to comprehend and anticipate the future spatial dynamics of roads and buildings, which are fundamental to the sustenance and evolution of urban landscapes. The theoretical underpinning of the interdependence between land use and infrastructure networks is encapsulated in the infrastructure land-use feedback cycle. This cycle illuminates the bidirectional relationship wherein the development of infrastructures, such as roads, enhances local accessibility, thereby escalating the demand for urban development. Conversely, urbanization intensifies local transport movements and subsequently amplifies the demand for transport networks (Kasraian et al., 2016). This cyclical interaction underscores the significance of roads and buildings as dynamic agents in urban ecosystems, necessitating a focused analysis of their future spatial changes.

In this regard, land use and land cover change (LULCC) models emerge as potent tools to simulate these future spatial transformations. LULCC, characterized by its spatiotemporal pattern changes, such as urbanization, encapsulates dynamic processes where land transitions adhere to specific rules or relationships (Sohl and Claggett, 2013; Wang et al., 2022). This dynamicity is a fundamental aspect of LULCC, rendering it a comprehensive framework to examine and project changes in land use patterns. LULCC models can assimilate and quantify the combined effects of anthropogenic and environmental drivers on landscape patterns. Moreover, by incorporating dynamic elements of urban growth and infrastructure development, it harnesses the dynamic nature of LULCC to provide comprehensive insights into the future of urban infrastructure, thereby enabling more informed and sustainable urban planning and development.

## 1.2 Research problem statement

Buildings and road networks not only facilitate essential services and societal activities but also represent major sources of material consumption and waste

generation, accumulating vast quantities of construction materials such as steel, cement, aggregate, and timber. These materials constitute the second-largest mass flow into urban areas only after water, and are the primary contributors to urban waste (Augiseau and Barles, 2017; Krausmann et al., 2017). Furthermore, the extraction, production, and utilization of these virgin construction materials exert a substantial impact on the global environment. Currently, decoupling MS from socioeconomic growth is a critical strategy in addressing the environmental challenges posed by the current economic development, and is vital for supporting sustainable, resilient, and equitable development. To fulfill this objective, it is imperative to address key research questions that form the foundation of MS dynamics: What are the factors influencing MS, and what mechanisms underlie these influences?

On the other hand, Japan is experiencing a significant population decline and an increasing proportion of elderly citizens. Japan's estimated future total population is expected to decrease to 70% of the current population in 50 years, with people aged 65 and over accounting for about 40% of the population (National Institute of Population and Social Security Research, 2023). The demographic trajectory of Japan presents a unique challenge for urban planning and environmental management. This demographic shift profoundly impacts land use, necessitating a re-evaluation of infrastructure practices and environmental strategies, particularly in Japan's major metropolitan areas. This raises another question: How are these stocks expected to transform in the future based on current trends and future scenarios? Understanding the MS of these infrastructural elements is vital for sustainable urban development, particularly in the face of Japan's declining population. This forward-looking study not only contributes to the understanding of infrastructure and material use but also informs policymakers and urban planners in developing strategies that align with demographic trends and sustainability goals.

### 1.3 Research objectives

In order to explore the retrospective progress and prospective trends of building and roadway MS from a spatiotemporal perspective, the following questions are studied:

(1) Factors affecting building MI: What are the attributes influencing MS, and how do these building attributes influence MI? (2) Historical evolution patterns: What patterns have historically characterized the evolution of buildings and roadways MS? (3) Future projections: How are the quantity and distribution of MSs expected to transform in the future based on current trends and future scenarios? (4) Simulation at future spatial scales: What will be the spatial distribution of roadways and buildings in the future, and what are the mechanisms underlie these changes?

#### 1.4 Framework of thesis

The thesis begins with introduction and literature review, followed by analyses of corresponding methods, results and discussions according to the research process. Finally, the main findings and research implications are summarized. Each chapter is introduced in detail below.

Chapter 1 introduces the critical role of MS in infrastructure, especially buildings and roads, in addressing environmental challenges and fostering sustainable urban development, as well as statements of research questions, research objectives, and thesis structure.

Chapter 2 begins with a review of theoretical foundations, and then delves into a literature review that thoroughly examines the state of the art of MS accounting based on bottom-up approach and the dynamic evaluation of MS through various methods.

Chapter 3 examines how various building attributes influence material intensity (MI) coefficient and a full hierarchical MI dataset of six selected building materials were predicted by the RF model.

Chapter 4 analyzes the spatiotemporal evolution of roadway's MS in Japan and forecasts the anticipated road MS in each prefecture by the year 2050 under Japanese SSPs.

Chapter 5 delves into the dynamics of building MS over time and its spatial distribution across different urban zones within three major metropolitan areas in Japan and predicts the future building MS by 2050 under Japanese SSPs.

Chapter 6 explores the potential mechanisms driving infrastructure MS in the same

three metropolitan areas. The focus expands to include various land use types including buildings and roadways. This chapter also analyzes the historical changes in land use types in these areas, utilizing the patch-generating land use simulation (PLUS) model to predict the future land use distribution and changes by 2050.

Chapter 7 concludes the findings of chapters 3, 4, 5, and 6. Implications for urban sustainability of this research are explained. Finally, limitations and future work of this research are stated.

## **2. Theories and state of the art**

### 2.1 Theoretical foundations

#### 2.1.1 Industrial ecology and sustainability

The origin and development of industrial ecology (IE) are rooted in the quest to understand and optimize the circulation of materials and energy flows within industrial systems, aligning them more closely with the functioning of natural ecosystems, aiming to restructure industrial processes to mimic the function observed in natural ecosystems (Erkman, 1997). The field of IE was significantly shaped by the introduction of the concept of industrial metabolism by Robert U. Ayres in 1988. This concept plays a key role in IE, focusing on understanding the societal use of natural resources and comprehensively assessing their environmental impacts (Anderberg, 1998). IE has evolved from recognizing the inadequacies of traditional industrial waste treatment to developing a holistic approach that seeks to emulate the efficiency and sustainability of natural ecosystems. It represents a significant paradigm shift in how industrial processes are understood and managed, with a focus on sustainability and environmental management (Saavedra et al., 2018).

IE is usually portrayed as the scientific component of sustainability, focusing on the industrial sector's metabolism within an ecological framework. In IE, resource flows in industrial systems undergo transformations. However, IE doesn't limit itself to material and energy flows but also considers information flows and interactions between different system components, including government, society, and industry.

This holistic approach incorporates aspects of social ecology. A key principle in IE is the concept of waste minimization, inspired by natural ecosystems where waste from one process serves as input for another, exemplifying a circular approach to resource use (Jonker and Harmsen, 2012). It integrates ecological principles into industrial processes, emphasizing sustainability, waste minimization, and efficient resource use. IE provides knowledge essential for comprehensive design context understanding and assessing design outcomes. It forms the scientific basis for industrial-oriented sustainable development and guides principles like design for environment and sustainability, and it also emphasizes the importance of tools like life cycle assessment for sustainable design (Jonker and Harmsen, 2012).

#### 2.1.2 Material flow and stock analysis

Material flow analysis (MFA) and MS analysis are essential methodologies in the realm of IE, each playing a pivotal role in the sustainable management of material and energy flows within various systems. MFA is a technique primarily utilized to quantify and assess the flow of materials within a spatially and temporally defined system, which could range from a specific industrial process to broader regional or sectoral scales. Its principal objective is to systematically evaluate the inputs, outputs, and transformations of materials and energy, thereby elucidating the "metabolism" of industrial systems. This approach is crucial for understanding the dynamics of material use and waste generation. It enables the identification of efficient pathways for resource utilization, waste minimization, and overall environmental impact reduction. MFA has been effectively applied in diverse contexts, from national level assessments to urban metabolism studies, offering valuable insights for environmental policy and management (Broto et al., 2012; Graedel, 2019).

In contrast, MS analysis focuses on the accumulated materials within a system, such as in buildings, infrastructure, or products. This analysis is instrumental in understanding the dynamics of MS accumulation over time and evaluating the relationships between stocks, flows, and services. It provides an in-depth perspective on the potential for secondary resource recovery and the implications of embodied

carbon emissions in various materials. By quantifying the materials accumulated in built environments and other infrastructures, MS analysis plays a critical role in guiding sustainable resource management and promoting circular economy practices (Fishman et al., 2016; Gillott et al., 2023). While MFA offers insights into the movement and transformation of materials within a system, MS analysis complements this by shedding light on the accumulation and potential reuse of materials.

So far, the evolution of MS research can be mainly divided into three phases, each with distinct characteristics as illustrated in Fig. 1 (Fu et al., 2021). The first phase established the groundwork for material stock research, with a simple keyword network focusing on "material flow analysis," "copper," and "metal." Research topics included material account, waste management, and macro-resource management for metal stocks. Next it developed into the second phase: extensive exploration. This phase saw a significant expansion in thematic exploration, involving a complex network. The focus shifted to resource recycling in the field of "industrial ecology," with "in-use stock" and "material flow analysis" emerging as dominant topics. Research in this phase expanded to include various metals like iron, steel, aluminum, and nickel, with studies often employing a top-down approach based on MFA. In addition, there was an increased interest in hibernating stocks (obsolete materials with future urban resource exploitation potential) and more specific product stocks. The third phase presented a concentrated development, marking a further condensation and clarity in research topics. In this phase, the research continued to focus on "in-use stock" and MFA, but with an increasing emphasis on "material stocks" instead of flow, and on "construction" environmental stock. There was a notable shift towards bottom-up stock analysis methods. Studies began to concentrate more on the role and function of MS, considering the influence of stocks in the complex societal context. There was also a development of comprehensive MS studies at smaller scales, providing insights for high-resolution resource management policies. The MS analysis has provided a framework for analyzing and optimizing the use of materials and energy, supporting the transition towards more sustainable industrial and societal systems, and is vital for policy

development, efficient resource management, and the advancement of a circular economy.

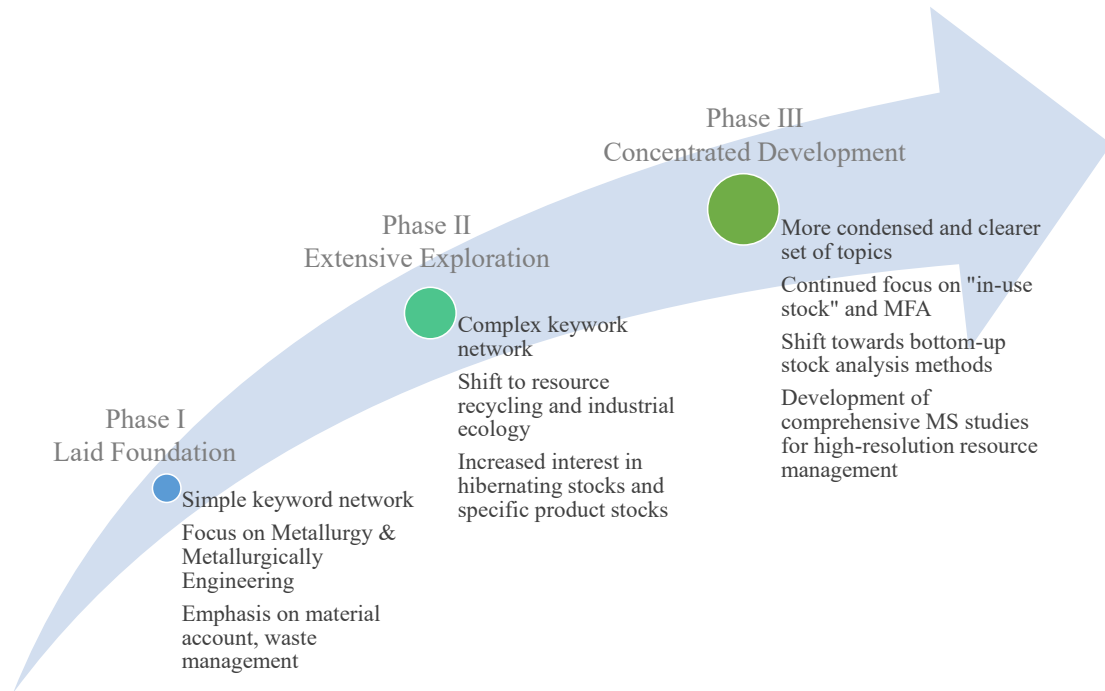


Fig. 1 Three phases of MS analysis in the evolutionary process (Fu et al., 2021)

## 2.2 Literature review and state of the art

### 2.2.1 Bottom-up approach in material flow and stock accounting

Material flow and stock accounting is crucial for understanding and managing material use in the context of sustainability, urban planning, and environmental conservation. The estimating approaches which are generally categorized into top-down, bottom-up, and their combination and extension (Lanau et al., 2019).

The top-down method estimates MS by analyzing aggregate data over large spatial and temporal scales. It calculates stock based on the cumulative difference between material inflows and outflows, using data such as national material flow statistics. This method often includes socioeconomic variables to refine calculations, making it suitable for national-level or larger regional assessments. While the top-down method is relatively quick to compile, it generally lacks spatial distribution details and depends heavily on the accuracy of lifetime distribution assumptions and parameters (Miatto et al., 2017a; Zhang, Y.P. et al., 2019). In contrast, the bottom-up method constructs with

the MI coefficient (for building MS, i.e., material mass per unit of building inventory) and a physical inventory of MS at a specified level, such as individual buildings or products, and aggregates this information to estimate total stocks (Arora et al., 2019; Mesta et al., 2019). Compared with a top-down manner, bottom-up stock accounting results are considered more accurate in terms of space and content variation as providing a granular view of MSs, including their spatial distribution, which is particularly useful for local or city-level assessments and is beneficial for identifying secondary resource sources and for more precise material recycling and recovery strategies (Arora et al., 2019; Lanau et al., 2019; Schiller et al., 2017). Thus far, the bottom-up method has been extensively applied to quantify material stocks at different spatial resolution, ranging from a section of a city (Marcellus-Zamora et al., 2016), to urban (Huang et al., 2017), national (Han et al., 2018; Tanikawa et al., 2015), and global scales (Deetman et al., 2020; Marinova et al., 2020), with temporal scopes containing a snapshot of a specific year (Guo et al., 2014) and the evolution over time (Han et al., 2018; Hong et al., 2016; Nageli et al., 2020), using diverse source data such as statistics (Huang et al., 2013; Shi et al., 2012) and geographical information system (GIS) (Heeren et al., 2013; Miatto et al., 2019; Tanikawa and Hashimoto, 2009).

In the bottom-up method, MI is a crucial coefficient for converting the physical number of objects into mass stock and flow regardless of the spatial and temporal scales (Kavgic et al., 2010; Lanau et al., 2019). The uncertainty of MI is directly propagated to the stock estimation results. MI varies with different building-level attributes such as structures, building service types, construction years, regions, and even case by case in the real world. This, on the one hand, implies the MI is barely likely to capture the true MS value. On the other hand, the collection from an on-site survey (Kleemann et al., 2016), construction company data (Marcellus-Zamora et al., 2016), construction standards (Tanikawa and Hashimoto, 2009), and integration of high-quality and representative MI data have always been challenging, making it scarce and only applicable to limited areas without random sampling (Heeren and Fishman, 2019; Sprecher et al., 2022), and only a handful of studies randomly selected samples such as

(Lederer et al., 2021). However, for regions that have experienced substantial urban construction and thus where rapidly growing stock needs to be properly managed, no harmonized dataset has been created so far. In the case of China, the Construction Project Investment Estimation Handbook (Yu and Li, 1999) and building sample survey (Liu and Hu, 2006; Gu, 2009) are the sole sources of MIs used for most previous studies on Chinese building MS accounting owing to the lack of a compiled MI dataset (Guo et al., 2019; Hu, M. et al., 2010; Huang et al., 2013; Shi et al., 2012).

The diversity of data sources renders inconsistency to the categorization basis of MI in different regions. The MI of buildings in Japan is usually presented by distinct structures (e.g., wooden, steel, and reinforced concrete) (Tanikawa et al., 2015; Tanikawa and Hashimoto, 2009), while in Europe and the USA, it is classified by utilization purpose (i.e., residential and non-residential) (Daxbeck et al., 2009; Haberl et al., 2021; Kleemann et al., 2017), occupation status (Gonti et al., 2018; Reyna and Chester, 2015; Wiedenhofer et al., 2015), and cohorts (Kleemann et al., 2017; Miatto et al., 2019; Schebek et al., 2017). Efforts have been made to harmonize MI values for comparison and transferability; for example, Schiller et al. (2019) discussed the options and limitations of the transferability of domestic building's MIs between German and Japanese, while Lederer et al. (2021) addressed the question of the unit of the building inventory, which can be ground area, gross and net floor area, or even the volume (Heeren and Fishman, 2019). However, the following questions still prevail: which building attribute is the most important for MI? Or do these attributes have the same level of influence on building MI? These questions are critical for the harmonious study of the building MS in different regions of the world; however, no single study has provided the answer to them.

Efforts have been made to explore the plausible solutions. To explore the extent building features can explain the MI variance, Heeren and Fishman (2019) conducted a statistical tool of analysis of variance (ANOVA) to detect whether apparent MI differences occur between publications from distinct journals. Ordinary least squares regression can be deployed to investigate how MI changes when a certain building

feature varies from one level to another level, where all building features are input into the model as a series of dummy variables (Heeren and Fishman, 2019). However, these methods are usually developed with strict examination of assumptions (e.g., normal distribution, independence, and homogeneity of the variances), under which realistic observation data likely fail. Meanwhile, researchers usually use average MI values as the important coefficient for material stock accounting (Hu, M. et al., 2010; Huang et al., 2013; Kleemann et al., 2017). To avoid the arbitrary determination of the MI, (Cao et al., 2018) identified the probability distribution of MI and estimated material stock using the Monte Carlo process through pseudo-random sampling, which reveals the uncertainty in providing the confidence interval, though this greatly increases the volume of calculations. (Arceo et al., 2021) investigated the MI variability of wood framed buildings by quantifying the MI of 40 single-family residences in Toronto, Canada, but with limited data sources and a single building type. (Vilaysouk et al., 2022) proposed a semisupervised machine learning method to classify MI for clustering building MI dataset and presented the probability distribution of residential buildings' MI for five clusters. However, the use of limited data from different regions of the world provided by Heeren and Fishman (2019) makes the representativeness of the results an obvious concern.

Is there a feasible way to identify the importance of each attribute while reducing the uncertainty associated with the average value? This needs to be supported by novel tools that can simultaneously consider multiple variables affecting MI and identify the respective importance of different variables. RF is a machine-learning technique developed to represent the superstructure of a ready-made decision tree data mining technique (Lin et al., 2021a; Lin et al., 2021b; Wang et al., 2018). RF effectively integrates the strengths of both statistical and machine learning methodologies. In this research, the RF model was employed, inputting a database of MI from Chinese buildings to identify the building attribute most crucially affecting MI (Yang et al., 2020). To measure the degree of influence of different variables on MI and gain a deeper insight into their relationships with MI, partial dependence analysis was implemented.

Furthermore, a hierarchical MI dataset was predicted using the RF model. This approach departs from traditional average-based methods by incorporating the importance of different building attributes. This technique has the potential to extend the structural hierarchy of MI according to available information levels, offering a possibility to alleviate the data limitations in current built environment studies.

### 2.2.2 The evolution and projection of MS

The SSPs have emerged as a pivotal tool for comprehending the potential impacts of climate change across various societal dimensions. These pathways depict the possible future trajectories of global social and economic development in the 21st century, influenced by factors such as demographics, economic development, and income disparities (O'Neill et al., 2017; Riahi et al., 2017; Schandl, Heinz et al., 2020). Represented by SSP1-5, these scenarios encapsulate coherent narratives portraying sustainability, middle-of-the-road development, regional rivalry, inequality, and fossil-fueled development, respectively. Researchers have utilized these pathways to investigate diverse issues, addressing the intricate challenges posed by climate change (Bauer et al., 2017; Popp et al., 2017; Schandl, Heinz et al., 2020). While SSPs serve as global development scenarios for climate change mitigation and adaptation, constructing regional or local extended versions of these scenarios is essential to ensure their applicability to specific areas (Frame et al., 2018). This is imperative due to the potential lack of region-specific drivers, unique national policy perspectives, and the unification of data in global narratives. For instance, Japan's specific challenges, such as an aging society and the need to obtain labor force from abroad, may not be explicitly incorporated in global scenarios (Chen et al., 2020). Given the crucial role of buildings and roads in the whole infrastructure and their impact on economic development, societal dynamics, and environmental sustainability, projecting future scale based on regional or local socioeconomic scenarios that reflect unique local circumstances becomes imperative.

Several studies have been focusing on projecting the future building development trends. For instance, (Arehart et al., 2022) specifically examines the evolution of

structural systems and estimates the floor space in the U.S. building stock from 2020 to 2100 under four SSP scenarios. (Le Boulzec et al., 2023) is more focused on the material requirements and energy demand of the materials production for the building sector up to the year 2100 under the SSP scenarios. Despite their insightful contributions, (Arehart et al., 2022) focus on the US building stock but with the scenarios of global trends, which may not capture possible local characteristics in the future. However, the extrapolation of historical data in (Le Boulzec et al., 2023) might not account for regional variations in building practices, materials, and regulations.

On the other hand, the literature on road infrastructure and the transportation sector has overlooked the resource-related aspects of adaptation measures in the transportation sector, despite the significant role of transport infrastructure in societal material turnover (Augiseau and Barles, 2017; Tanikawa et al., 2015; Tanikawa and Hashimoto, 2009). Although research on climate change impacts on road infrastructure and the transportation sector has grown, they mainly focus on identifying adaptation measures and assessing their effectiveness (de Abreu et al., 2022; Eisenack et al., 2012), so there is still insufficient in providing detailed, site-specific adaptation measures for countries with distinctive future regional development features like Japan.

Given the long lifespan of infrastructure and its profound impact, evaluating future resource requirements at an early stage is crucial (Gassner et al., 2021). This research employed material flow analysis and MS analysis to depict the evolution of MS in road networks and buildings, aiming to project the expected MS in Japan by 2050 based on the national SSPs, ensuring that local unique characteristics are thoroughly considered. The evaluation of the anticipated MS allows for a detailed assessment of whether there will be continued demand or a potential decline, particularly considering factors such as population decrease and the consequent reduction in facility utilization. A comprehensive understanding of the relationship between MS evolution and material consumption can offer critical insights for informed decisions to optimize resource utilization and minimize adverse environmental impacts. Moreover, it is integral to developing sustainable infrastructure policies and practices that are responsive to

evolving demographic and economic trends.

### 2.2.3 Dynamic simulation of future land use types

Given the dominant role of the MS of buildings and road networks in the overall MS of infrastructure, it is fundamental to understand and simulate the spatial changes of roads and buildings for sustainable urban and regional planning. These simulations are vital for anticipating future development patterns, managing natural resources efficiently, and mitigating environmental impacts. Land use and land cover change (LULCC) models serve as essential tools in this context as it can effectively simulate the dynamics of land-use systems, revealing critical interactions between land use changes and environmental consequences, thus providing insights into the dynamics of urban and infrastructural expansion (Wang et al., 2022). It transcends traditional static planning approaches by incorporating dynamic elements of urban growth and infrastructure development. This capability is crucial in understanding the evolving patterns of roads and buildings, which are central to urban development. By offering a clear view of these dynamics, LULCC models aid policymakers and urban planners in making informed decisions, especially in strategic planning where decisions have long-lasting socio-economic and environmental implications (Jantz et al., 2004; Pongratz et al., 2021). Furthermore, LULCC models can project future land-use patterns under various scenarios (Le Boulzec et al., 2023; Yang et al., 2019; Zhang et al., 2017), allowing planners to anticipate and prepare for future expansions or modifications in road networks and building distributions.

The integration of LULCC models with other systems such as cellular automata and dynamics models enhances their applicability in urban planning by improving the accuracy of urban expansion simulations (Berberoğlu et al., 2016; Clarke, 2008; Wang et al., 2022). This integrative approach helps in optimizing land-use patterns and improving sustainable land management. Therefore, LULCC models play a pivotal role in guiding sustainable urban and regional planning efforts, making them indispensable in modern urban development and environmental conservation strategies. This research utilized LULCC model along with GIS tool for simulating the spatial changes of land

use changes in Japan's three major metropolitan areas, especially for construction areas and road networks. Unlike traditional data analysis models that may overlook the spatial dimension, GIS explicitly incorporates geographic and spatial data, allowing for a more nuanced understanding of spatial patterns. At the same time, LULCC Models integrate spatial data with temporal dynamics, enabling a deeper understanding of how land use and land cover have evolved over time and how they might change in the future.

Japan's three major metropolitan areas – the Greater Tokyo area, Keinki metropolitan area (Osaka), and Chukyo metropolitan area (Nagoya) was selected as the focus area for analyzing and predicting land use changes, particularly in road and construction sectors. As principal economic hubs of Japan, these metropolitan areas contribute substantially to the national Gross Domestic Product (GDP). Their dense population presents both challenges and opportunities in urban planning and land use management. On the other hand, Japan's population continues to decline and age, the demand for infrastructure and its utilization patterns will undergo significant changes. In terms of infrastructure adaptation, with a declining population, there is less stimulus for new infrastructure development, allowing for a more efficient allocation of resources towards the maintenance and optimization of existing structures. Furthermore, the aging population necessitates a shift towards enhancing accessibility and safety for the elderly. Additionally, the aging and reduction in population are expected to lead to a decrease in housing demand, particularly in suburban and rural areas, resulting in a rise in vacant properties, thus potentially leading to urban decay and land underutilization. By providing spatially explicit and temporally dynamic predictions, these models can help in identifying potential areas for urban development, infrastructure needs, resource management, or conservation efforts, grounded in a spatial understanding of the landscape. By focusing on road and construction areas within these regions, the study can provide critical insights into infrastructure needs and urban growth trends, which are essential for addressing the requirements of a densely populated area and planning for sustainable urban expansion. Furthermore, urban expansion, particularly in road and construction sectors, has profound environmental

consequences. The insights derived from such analyses are pivotal in informing urban planning and policy decisions, aiming to optimize land use for material metabolism, environmental sustainability, and societal wellbeing.

#### 2.2.4 Comparative analysis of MS prediction models

Understanding the current MS of roadways and buildings is vital for optimizing infrastructure management and assessing the ecological footprint of construction and maintenance activities. Long-term prediction of MS is essential for ensuring the continued functionality, safety, and sustainability of infrastructure, enabling informed decisions about future resource allocation and investments in construction, maintenance, and upgrades. However, research on future MS estimation of road network infrastructure remains scarce, with data-driven methods such as machine learning primarily concentrated in road safety (Shaik et al., 2021; Sohail et al., 2023; Tang et al., 2020). Few previous studies have either focused solely on past road stock in regions (e.g., Burghardt et al., 2022; Miatto et al., 2017b; Nguyen et al., 2019) or on disaster response scenarios. For instance, (Yuan et al., 2022) predicted near-future flooding status of road segments by employing a deep learning framework on fine-grained traffic data of their own and adjacent road segments. In contrast, Laurance et al. (2014) and Meijer et al. (2018) provided a global perspective on road length and estimated a significant increase in road length by 2050. In contrast, research on predicting future building MS is relatively abundant, using methods such as scenario analysis (Hirvonen et al., 2021) and dynamic stock-driven approach (Göswein et al., 2018; Stephan and Athanassiadis, 2018; Zhang et al., 2023). However, there are few simulations and analyzes on future spatial scales.

In this context, this study stands out by examining historical road network changes over several decades, projecting future road and building in Japan based on regional SSP scenarios reflecting unique local conditions, and comparing various prediction models, including The Autoregressive Integrated Moving Average eXogenous Model (ARIMAX), Support Vector Regression(SVR), ARIMAX-SVR, Multiple Linear Regression (MLR), and other machine learning methods such as RF, Artificial Neural

Networks (ANN). Machine learning algorithms offer several significant advantages in analyzing and simulating data. Their abilities such as efficiently processing and analyzing large, complex datasets, adapting to new data, and capturing complex, non-linear relationships make them increasingly popular tools in environmental science and sustainability research. Through data-based analysis and projection, this research can offer a deeper understanding of the MS evolution of roads and buildings in Japan, thereby providing information on facilitating resource allocation and policy formulation in infrastructure management under different regional SSP scenarios.

### **3. Building MS accounting: exploring the role of MI**

#### **3.1 Data and variables**

The raw MI database was compiled using data from 813 building samples spanning across China, constructed between 1949 and 2015. This comprehensive dataset is thoroughly detailed in (Yang et al., 2020) and is accessible via Zenodo (Yang et al., 2019). A more intuitive introduction and the distribution and sample size of each material in the dataset are illustrated in Fig. 2. A total of 769 buildings were included as samples; among them, 767 building samples contained steel materials; 758 samples, cement, and samples containing gravel are the least (696). For building structures, the majority was brick-wood structure (54.62%), and the sample size of steel structure was the smallest, accounting for only 1.56%. In terms of construction period and use type, buildings constructed in 1980s and residential types are the most frequent, accounting for 38.75% and 48.89%, respectively. Buildings constructed in 2000s and industrial use were the least frequent, with percentages of 6.24% and 18.34%, respectively. The sample size of buildings in southern and northern region of China is relatively even, with the proportion of northern to southern buildings being 1.12 to 1.

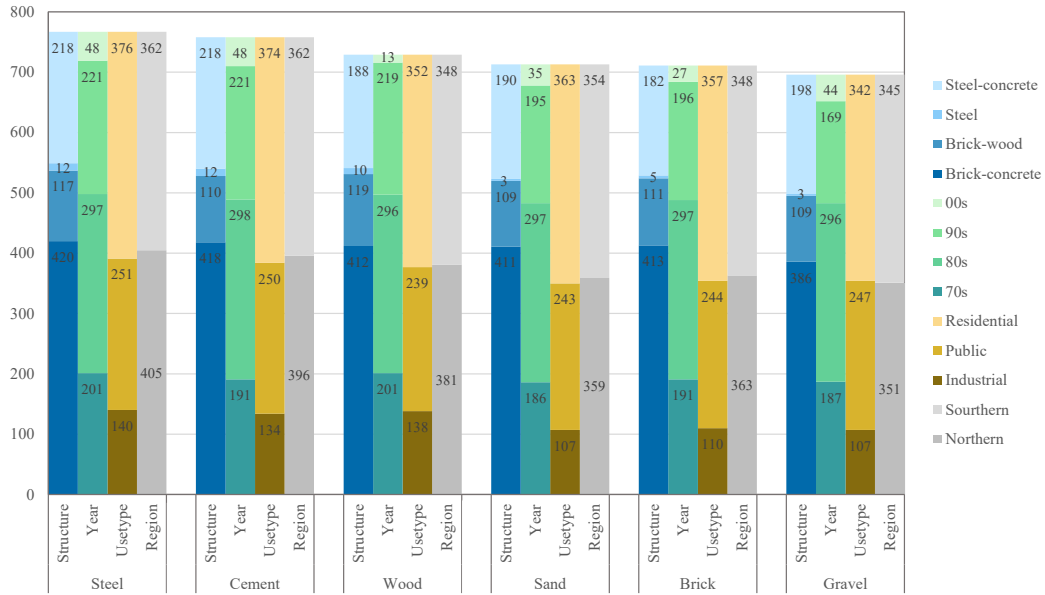


Fig. 2 Size and composition of building samples

The MI values were calculated by dividing the mass of each building material by the corresponding building's gross floor area. The original database encompassed 10 construction materials used in foundations and structural components of buildings. In subsequent analyses, six key materials - cement, steel, sand, gravel, wood, and brick - were chosen due to: (1) the sum of their MI values accounted for approximately 95% of the total value at average level, which is consistent with the results from other regions (Gonti et al., 2018; Guo et al., 2019), and (2) there are relatively more sufficient MI data samples for these materials than the others. Each building in the database was categorized based on four attributes: geographic location (i.e., northern or southern regions of China), use type (i.e., industrial, public, or residential), structural composition (i.e., steel, brick-concrete, brick-wood, or reinforced concrete), and construction era (i.e., 1970s and before, 1980s, 1990s, 2000s and after). These categories were selected to ensure a sufficient sample size and are considered as factors impacting MI, with their importance estimated in the subsequent sections. Wooden structures were excluded because of the small number of its samples in the original MI database and the scarcity of wooden buildings in current China (Luo et al., 2018).

### 3.2 Correlation analysis

Several studies have indicated that high feature correlations can influence the feature importance measures in RF models, but a clear consensus on this impact is yet to be established (Gregorutti et al., 2017; Tolosi and Lengauer, 2011). Therefore, a correlation analysis was conducted to examine potential associations between features and their strength of the associations. Given that the four variables in this study are categorical variables, the chi-square test was employed to investigate whether there is an association between the variables, and to measure the pairwise correlations between four categorical variables. While the chi-square test effectively identifies the significance of the associations, it does not quantify the strength of the association. To address this, Cramer's V coefficient, which is a Pearson's chi-squared test-based measure, was utilized to quantify the strength of the association between two variables. This coefficient is not affected by sample size and therefore useful for large sample sizes as in the present study. The bias-corrected Cramer's V was applied to further evaluate the strength of pairwise correlations between the four categorical variables (Bergsma, 2013). Cramer's V ranges from 0, indicating no association, to 1, indicating a complete association between two categorical variables. In addition, the association between building materials was quantified using Pearson's correlation coefficient, which lies between -1 and 1. A correlation coefficient nearing the absolute value of 1 suggests a stronger association between the variables.

### 3.3 Methodology: RF regressor

The RF algorithm is an ensemble tool relying on the integration of multiple decision trees, encompassing both classification and regression trees used for predicting discrete and continuous variables, respectively (Dou et al., 2019). An individual regression tree is prone to high variance, resulting in unstable and imprecise predictions. Bagging regression tree enhances prediction performance by aggregating multiple models, which averages the outputs to minimize the variability inherent in single trees and reduces the risk of overfitting. However, the effectiveness of bagging can be compromised by correlations between trees, potentially diminishing the model's overall performance. RF addresses this issue by constructing a large collection of decision trees,

which is an evolution and refinement of bagging approach. Each component tree within the RF framework is developed through randomness, distinguishing RF as an enhanced tool of single decision tree. This learning algorithm is generally recognized for its good prediction accuracy, demonstrating robust and accurate performance in dealing with complex datasets (Dou et al., 2019; Wang et al., 2018).

### 3.3.1 RF model development

RF procedures are conducted in a series of steps: a) random resampling from the original dataset with the bootstrap method; b) constructing a regression tree for each bootstrapped dataset, selecting the best variable from a random subset when the node is split; c) repeating the first two steps to build numerous trees, until the predetermined number of trees is reached; d) aggregating information of all decision trees to make predictions by averaging the outputs from all the trees (Nguyen et al., 2013).

Within this procedure, three parameters are crucial for RF modeling and need to be determined: *n<sub>tree</sub>* (the number of trees established in the RF model), *m<sub>try</sub>* (the number of variables sampled randomly for splitting at each node), and *n<sub>odesize</sub>* (the minimum size in terminal nodes). The *n<sub>tree</sub>* parameter controls the number of trees grown in the RF model; a higher number of trees can stabilize model, but an excessively high number of trees increases computational demands without proportional efficiency gains (Wang et al., 2018). In this research, after computational tests (illustrated in Fig. 3), the default *n<sub>tree</sub>* parameter of 500 trees was applied. Regarding *m<sub>try</sub>* parameter, when the total number of variables is used, model is equivalent to bagging; when setting *m<sub>try</sub>* to 1, the completely random splitting variable can lead to over-biased results. Given the presence of four variables in this research, the *m<sub>try</sub>* parameter was set to 3, and the corresponding test results of *m<sub>try</sub>* are detailed in Table 1. The *n<sub>odesize</sub>* parameter affects tree depth and computation time; larger *n<sub>odesize</sub>* results in shallower trees and less computation time, but limited nodes would result in some patterns in the data to be unlearnable. The default *n<sub>odesize</sub>* value of 5, widely used in prior research, was also employed here (Sun et al., 2016; Wang et al., 2018).

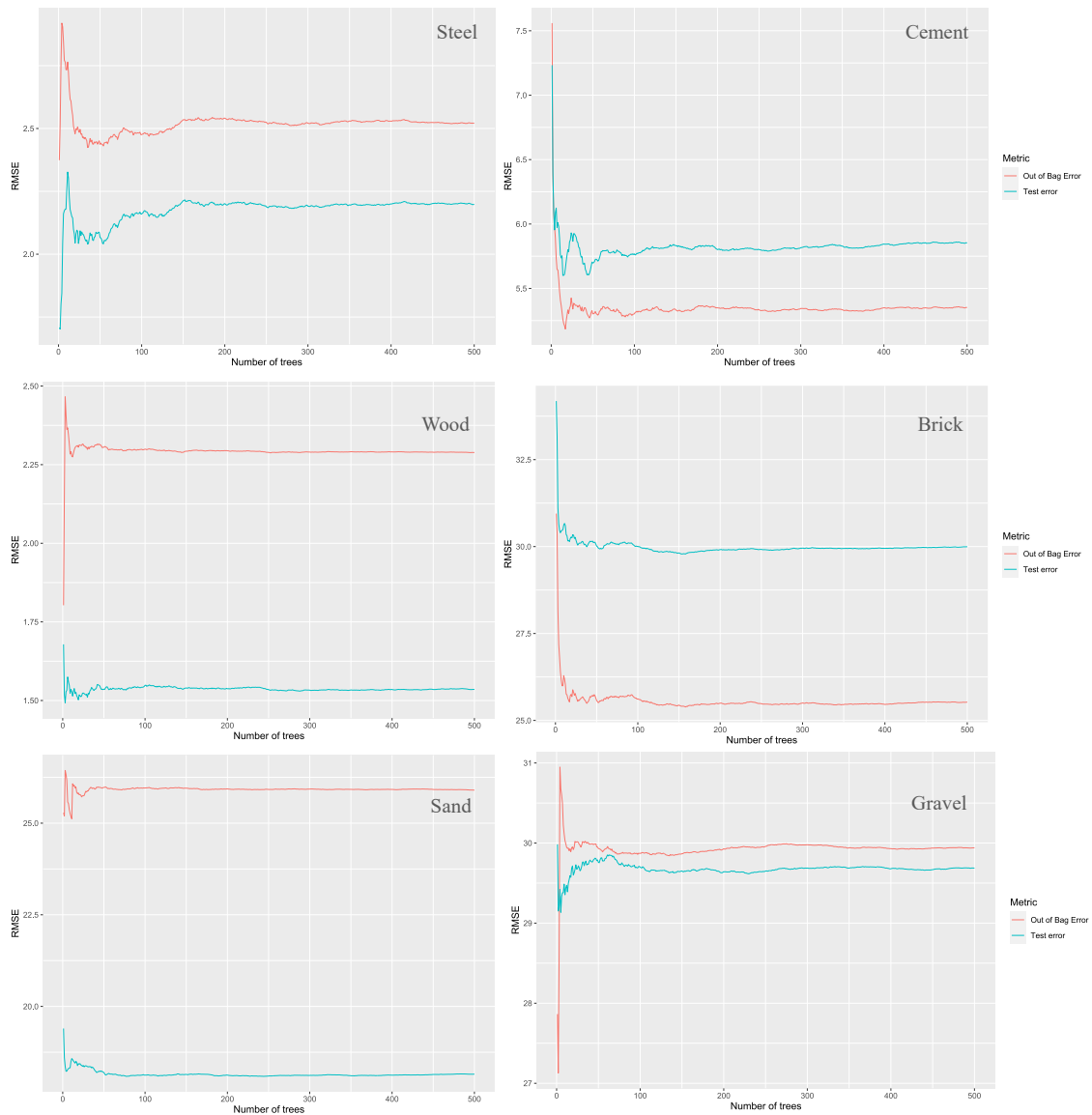


Fig. 3 Computation test of the number of trees (*ntree*)

Table 1 Test results of *mtry* parameter

	Steel	Wood	Cement	Brick	Sand	Gravel
<i>mtry</i> =2	0.238	0.747	0.620	21.273	27.335	30.339
<i>mtry</i> =3	0.069	0.561	0.114	4.980	8.602	14.474

The methods in this section were executed using the open-source R statistical computing environment, incorporating the following packages: randomForest (Breiman, 2001) for classification and regression based on a forest of trees using random inputs, caret (Kuhn, 2015) for data splitting and generating stratified bootstrap

samples, and DALEX (Maksymiuk et al., 2020) for assessing variable importance and partial dependence.

### 3.3.2 Identification of the building feature importance

There are three measures of RF variable importance, namely, selection frequency, Gini importance, and permutation accuracy importance (Strobl et al., 2007). The technique of randomly permuting variable values can disturb the original association between the variables and the output: if a variable is associated with the output, substituting it with the randomly permuted one can significantly decrease the model's predictive performance (Wang et al., 2018). Therefore, the importance of variables was evaluated by measuring the model performance loss after the permutation of a selected variable. The method to measure variable importance is described in the literature (Biecek and Burzykowski, 2021). The Root Mean Square Error (*RMSE*) was utilized to evaluate the model's goodness-of-fit and overall performance. *RMSE* can identify large errors and evaluates fluctuations in the model response with respect to variance. *RMSE* is the square root of the Mean Squared Error (*MSE*) and indicates the sample standard deviation of the residuals. *RMSE* is defined as follows:

$$RMSE = \sqrt{MSE} = \sqrt{\frac{1}{n} \sum_i^n (\hat{y}_i - y_i)^2} = \sqrt{\frac{1}{n} \sum_i^n r_i^2} \quad (1)$$

where  $n$  is the number of observations available;  $\hat{y}_i$  is the predicted value for the  $i$ -th observation;  $y_i$  is the observed value of the dependent variables for the  $i$ -th observation; and  $r_i$  is the residual for the  $i$ -th observation. In this analysis, 50 permutations were performed for each variable to measure the effect on the model caused by randomly permuting the values of variables. The importance for each variable was then quantified as follows:

$$VI_{X,j} = \frac{\sum_{i=1}^m (RMSE_j^i - RMSE_j^0)}{m} \quad (2)$$

where  $VI_{X,j}$  represents the variable importance for building feature  $X$  (i.e., structure, construction year, use type, and region) for material  $j$  after  $m$  permutations;  $m$  means the number of permutations ( $m = 50$  in this analysis);  $RMSE_j^i$  means the *RMSE* value for the  $i$ -th permutation for material  $j$ ; and  $RMSE_j^0$  means the *RMSE* value for the original, unpermuted data for material  $j$ .

In built environment stock studies that simultaneously measure multiple building materials, it is essential to maintain a consistent categorization of MI across different material types for convenient and efficient MI utilization. Thus, to measure and compare the overall importance of the four features across all materials, a normalization analysis was conducted to establish a consistent order of feature importance. The importance of each variable for each material was normalized using the most important variable as the criterion. The normalized variable importance is given by:

$$NVI_{X,j} = \frac{VI_{X,j}}{VI_{MX,j}} \quad (3)$$

where  $NVI_{X,j}$  denotes the normalized importance of variable  $X$  for material  $j$ , and  $VI_{MX,j}$  represents the importance of the most important variable for material  $j$ . The overall variable importance was then determined as the average importance across all materials.

### 3.3.3 Effects of building features on MI: partial dependence

Partial dependence (PD) plots were depicted to further analyze the relationships between MI and various building properties in the RF model. PD plots, introduced by (Friedman, 2001), graphically represent how the expected outcome of the model varies with alterations in a specific explanatory variable, while holding all other variables constant, in other words, showing the corresponding behavior of the expected model value with the changes in only a selected explanatory variable. A thorough explanation of this method is available in (Biecek and Burzykowski, 2021). The PD plots are particularly valued for their intuitiveness and have been widely applied as they allow to understand what influence the explanatory variable has on the model's predictions separately.

### 3.3.4 RF-based MI estimation

The final MI values, based on the RF model, were estimated by averaging individual prediction of each tree across all 500 developed trees. A hierarchical structure for MI was constructed, reflecting the established order of overall variable importance. In this hierarchical MI estimation, upper-level MIs were calculated by averaging the MIs of all buildings within each upper category. The overall framework of this analysis is illustrated in Fig. 4. This joint prediction approach enhances the

stability of the RF model and reduces the risk of major errors by equalizing the effects of the training data (Wang et al., 2018).

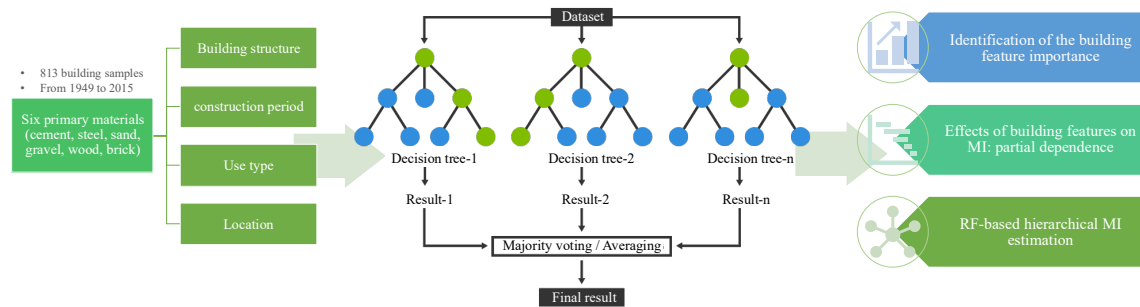


Fig. 4 The overall framework of building MI analysis using RF model

### 3.4 Results

#### 3.4.1 Correlation analysis

The Cramer's V coefficients, illustrating the relationships between four categorical variables for each building material, are displayed in Fig. 5, with all associated  $p$ -values are below 0.01. Across all materials, the strongest association was observed between construction year and region, as indicated by the highest Cramer's V value, suggesting a significant correlation. Moreover, the structure showed a moderate association with the construction year, and relatively high Cramer's V values, approximately 0.4, were also noted between structure and region. It should be noted that the dataset in this study might exhibit uneven sample distribution across different categories, potentially influenced by external factors during sampling, which could contribute to the observed strong correlations between certain categories.

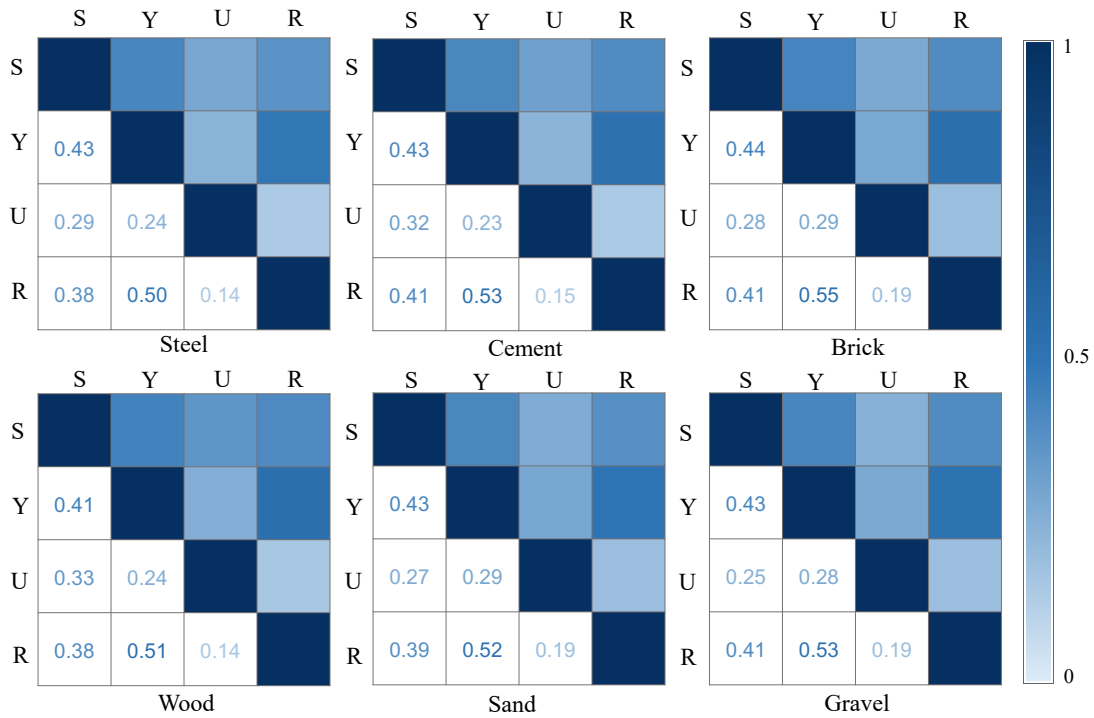


Fig. 5 Correlation analysis: Cramer's V test results of categorical variables. S: structure; Y: construction year; U: use type; R: region

Pearson's correlation coefficients between six building materials are presented in Fig. 6. A notable high correlation coefficient of 0.62 was observed between steel and cement, consistent with findings in other research (Heeren and Fishman, 2019). Additionally, sand displayed a moderate correlation with cement. The following section will individually measure the variable importance for the MI of each building material.

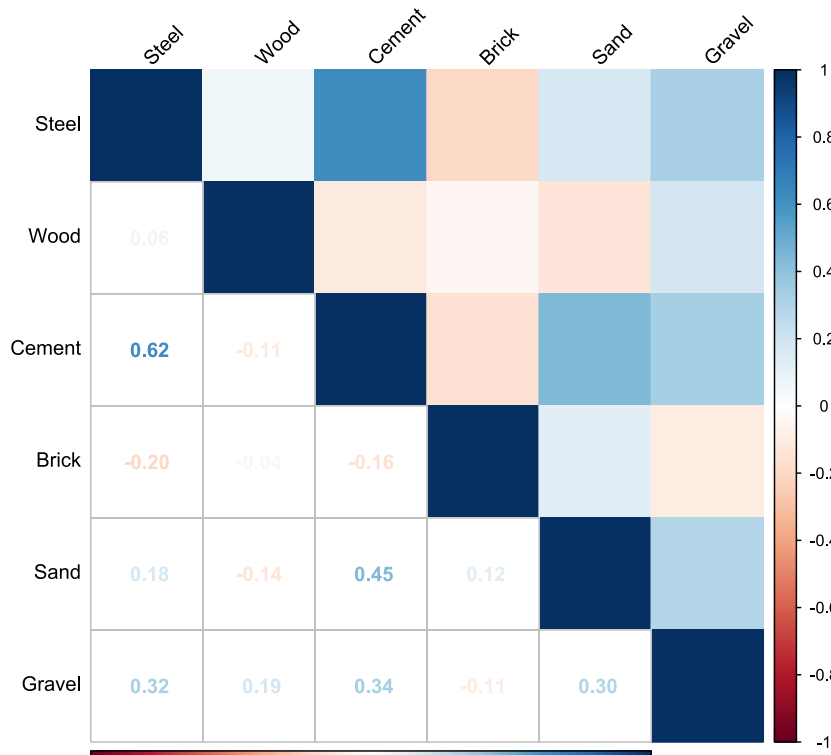


Fig. 6 Correlation analysis: Pearson's correlation test results of building materials

### 3.4.2 Building feature importance

Fig.7 illustrates the variable importance measures in the RF model, derived from 50 permutations. The length of each bar reflects the average variable importance (RMSE loss value) across 50 permutations, with longer bars indicating greater importance due to higher loss upon random permutation. The accompanying box plots on the bars represent the distribution of RMSE loss values over the 50 permutations. Different patterns emerged for the four building attributes across different materials. For steel and brick, the structure was identified as the most influential variable, followed by construction year. In the case of cement, structure was also most influential variable, with use type and construction year showing comparable levels of importance. For the other materials, construction year emerged as the most important feature. Sand and gravel displayed similar patterns in variable significance, whereas wood differed, showing comparable importance for region and construction year.

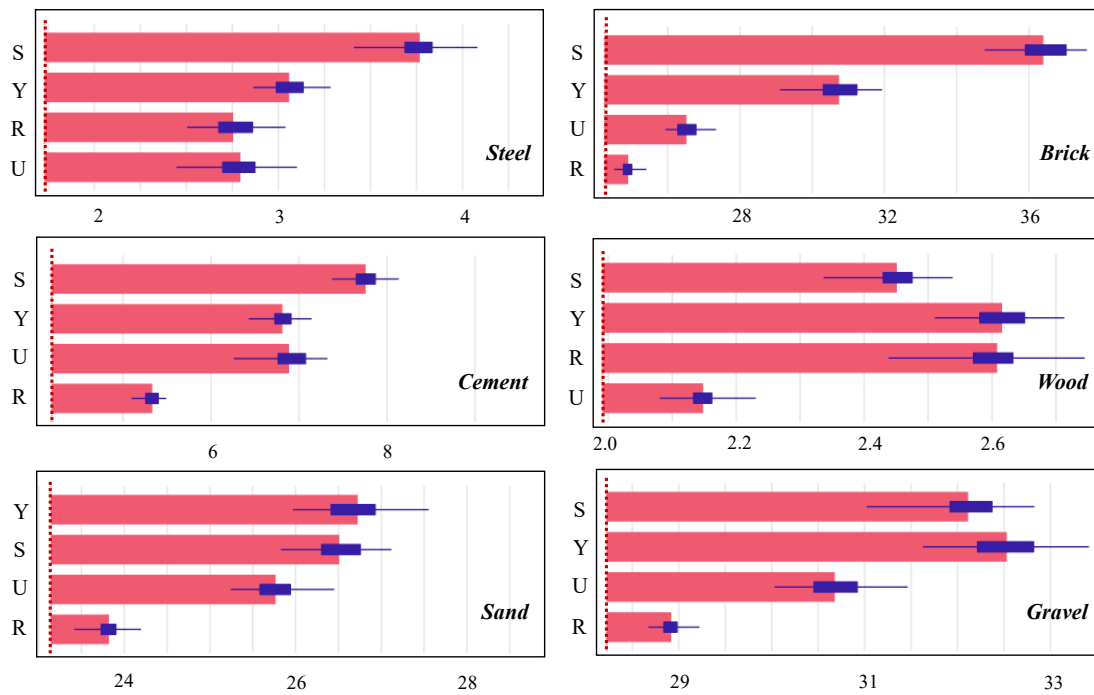


Fig. 7 Building feature importance: Means of variable importance measures over 50 permutations with RMSE as the loss-function for the RF model; Values on the horizontal axis represent mean RMSE loss values and left edge of horizontal axis as shown in dashed lines represents the loss function for the full model (before variables are randomly permuted) over 50 permutations. S: structure; Y: construction year; U: use type; R: region

To further investigate the impact of variable correlations on importance and assess the robustness of feature importance, new models with three of the variables were established after excluding one of the variables. These new models were performed using 50 permutations to calculate the mean variable importance (RMSE loss value) of three variables for each material (shown in Fig. 8). The most notable correlation, as depicted in Figure 5, was between construction year and region across all materials. Excluding the construction year variable revealed that structure became the most critical variable for all materials except wood. Removing the region variable also yielded an importance order for all materials other than wood consistent with findings of Fig. 7. Given the significant influence of construction year and region on wood's MI, their strong correlation likely affected the model in assessing wood's variable

importance. When both construction year and region were included (i.e., excluding only structure or use type), the importance order for wood aligned with Fig. 7. For sand and gravel, structure became more important than construction year upon the exclusion of use type. When structure was removed, the importance of region increased for steel, cement, brick, and gravel, as compared to Fig. 7. Overall, these findings reaffirmed that structure and construction year were the two factors that had the greatest impact on MI across these materials after removing one of the variables.

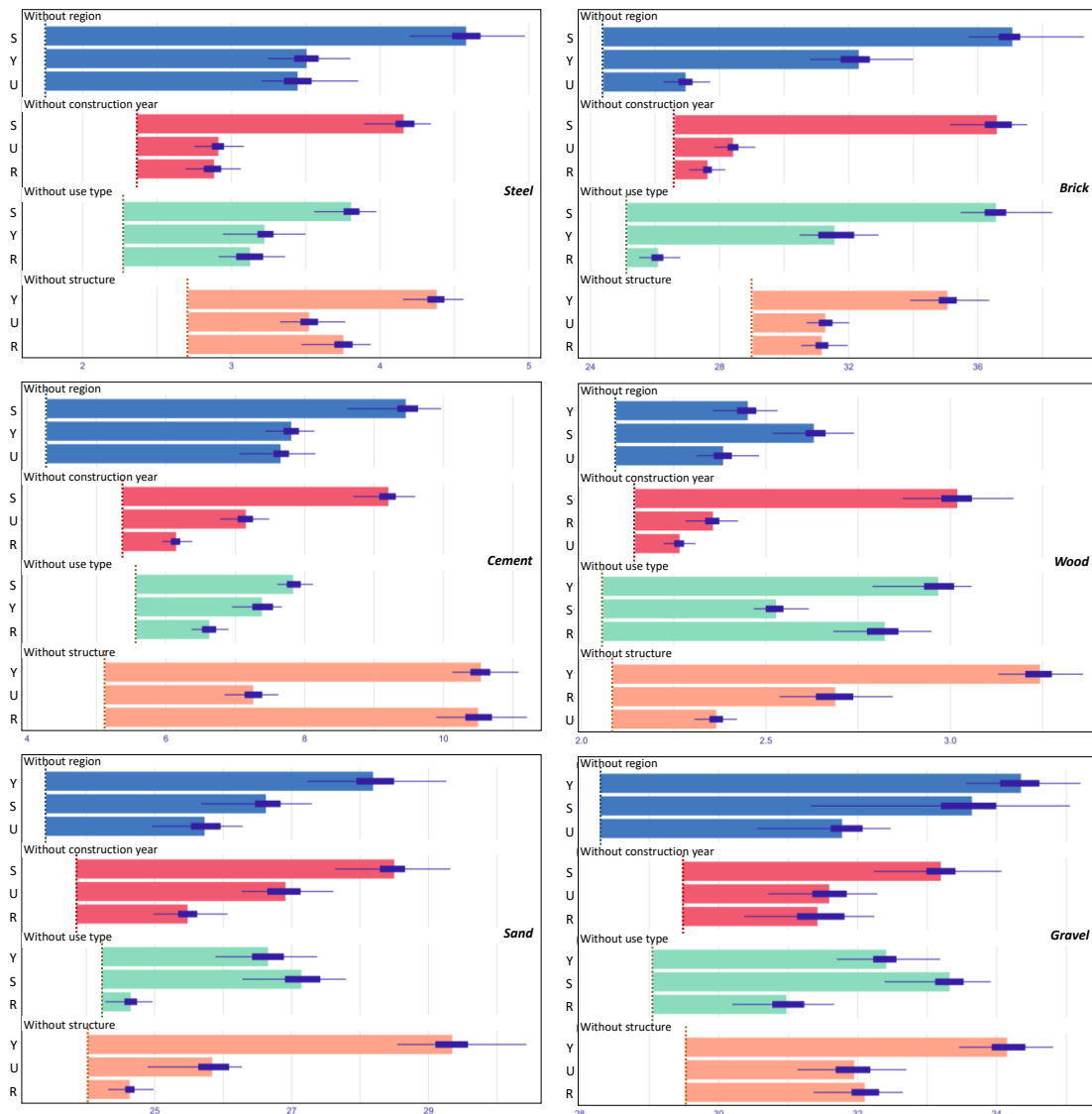


Fig. 8 Building feature importance: Means of variable importance measures over 50 permutations with RMSE as the loss-function for the RF model after removing one of the variables. Values on the horizontal axis represent mean RMSE loss values and left edge of horizontal axis as shown in dashed lines represents the loss function for the full

model (before variables are randomly permuted) over 50 permutations. S: structure; Y: construction year; U: use type; R: region

The variable importance results were normalized to harmonize importance of various building attributes across materials, as shown in Fig. 9. Structure and construction year were found to be relatively more influential for the MI of these six analyzed materials. Use type and region, though of some importance, were not the major variables affecting material intensities of steel, brick, sand, and gravel. In contrast, for wood and cement, region and use type respectively demonstrated relatively high importance. The overall analysis underscored structure as the most significant variable impacting a building's MI, followed by construction year, with use type ranking third but showing a considerable gap in importance from construction year. The region was identified as the least impactful variable among the four building attributes.

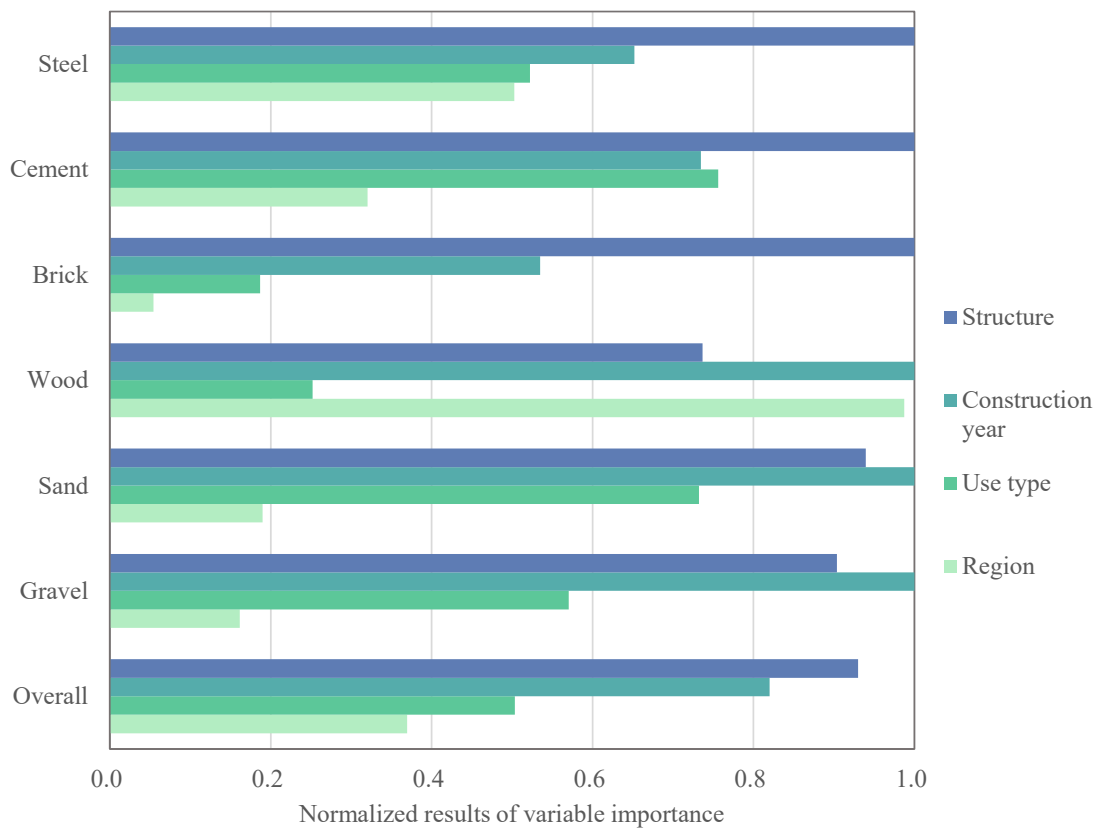


Fig. 9 Normalized variable importance for the RF model

### 3.4.3 Effects of building features on MI

In Fig. 10, PD plots are utilized to depict the impact of selected variables on predictions made by the RF model. The vertical axis of each plot represents the model's response to a specific variable, assuming all other variables remain constant at their average levels.

For the six materials analyzed, PD plots relating to structure reveal that steel buildings significantly influence the MIs of steel, cement, sand, and gravel, more so than other building types. Conversely, MIs of brick and wood are highly dependent on buildings related to brick (i.e., brick-wood and brick-concrete) and wood (i.e., brick-wood), respectively. The PD plots in terms of construction year show a general trend in the MIs of different materials over time. For instance, the MIs of steel and cement exhibit an increasing trend, while those of brick and gravel have decreased since the 1980s. The MIs of wood and sand have remained relatively stable since the 1980s, with minor variations.

Despite use type and region being identified as less significant for MI compared to structure and construction year (as per Fig. 9), their PD plots still offer some interesting insights. Buildings intended for public use tend to consume higher material quantities per unit space, with the exception of brick and sand. In the right-hand column of Fig. 10, a consistent pattern across all materials indicates that buildings in the northern region of China have higher MIs than those in the southern region, particularly for steel, brick, wood, and cement. This distinction in MI between the two regions which has not been considered in previous studies (Hu, M. et al., 2010; Huang et al., 2013; Shi et al., 2012), and provides new insights into the refined research.

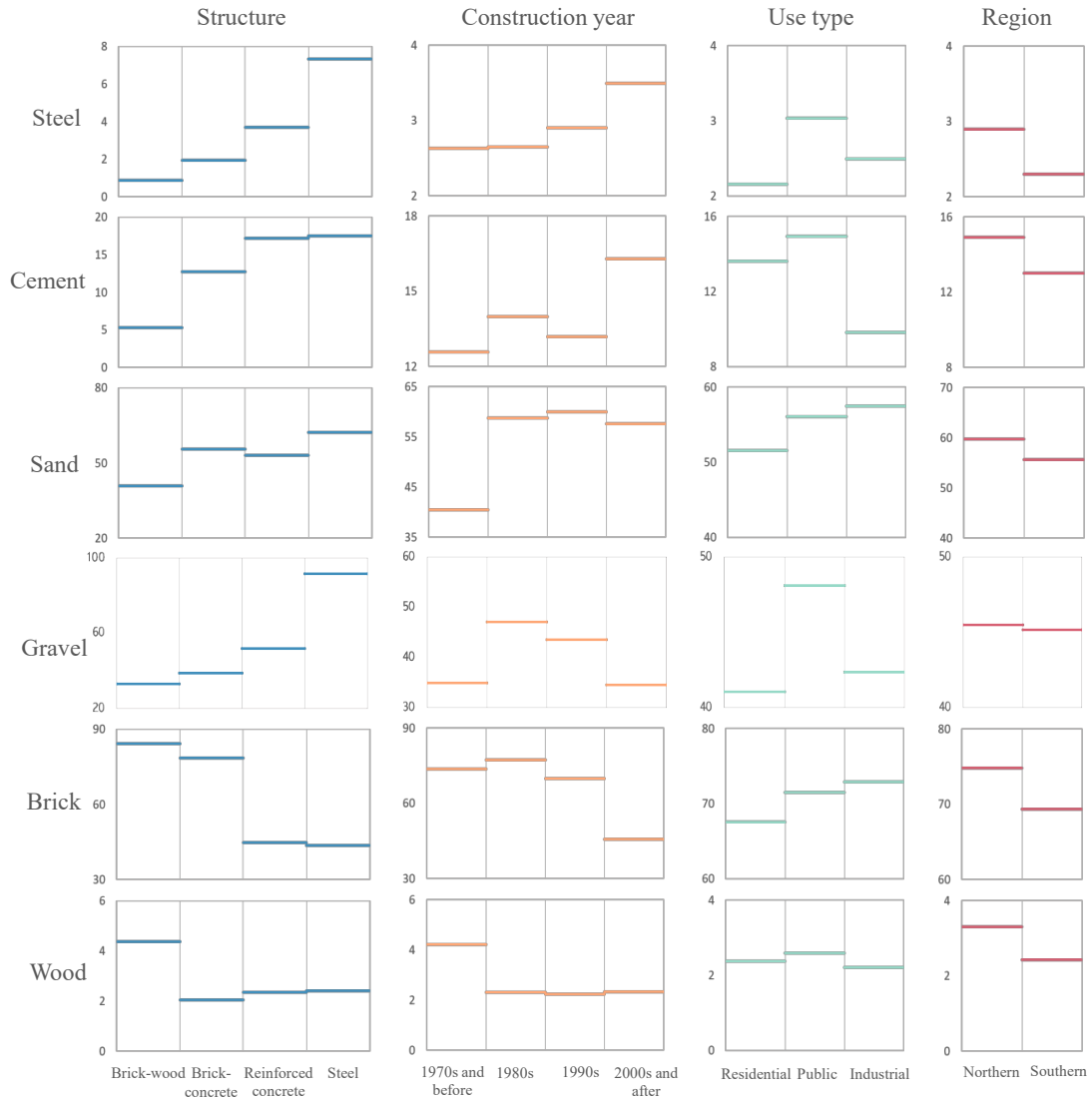


Fig. 10 Effects of building attributes on MI: partial dependence plots. The values on the vertical axis represent the predicted average marginal effects for a given variable

### 3.4.4 RF-based MI

A RF model was utilized to predict the MI of six building materials. The findings for building MI for one of key materials, cement, are presented in Fig. 11. The RF-based MI predictions of other materials is visualized in Appendix 1 and the dataset for all materials is also provided as Table in Appendix 2 so that researchers can easily access it and convert to other units as needed. Fig. 11 as well as Figures in Appendix 1 show the hierarchical RF-based MI results of six building materials. The leaves represent the MI of the corresponding category, and the size of the leaf reflects the value of the MI. The darkness of leaf color indicates the uncertainty difference of MI

application results from inside to outside. The darker color indicates greater uncertainty and vice versa, as the MI of the upper category level considers fewer building attributes. For instance, the highest category level considers only structural attributes of the building, while the lowest level considers all four building attributes. The complete dataset for all materials is also accessible in an Excel format in Supplementary Information of (Zhang, R. et al., 2022), facilitating easy access and unit conversion for researchers. A quick MI calculator is provided in sheet "RF-based MI dataset". If MI with some building attributes is need, use the filter function of Excel to select the required attributes, and the filtered MI information of each material will be automatically calculated and displayed in cells of sheet.

Taking a branch as an explanatory example (highlighted in red in Fig. 11), if only taking structure into account, the cement MI for a reinforced concrete structure is estimated to be 18.5 tons per 100 square meters, the highest intensity among all structures. This high intensity is attributed to the structural reliance on reinforced concrete and structural steel in the load-bearing frames of cement-intensive reinforced concrete buildings (Wang et al., 2015). In contrast, brick-wood buildings exhibit the lowest cement MI. Further down the hierarchy, buildings constructed after 2000 in the reinforced concrete category required 21.22 tons of cement per 100 square meters. Delving deeper, the cement MI for public buildings is estimated at 26.41 tons per 100 square meters. Additionally, regional variations are considered at the lowest hierarchy, with cement MI for public buildings in northern and southern regions of China being 31.86 and 20.96 tons per 100 square meters, respectively.

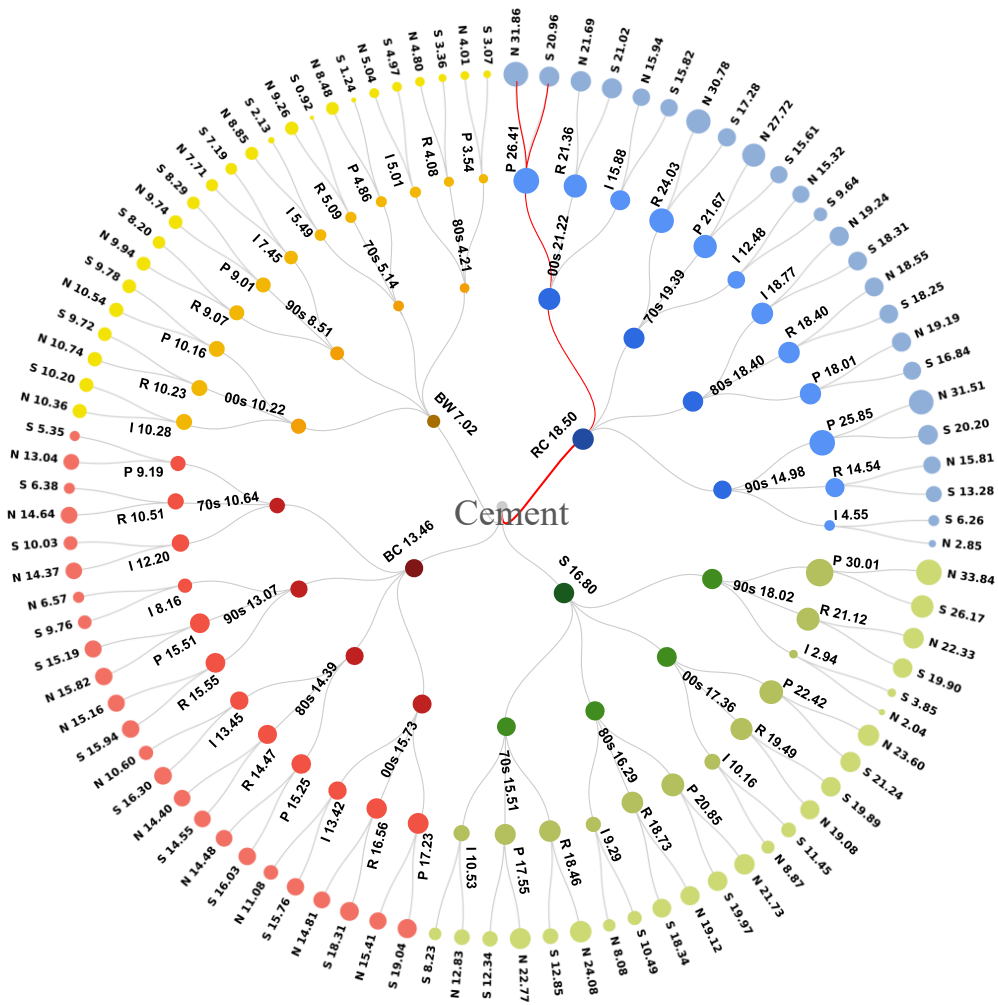


Fig. 11 RF-based MI for cement (Unit: ton/100 m<sup>2</sup>). BC: brick-concrete; BW: brick-wood; S: steel; RC: reinforced concrete; 70s: 1970s and before; 80s: 1980s; 90s: 1990s; 00s: 2000s and after; I: industrial; P: public; R: residential; S: southern; N: northern

### 3.5 Discussion

#### 3.5.1 Comparison with mean values of MI

Several previous studies on quantifying the MS of Chinese buildings have traditionally determined the MI of archetype buildings using mean values (Hu, M. et al., 2010; Huang et al., 2013; Shi et al., 2012), usually categorized based on structure (Guo et al., 2019; Hu, D. et al., 2010; Wang et al., 2015) and use type (Huang et al., 2013; Shi et al., 2012), occasionally incorporating construction year (Han and Xiang, 2013; Huang et al., 2013; Shi et al., 2012). This approach is executed by assigning equal weight to each influencing factor. For example, in calculating the average MI for a

building type defined by structure, other impacting factors like construction year, use type, and area are deemed equally important. However, our variable importance analysis (Fig. 7) suggests that these features vary in their importance for different materials. To validate the RF-based MI values and reveal the strength of hierarchical MI, results of this part were compared with mean values from (Yang et al., 2020) using the same MI database, as shown in Fig. 12.

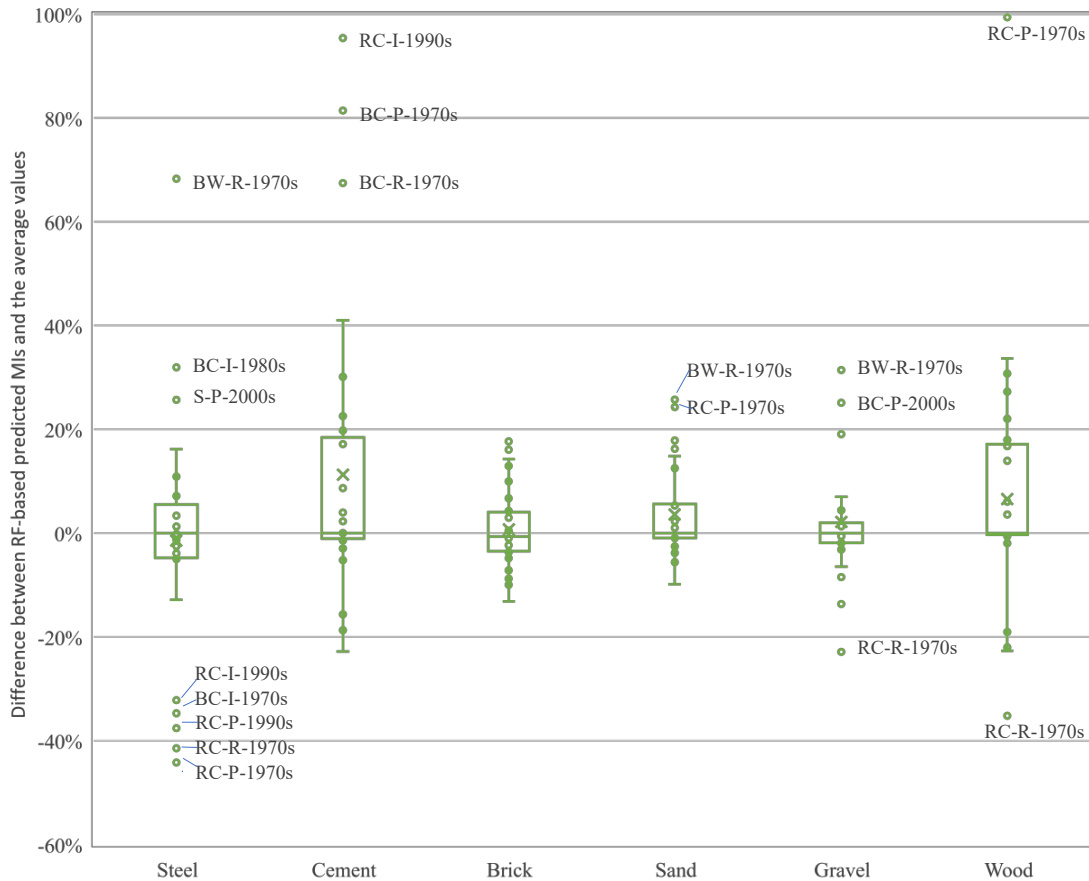


Fig. 12 Difference between RF-based MI and mean values of MI. The boundaries of the upper and lower whiskers represent the minimum and maximum (excluding outliers), respectively; the upper and lower boundaries of the box represent the upper and lower quartile, respectively; outliers are values that lie outside 1.5 times the interquartile range from either end of the box; the line in the middle represents the median and the blue mark represents the mean value

As region factor is not included in Yang et al. (2020), the RF-based MIs used for comparison also consider only the three factors—structure, use type, and construction

period. On an average, the RF-based MIs generally exceed the mean values for most materials, except for steel. Nonetheless, the median differences between RF-based values and the mean are negligible across all comparisons. Notably, many outliers were observed in categories from the 1970s, where data variability was high (Yang et al., 2020). A significant reason for these outliers is the averaging method's inability to account for regional variations due to incomplete sampling. For instance, the raw samples for the RC-I-1990s category comprised only data from China's northern region, regardless of differences in MI between the north and the south, making the average MI unrepresentative of the entire country. Similar regional biases were noted in other outlier categories, which only include data from the northern (e.g., RC-R-1970s, RC-P-1970s, RC-I-1990s, RC-P-1990s, and S-P-2000s) or southern regions (BC-P-1970s and BC-R-1970s). The average value's reliance on sampling data highlights its potential for bias, if some features in the current category is missing, then the feature cannot be fully represented, and the result will be biased. However, this is mitigated in the RF model by capturing intrinsic dataset features, thus showcasing the RF model's superiority over mean-based methods.

### 3.5.2 Application in material stock and flow analysis

In bottom-up approach of building MS accounting, the physical dimensions of buildings, such as floor area or volume, are crucial alongside MI. However, obtaining definite and comprehensive building information is challenging. So far, various methods, such as GIS-based data (Heeren et al., 2013; Kleemann et al., 2017; Miatto et al., 2019), remote sensing images (Haberl et al., 2021; Liang et al., 2017; Schandl, H. et al., 2020), and conventional statistical data (Han and Xiang, 2013; Hu, D. et al., 2010; Hu, M. et al., 2010), are commonly used to gather physical building inventories, but each with varying and limited capabilities in capturing building typology information. For instance, GIS tool has been widely used for their spatial explicitness and it has a relatively greater potential to obtain diverse properties (Heeren et al., 2013; Kleemann et al., 2017; Tanikawa and Hashimoto, 2009). In areas such as Japan, all these four building attributes are explicitly integrated with a GIS dataset (Tanikawa et al., 2015;

Tanikawa and Hashimoto, 2009), while some areas can only access building GIS data with limited features (e.g., location, shape, and size) (Guo et al., 2019; Wang et al., 2019). For remote sensing, the acquisition of physical quantity data with attributes is more limited compared with GIS. Remote sensing itself has been hard to identify building archetypes, despite with the development of auxiliary tools such as machine-learning methods (Haberl et al., 2021; Schandl, H. et al., 2020).

Given these challenges in data quality and availability in material stock and flow analysis, the RF-based MI dataset can offer substantial aid. In cases where information is lacking, the RF-based MI dataset estimated in this study can also be applied. For example, when building quantity data is limited to construction year and purpose of use, the adjusted MI can be derived from the RF-based MIs in Table 1, averaging the MIs under each category. This approach enables researchers to adapt the comprehensive RF-based MIs to available building feature data. A user-friendly MI calculator in (Zhang, R. et al., 2022) have also been developed. This hierarchical MI database significantly enhances MS and flow studies on Chinese buildings, especially when combined with the varied tools and methodologies discussed above.

Table 2 Estimated MI with construction year and use type information (Unit: ton/100 m<sup>2</sup>)

Construction year	Use type	Steel	Brick	Cement	Wood	Sand	Gravel
1970s and before	Industrial	3.95	76.37	10.18	4.26	54.22	36.58
	Public	4.93	81.00	13.32	4.39	40.67	55.07
	Residential	4.06	76.53	14.52	4.75	36.59	46.95
1980s	Industrial	3.54	69.69	11.63	2.64	58.05	61.55
	Public	3.89	70.23	14.41	2.59	58.22	58.59
	Residential	3.00	62.70	13.92	2.63	56.57	55.90
1990s	Industrial	4.12	64.10	5.78	2.52	58.74	56.89
	Public	7.48	58.89	20.10	2.88	60.74	67.68
	Residential	3.09	47.92	15.07	2.70	55.10	51.74

2000s and after	Industrial	4.19	41.24	12.44	2.61	60.05	40.95
	Public	5.51	34.43	19.05	2.95	66.95	42.50
	Residential	4.29	32.40	16.91	2.48	54.79	44.96

### 3.5.3 Rethinking the MI in different regions

The hierarchy for MI in buildings varies significantly across different studies. In Europe and the USA, buildings' MIs are often classified based on utilization purpose, such as residential or non-residential (Haberl et al., 2021; Kleemann et al., 2017; Marcellus-Zamora et al., 2016; Miatto et al., 2019). In contrast, Japanese studies typically categorize MIs based on construction technology, like wooden, steel, or reinforced concrete structures (Tanikawa et al., 2015; Tanikawa and Hashimoto, 2009). Such inconsistency in hierarchy (i.e., construction-based typologies and use-based typologies) and varying reference units (e.g., gross or net floor area, ground area, volume) not only hinders comparisons between studies but also hampers the transferability of MI data (Lanau et al., 2019; Schiller et al., 2019). These findings suggest that structural attributes are crucial for Chinese buildings, aligning with Japanese studies but diverging from studies in western regions. However, in studies focusing on use-based typologies, it has not been examined yet whether use type is indeed the most influential factor, because both national statistics and researchers in Europe omitted attribute of structure while collecting MI data. If the evidence proved so in the future, then the MIs obtained with different categorization systems in different regions should be considered equally reliable, and thus the transferability of MI would become unfeasible among regions due to inconsistent hierarchy.

Therefore, this underscores the importance of analyzing the influence of building features on MI, not only for estimating building MS but also for establishing local MI databases. Comprehensive and region-specific MI data collection through random sampling is essential, particularly in areas like Europe where buildings have longer lifespans and undergo extensive renovation activities. Considering the renovation status in these regions is vital. The RF-based approach used in this study offers a valuable

reference for identifying the most influential building attributes in different regions, once sufficient MI data is gathered.

#### 4. Roadway MS accounting: mapping historical patterns and projecting future trends

##### 4.1 Methodology

##### 4.1.1 Estimation of road MS in Japan with bottom-up method for 1965-2020

The historical road MS can depict the evolution of Japan's road system and serves as the cornerstone for predicting future road MS. The total road MS was determined using a bottom-up material flow analysis method, a common approach for detailed stock status evaluation in MS of materials or infrastructure (Arora et al., 2019; Dai and Yue, 2023; Gassner et al., 2020; Li et al., 2022) for its detailed description of stock status and the capability to display spatial differences in results (Lanau et al., 2019; Tanikawa et al., 2015). The methodology framework is outlined in Fig. 13. This quantification covered all prefectures in Japan, categorizing roads into highways, national roads, prefectural roads, and municipal roads. These roads were further segmented by width into five groups: greater than 19.5 meters, between 13.0 and 19.5 meters, between 5.5 and 13.0 meters, between 3.5 and 5.5 meters, and less than 3.5 meters. For the widest and narrowest categories, widths were standardized at 19.5 meters and 3.5 meters, respectively. For the middle three categories, the average width of each category was used. Additionally, national, prefectural, and municipal roads in each prefecture were classified into concrete and asphalt types, according to the local proportions of concrete and asphalt pavement in each type of road. All roads narrower than 3.5 meters were categorized as simple asphalt paving. The total road MS in Japan from 1965 to 2019 was calculated as follows:

$$MS_t = \sum_{p,i} (MS_{t-1,p,i} + NMS_{t,p,i}) \quad (4)$$

$$NMS_{t,i} = \sum_y (L_{t,y} - L_{t-1,y}) \cdot W_{t,y} \cdot MI_{t,y,i} \quad (5)$$

where  $MS_t$  represents the total road MS of Japan in a given year  $t$ ;  $NMS_{t,p,i}$  indicates the net addition to the MS of material  $i$  in prefecture  $p$  in year  $t$ ;  $L_{t,y}$  is the length of

road type  $y$  in year  $t$ ;  $W_{t,y}$  refers to the width of road type  $y$  in year  $t$ ; and  $MI_{t,y,i}$  stands for the MI of material  $i$  used in road type  $y$  in year  $t$ . Tanikawa et al. (2015) provide a more comprehensive explanation of MI. Due to the unavailability of 2020 data and the relative stability of road MS in recent years, the net addition to MS from 2019 to 2020 was estimated based on the 2018 to 2019 data, assuming that the net addition to MS of 2019 to 2020 was the same as that from 2018 to 2019. Data for Okinawa prefecture roads starts from 1971 due to historical data constraints.

After collecting MS data for each prefecture for four materials from 1965 to 2020 through material flow analysis, GIS software, specifically ArcGIS, was used to merge this road MS data with geospatial information for each prefecture. This was achieved by superimposing the MS data onto maps for each prefecture. The resultant thematic maps graphically display the distribution of road MS across different prefectures over various years. These maps utilize varying color gradients and legends to clearly indicate different levels of MS, facilitating easy interpretation and understanding of the spatial distribution of road MS.

#### 4.1.2 Models: ARIMAX, SVR, hybrid ARIMAX-SVR, ANN, RF, and MLR

The Autoregressive Integrated Moving Average (ARIMA) model is a prevalent tool for analyzing and forecasting time series data, using initial values of a given time series, lagged forecast errors, and lags. As MS growth can be driven by multiple processes, such as government policy and various forms of shocks, including international crises and price changes, the intrinsic trend and effects-based approach of ARIMA allows for forecasts of time-series data without explicitly identifying the causes of such trends and shocks (Fishman et al., 2016). In contrast, the ARIMAX model, which incorporates ARIMA's approach with additional explanatory variables, can provide more precise forecasts by integrating key historical data and relevant variables (Hossain et al., 2021; Yan et al., 2017). ARIMA model is delineated by 3 parameters:  $p, d, q$  where,

$p$  is the order of autoregressive (AR) term;

$q$  is the order of moving average (MA) term;

$d$  is the number of differences to make the time series stationary.

The "Auto Regressive" in ARIMA means a linear regression model using its lags as predictors.  $p$  is related to the number of lags.  $q$  is related to the number of lagged forecast errors that should comply with the ARIMA model. The ARIMA model can be written in backshift notation as follows:

$$(1 - \phi_1 B - \dots - \phi_p B^p)(1 - B)^d y_t = \mu + (1 + \theta_1 B + \dots + \theta_q B^q) a_t \quad (6)$$

where  $y_t$  ( $1 \leq t \leq n$ ) is the time series at time  $t$ ;  $\mu$  is the mean term;  $B$  is the backshift operator ( $B y_t = y_{t-1}$ );  $\phi_i$  is the coefficient of AR term of lag  $i$ ;  $\theta_i$  is the coefficient of MA term of lag  $i$ ; and  $a_t$  is the random error or white noise.

ARIMAX model is an extension of Arima model, and it is a combination of AR model (using previous states), MA model (using past residuals); and ordinary regression model (using external variables on integrated series) (Bolanle and Oluwadare, 2017). An ARIMAX model can be expressed as:

$$y_t = \sum \beta_j X_{t-j} + \phi(B)^{-1} \theta(B) a_t \quad (7)$$

where  $X_t$  is a covariate at time  $t$ ;  $\beta$  is the coefficient of the covariate;  $\phi(B)$  is the AR operator; and  $\theta(B)$  is the MA operator; where

$$\phi(B) = 1 - \phi_1 B - \dots - \phi_p B^p \quad (8)$$

$$\theta(B) = 1 + \theta_1 B + \dots + \theta_q B^q \quad (9)$$

The stationarity of time series for each prefecture was tested using the Kwiatkowski-Phillips-Schmidt-Shin (KPSS) test. The order of AR term ( $p$ ) and MA term ( $q$ ) were selected by minimizing the value of Akaike's Information Criterion (AIC) to decide the suitable model for each prefecture. The utilized methods were implemented using the open-source R statistical computing environment using R's forecast package. The residual diagnostics was performed by Ljung-Box test and autocorrelation function and partial autocorrelation function plots. More detailed information of the ARIMAX model, and model selection and fitting procedures can be found in the references (Bolanle and Oluwadare, 2017; Hossain et al., 2021; Hyndman and Athanasopoulos, 2018; Hyndman and Khandakar, 2008).

SVR is a non-parametric machine learning method based on Support Vector

Machine principles, tailored for regression problems (Awad and Khanna, 2015; Smola and Schölkopf, 2004). Unlike traditional regression, SVR does not assume a specific statistical distribution for input data. It uses kernel functions for fitting nonlinear data and focuses on finding the optimal hyperplane that maximizes the margin between predicted and actual values (Awad and Khanna, 2015; Ma et al., 2022; Mechelli and Viera, 2019), making it effective for handling complex datasets characterized by high variability and nonlinearity and has been widely used to solve various regression problems (Dash et al., 2021; Fan et al., 2021; Zhong et al., 2019).

The ARIMAX-SVR hybrid model combines ARIMAX's and SVR's strengths. Assuming that the time series comprises both a linear autocorrelation component and a nonlinear residual component, it first utilized ARIMAX to predict future MS values, treating the deviation between these predictions and actual values as the residual, which was subsequently recorded as the nonlinear component. This residual was then used to build SVR model for future residual predictions (Xu et al., 2020). The outputs from both models were combined for a final and comprehensive MS forecast. ARIMAX models the linear aspects and external variables of the time series, while SVR addresses the nonlinear relationships. This hybrid approach leverages the strengths of both linear and nonlinear models and is expected to improve prediction accuracy compared to using either model alone. It has found application in diverse fields (Che and Wang, 2010; Staffini, 2022; Xu et al., 2020; Xu et al., 2022; Zhang, Y.M. et al., 2019).

Different models possess unique strengths and limitations, and their suitability for specific regression problem domains varies. For a holistic evaluation of these models, a comparative analysis involving three popular machine learning techniques—SVR, ANN, and RF—along with the widely used statistical method, MLR was conducted.

ANN is a computational model that emulates the structure and function of biological neurons, consisting of interconnected layers of nodes that process information and learn from data. ANNs are particularly well-suited for various regression tasks, especially when dealing with large datasets and complex patterns. They excel in capturing intricate relationships and handling noisy data (Krogh, 2008;

Yegnanarayana, 2009). RF, an ensemble of decision trees, is robust against outliers and noisy data. Additionally, it demonstrates notable performance in the presence of irrelevant features and effectively handles missing data (Breiman, 2001; Cutler et al., 2012). MLR serves as a baseline for comparison against the other machine learning methods. By including multiple independent variables to predict a continuous dependent variable, MLR aims to determine the best-fitting linear equation that explains the variation in the target variable based on the values of the predictors. This can provide insights into the strengths and weaknesses of machine learning models relative to traditional statistical approaches.

#### 4.1.3 Explanatory variables

Four explanatory variables were utilized to forecast the expected future road MS: population, gross regional product (GRP), passenger transportation (measured in passenger-kilometer, pkm), and cargo transportation (measured in tonne-kilometer, tkm). Population and GRP were chosen for their comprehensive representation of both demographic and economic aspects as covering both population and affluence, recognized as two main ultimate drivers of environmental impact (Ehrlich and Holdren, 1971; Meijer et al., 2018). The transportation data, divided into passenger and cargo transportation, reflects the demand and supply dynamics of transport services in a given region. Vehicle ownership was a critical factor in predicting transportation trends, as it directly influences traffic patterns and holds immense potential in anticipating and explaining future travel behaviors (Moody et al., 2021; Yang et al., 2017). Transportation data was computed by multiplying the number of vehicles and the individual vehicle transport index (IVTI) (MLIT, 2023a).

Vehicles were categorized into passenger and commercial types. Passenger vehicles included private cars and buses, while commercial vehicles encompassed trucks and other commercial vehicles in addition to buses. In 2020, private passenger cars made up 79% of total vehicles, and there was a strong correlation between the number of passenger vehicles and the GRP in each prefecture. Consequently, linear regression models were established for each prefecture to predict the number of

passenger vehicles up to 2050, based on GRP projections for five SSPs (Wu et al., 2014). The R-square values and significance of these regression models are detailed in Table 3. For commercial vehicles, which typically respond to population needs, future numbers were estimated based on the population projections of the five SSPs for each prefecture. It was noted that the ratio of commercial vehicles per capita had stabilized in recent years in each prefecture.

Table 3 R-square and significance of linear regressions for each prefecture in Japan  
between the number of passenger vehicles and GRP

Prefecture	R <sup>2</sup>	Adjusted R <sup>2</sup>	Significance
Hokkaido	0.90	0.89	***
Aomori	0.86	0.86	***
Iwate	0.84	0.84	***
Miyagi	0.89	0.89	***
Akita	0.81	0.80	***
Yamagata	0.85	0.85	***
Fukushima	0.85	0.85	***
Ibaraki	0.93	0.93	***
Tochigi	0.91	0.91	***
Gumma	0.90	0.90	***
Saitama	0.95	0.95	***
Chiba	0.94	0.94	***
Tokyo	0.96	0.96	***
Kanagawa	0.97	0.97	***
Yamanashi	0.80	0.79	***
Niigata	0.85	0.84	***
Toyama	0.85	0.84	***
Ishikawa	0.87	0.87	***
Nagano	0.89	0.89	***
Fukui	0.88	0.88	***
Gifu	0.90	0.90	***
Shizuoka	0.92	0.92	***
Aichi	0.93	0.93	***
Mie	0.94	0.94	***
Shiga	0.89	0.89	***
Kyoto	0.94	0.93	***
Osaka	0.92	0.92	***
Nara	0.89	0.88	***
Wakayama	0.89	0.88	***
Hyogo	0.91	0.91	***
Tottori	0.73	0.72	***

Shimane	0.86	0.86	***
Okayama	0.85	0.84	***
Hiroshima	0.84	0.84	***
Yamaguchi	0.90	0.90	***
Tokushima	0.95	0.95	***
Kagawa	0.86	0.85	***
Ehime	0.85	0.84	***
Kochi	0.85	0.85	***
Fukuoka	0.91	0.91	***
Saga	0.87	0.87	***
Nagasaki	0.85	0.84	***
Kumamoto	0.85	0.84	***
Oita	0.85	0.84	***
Miyazaki	0.89	0.88	***
Kagoshima	0.88	0.88	***
Okinawa	0.90	0.90	***

\* \*\* p \*\*\* p<0.01

#### 4.1.4 Forecast of road MS in Japan by 2050

The estimation of future road MS until the year 2050 was conducted by incorporating prospective explanatory variables, namely population, GRP, passenger transportation, and cargo transportation, for each prefecture across five SSPs. The evaluation of the relationship between road MS and these explanatory variables involved a multistep process, as illustrated in the overview figure of Fig. 13.

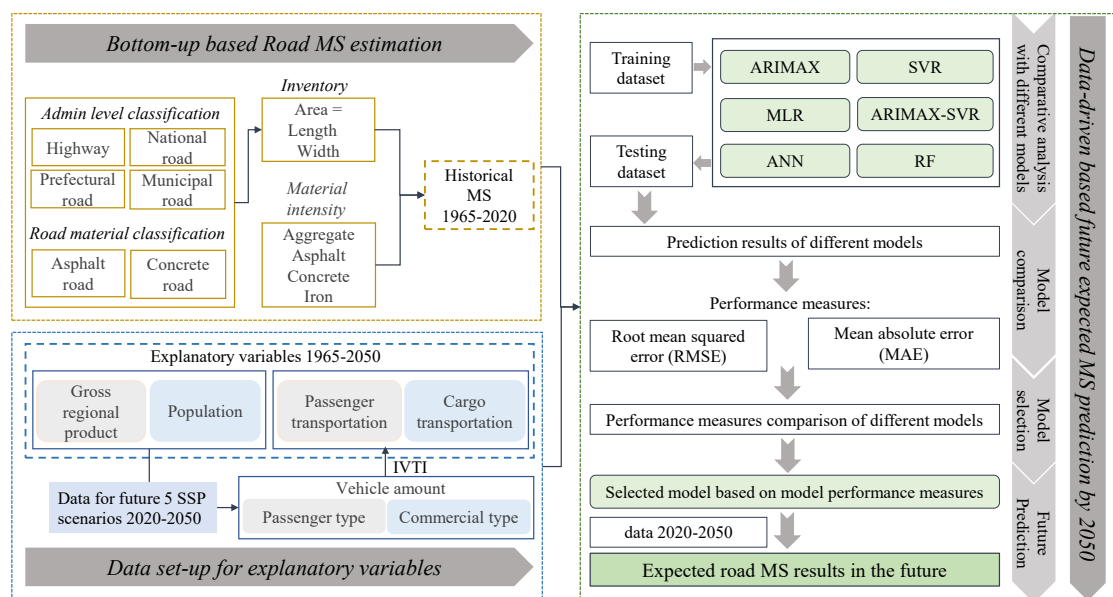


Fig. 13 Overview and research methodology

Initially, the ARIMAX model was developed for time series data spanning from 1965 to 2020. The dataset was partitioned into training data (1965 to 2015) and testing data (road MS data after 2015). Akaike's Information Criterion (AIC) was used to select the most suitable model, considering its performance on predicting the testing dataset. Model performance was assessed using the RMSE and mean absolute error (MAE) metrics, which are negatively-oriented and lower values indicated higher prediction accuracy. They are calculated as follows:

$$\text{RMSE} = \sqrt{\frac{\sum_{i=1}^n (y_i - \hat{y}_i)^2}{n}} \quad (10)$$

$$\text{MAE} = \frac{\sum_{i=1}^n |y_i - \hat{y}_i|}{n} \quad (11)$$

where  $y_i$  denotes the actual value;  $\hat{y}_i$  represents the predicted value;  $n$  means the number of observations.

Subsequently, the SVR model was employed to predict the residuals of the ARIMAX model. Understanding the order of SVR model residuals and their impact on subsequent period residuals was crucial. To achieve this, a series of  $k$  time-ordered residual data was collected at each time point, arranged chronologically, and the aligned matrix was used as input for the SVR model. The SVR model outputs  $k + 1$  data points, preserving the data error (Xu et al., 2020). The grid search algorithm was applied to optimize the epsilon parameter and cost parameter of the SVR model.

Finally, the prediction results from both the ARIMAX and SVR models were combined to derive integrated results from the ARIMAX-SVR model. To address multicollinearity, the performance of the ARIMAX-SVR model and the ARIMAX model alone was examined, incorporating population and GRP as explanatory variables after excluding transportation data. The final model, demonstrating the highest prediction accuracy, was selected. All methodologies were implemented using the open-source R statistical computing environment.

For MLR, SVR, ANN, and RF models, 10-fold cross-validation was applied to relate road MS for each prefecture to explanatory variables. Evaluation metrics, RMSE and MAE, were used, and these methods were implemented on the Weka platform, a

popular and widely used open-source software suite for data mining and machine learning tasks, primarily based on the Java programming language (Eibe et al., 2016; Hall et al., 2009). Hyperparameters for these models are provided in Table 4. This study did not consider qualitative differences between SSPs, such as technological development (Fishman et al., 2021; Meijer et al., 2018; Yokoi et al., 2022). The comprehensive analysis and comparison of these machine learning models offer insights into their performance for road MS prediction.

Table 4 Information and parameters for MLR, SVR, ANN, and RF models on Weka platform

Models	Information and parameters
MLR	Eliminate colinear attributes: True
SVR	Kernel: Polynomial Kernel; Exponent:1.0; Parameter C: 1.0
ANN	Learning rate: 0.2; Momentum: 0.2; Number of Epochs: 500
RF	ntree: 500; number of randomly chosen features: 3;

\*For other hyperparameters not showed, the default values of the Weka software were utilized.

#### 4.1.5 Data sources

Historical road statistical data and road MI from 1965 to 2020 for each prefecture were obtained from the Ministry of Land, Infrastructure, Transport and Tourism of Japan (MLIT, 2022) and (Tanikawa et al., 2015), respectively. Data on historical population in Japan were collected from the portal site for Japanese Government Statistics (e-Stat, 2022), while data on future population under the five SSPs were obtained through the Adaptation Information Platform of Japan (A-PLAT, 2022). Historical GRP data were retrieved from the Cabinet Office, Government of Japan (COGA, 2022), and the average future GRP of each prefecture under the five Japanese SSPs were obtained from (Honjo et al., 2021). Historical data on vehicle numbers and transportation were collected from the Automobile Inspection and Registration Information Association of Japan (AIRIA, 2023) and the Ministry of Land,

Infrastructure, Transport and Tourism of Japan (MLIT, 2023a), respectively.

## 4.2 Results

### 4.2.1 Evolution trends and material decomposition of road MS over the past half century

Fig. 14 illustrates the material and regional composition as well as the chronological distribution of road MS. In this diagram, the width of nodes on the left denotes the quantity of road MS in each prefecture, the width of nodes in the middle corresponds to the amount of different types of road materials, and on the right, the width of nodes represents the distribution of road MS across different years. Through the analysis of the inter-node flow, this diagram facilitates the identification of disparities in road MS among various regions and variations in the quantities of materials utilized. Consequently, this graph offers an intuitive understanding of the distribution of road MS and its changes over time.

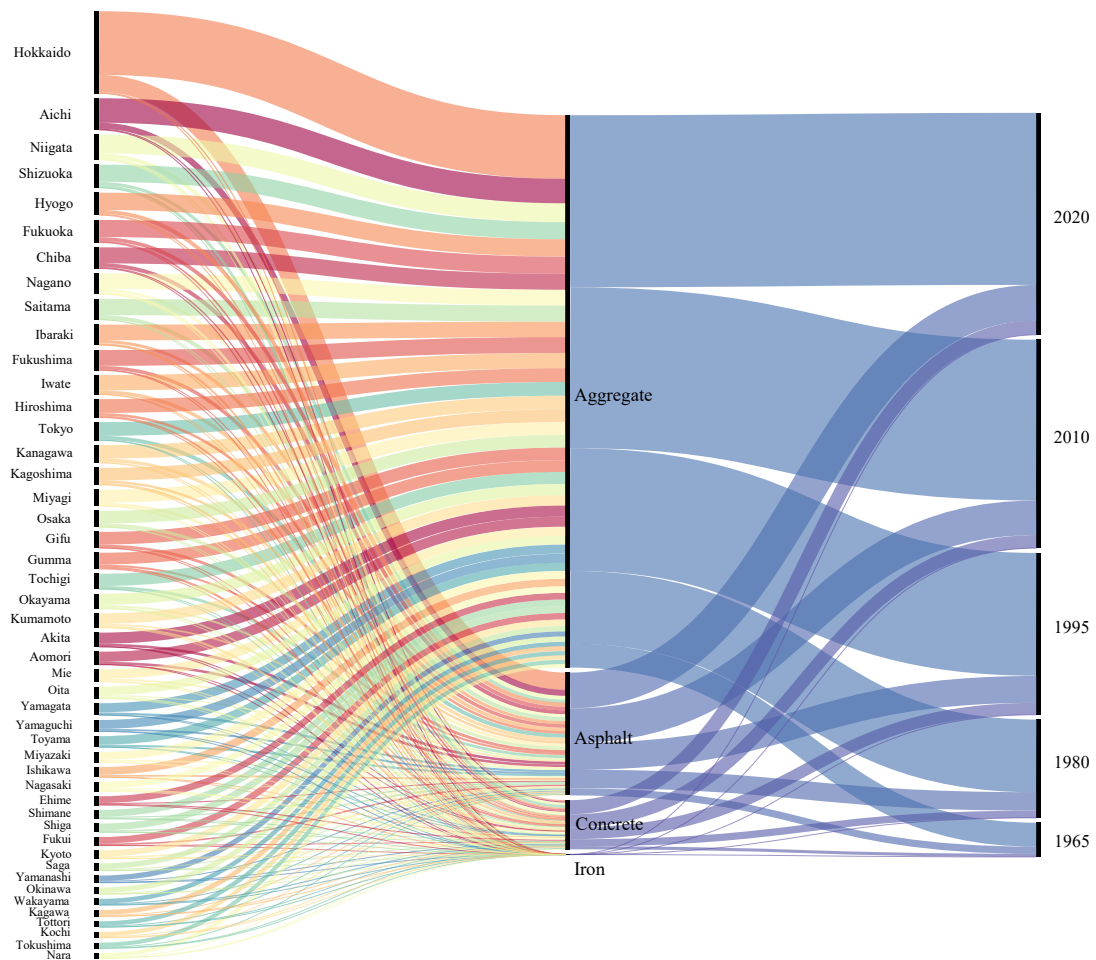


Fig. 14 The material and regional composition

Hokkaido, the prefecture with the largest amount of road MS, contributed 7.6% to 12.4% and 9.4% to 15.2% of aggregate and asphalt, respectively, across the four periods. However, only 2% to 3.1% of concrete and 2.5% to 3.5% of iron were attributed to Hokkaido. The distribution of asphalt, concrete, and iron in each prefecture to some extent reflects variations in road types across different regions. For instance, clear flows from Hokkaido and Aichi are visible in asphalt, while in concrete, Shizuoka, Nagano, and Niigata contribute relatively substantial flows (Fig. 14).

Fig. 15 presents the material composition with values in each prefecture for different periods and Fig. 16 illustrates the change in the percentage of each material from 1965 to 2020. Aggregate emerged as the predominant material in road MS, constituting over 70% in each period, followed by asphalt, ranging from 16% to 21%. The contribution of iron was minimal, as it was only included in concrete roads, with asphalt roads being more prevalent than concrete roads in Japan.

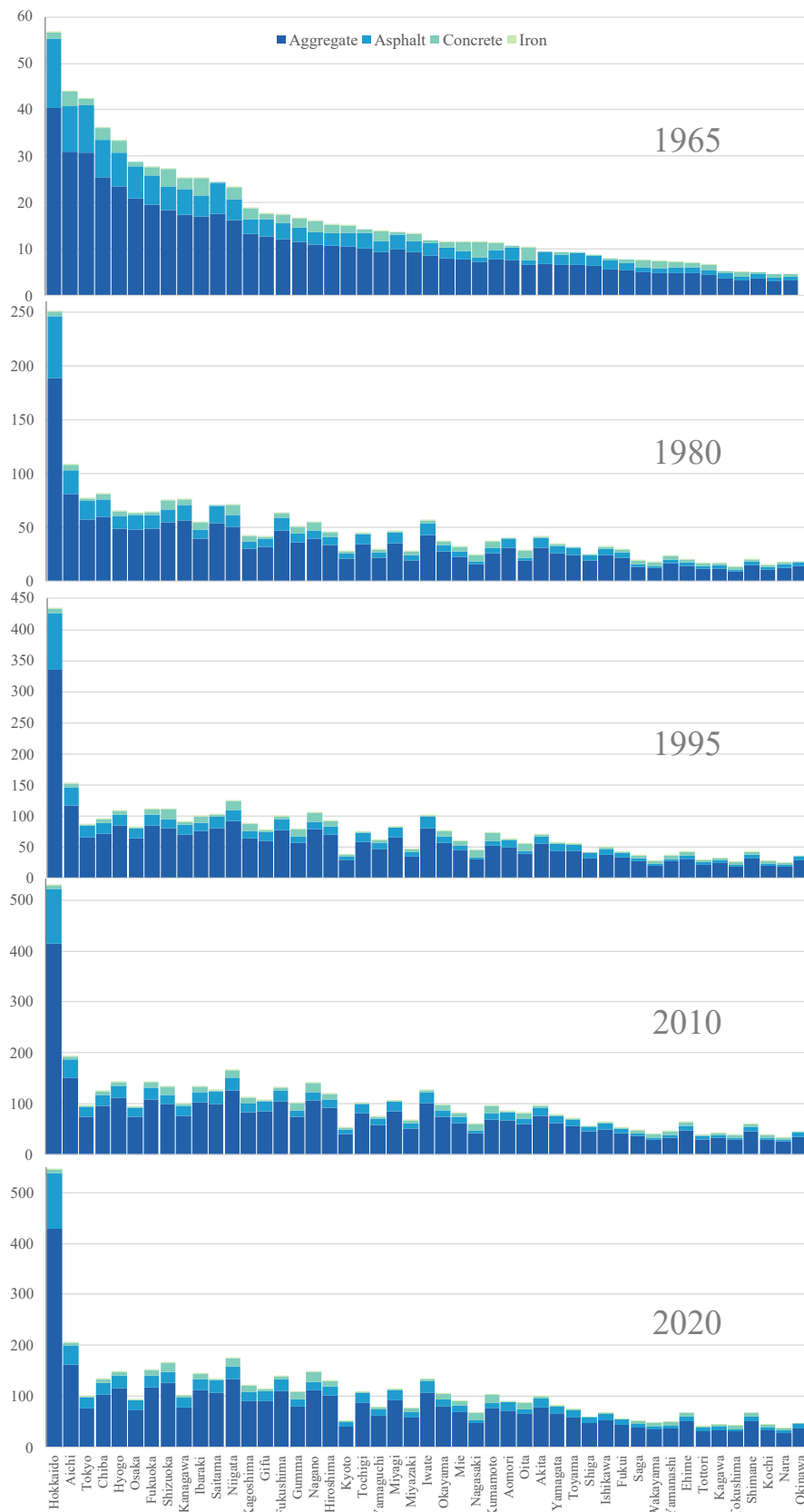


Fig. 15 The material composition with values in each prefecture for different period

(Unit: Mt)

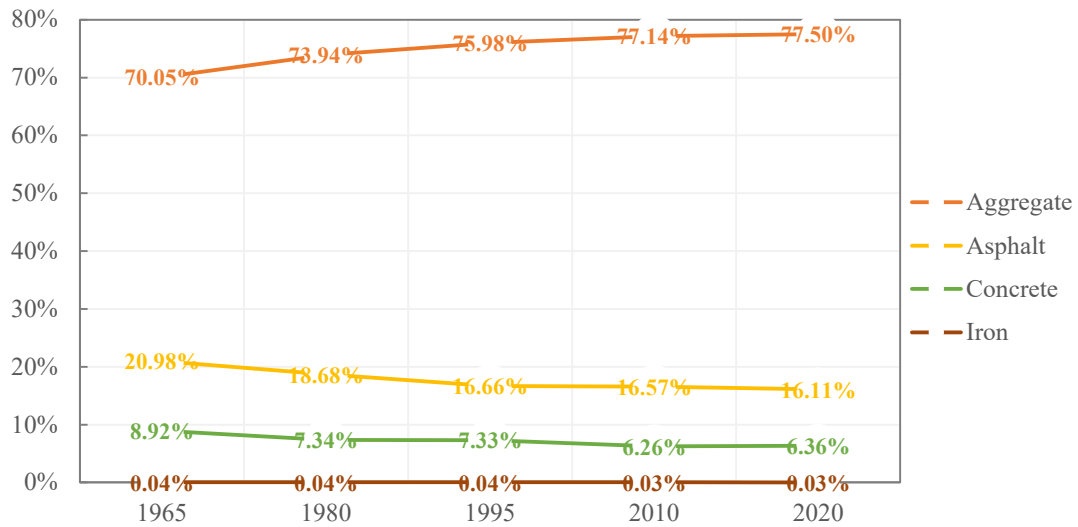
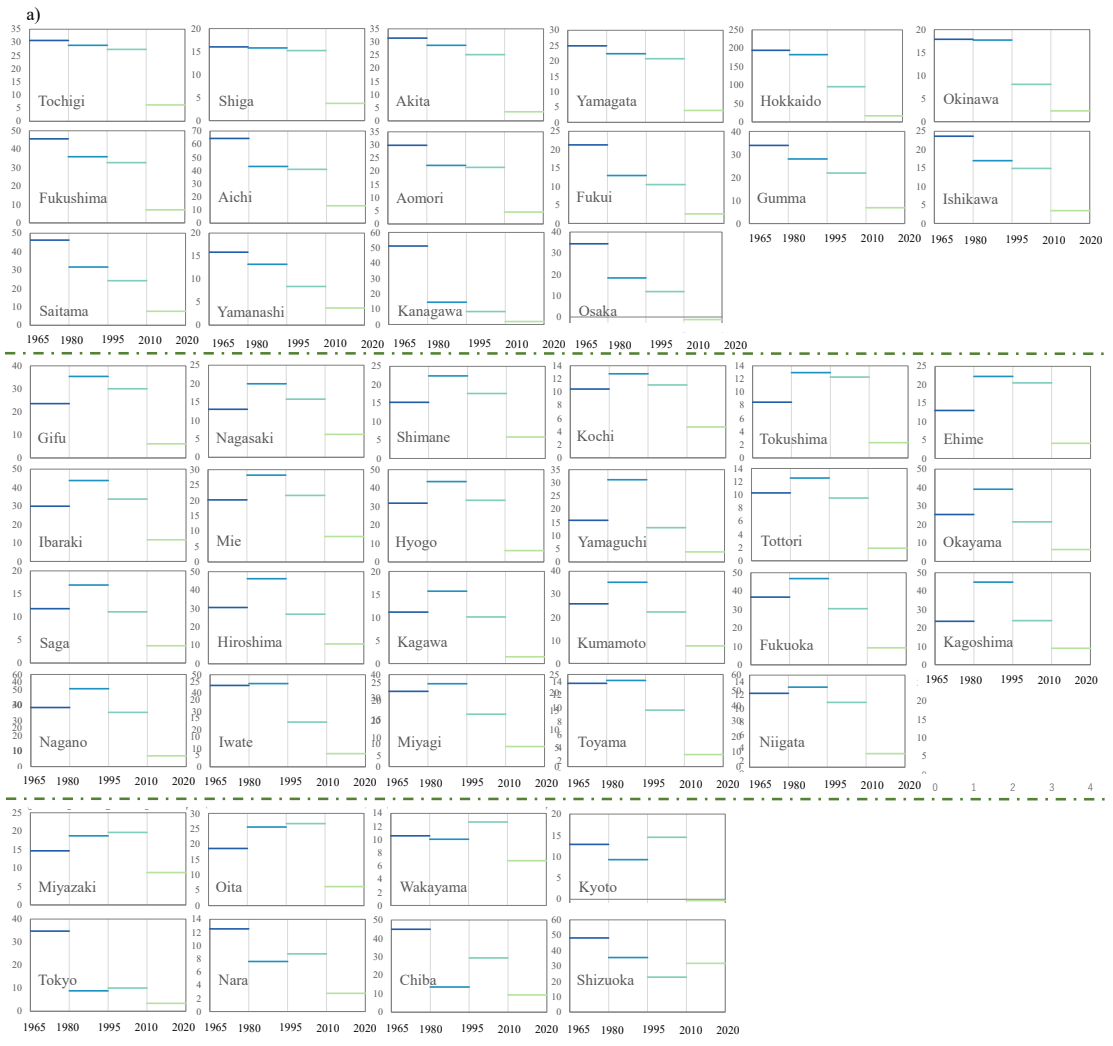


Fig. 16 The change in the percentage of each road material from 1965 to 2020

Fig. 17 presents the growth in road MS and the Average Annual Growth Rate (AAGR) for each prefecture across four periods (i.e., 1965-1980, 1980-1995, 1995-2010, and 2010-2020). While the growth varied regionally, the AAGR exhibited a consistent trend. Owing to its expansive area and ongoing road system development, Hokkaido demonstrated a notably higher road MS growth over the past few decades compared to other prefectures (Fig. 17a). It is noteworthy that, during 1965-1980, due to a lack of initial year data in Okinawa, the road MS in Okinawa in 1980 is presented instead of the increase from 1965 to 1980. In the first two periods (1965-1980 and 1980-1995), most prefectures experienced substantial growth. Conversely, in the last decade, Osaka and Kyoto even witnessed a decline in road MS by 1.21 and 0.32 Mt, respectively. In terms of AAGR, the majority of prefectures exhibited a gradual decrease over the four periods, particularly in the last decade, suggesting that the road MS is reaching saturation. The AAGR, initially ranging from 6% to 10% in the first fifteen years, dropped to 0.19% to about 1% in the last decade, except for Shizuoka, Osaka, and Kyoto. Shizuoka was the sole prefecture with an improved AAGR compared to 1995-2010, while Osaka and Kyoto recorded AAGRs of -0.13% and -0.06% over the last ten years, respectively.



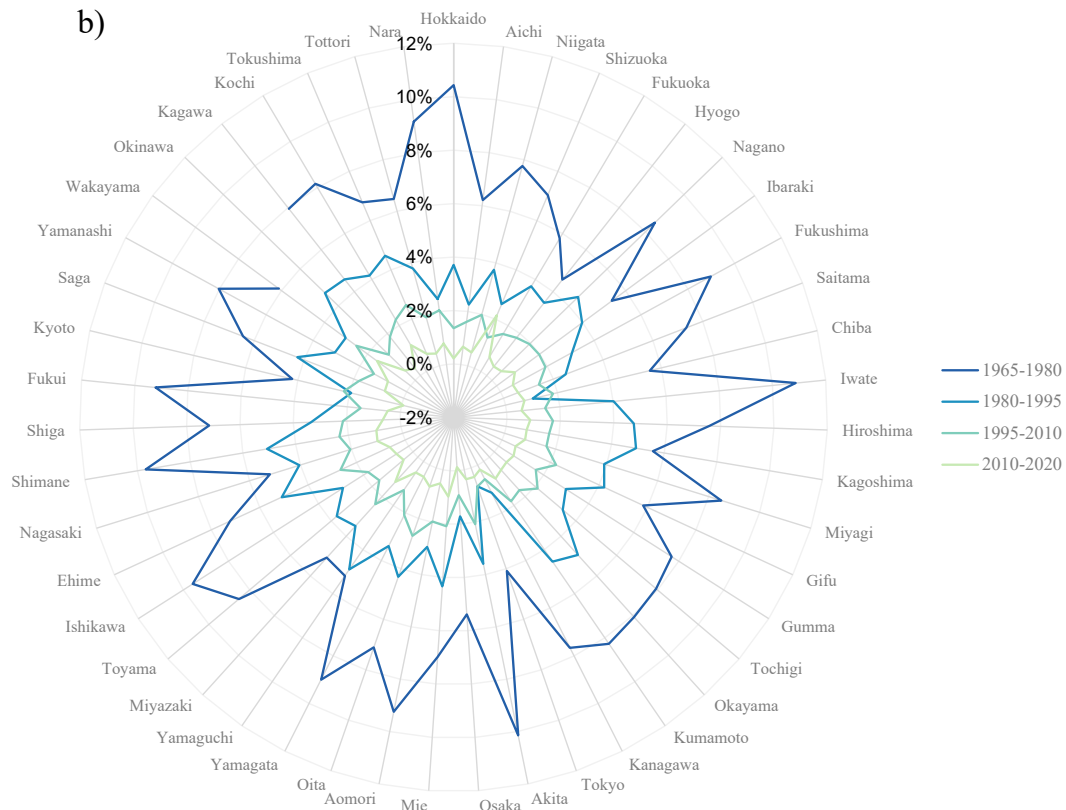


Fig. 17 Trends in road MS over the past half century: a) The amount of road MS growth for each prefecture (Unit: Mt); b) The average annual growth rate for each prefecture

#### 4.2.2 Spatiotemporal evolution and prefectural differences of road MS in Japan

Fig. 18 illustrates the evolution of total road MS for each prefecture in Japan in 1965, 1980, 1995, 2010, and 2020. Over 55 years, the total road MS in Japan increased by 5.5 times, rising from 758.39 Mt in 1965 to 4917.92 Mt in 2020, with significant growth observed in the eastern, central, and southern regions in each period. In 2020, Hokkaido prefecture contributed over 11% of the national total road MS, experiencing an 8.6-fold increase from 1965 to 2020. Aichi prefecture followed, comprising more than 4% of the country's total road MS in 2020, while the growth was much less compared to Hokkaido, with a growth of less than four times over 55 years. Nevertheless, the regions with substantial road MS did not necessarily exhibit the fastest growth. For instance, the road MS of Shimane prefecture soared from 5.07 Mt in 1965 to 66.18 Mt in 2020, an increase of 12 times, followed by a tenfold increase of Iwate prefecture, from 11.93 Mt in 1965 to 132.8 Mt in 2020. In contrast, Tokyo, Osaka,

and Kyoto showed more modest growth rates of 1.4, 2.2, and 2.4 times, respectively, over the past five decades, collectively accounting for 2%, 1.9%, and 1% of the national total road MS in 2020.

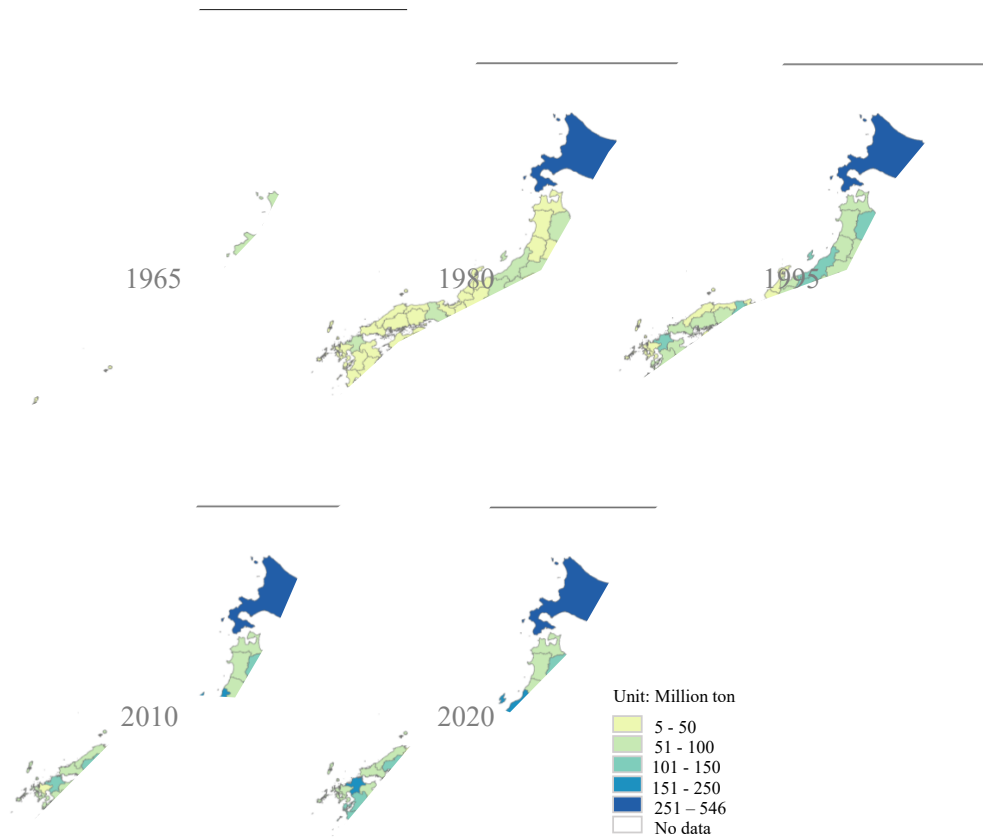


Fig. 18 The evolution of the total road MS in 1965, 1980, 1995, 2010, and 2020

#### 4.2.3 Projection of expected road MS by 2050

The model information and performance metrics of the ARIMAX-SVR and ARIMAX models for each prefecture, considering various combinations of explanatory variables are presented in Table 5. In Table 6, the model performance of MLR, SVR, ANN, and RF models is evaluated based on RMSE and MAE, considering all explanatory variables. Among these four models, both ANN and RF demonstrated superior performance when compared to MLR and SVR. However, only specific prefectures, such as Chiba and Aichi, exhibited significantly improved predictive performance compared to ARIMAX and ARIMAX-SVR models. Interestingly, the hybrid ARIMAX-SVR model did not outperform the ARIMAX model alone in many prefectures, as evidenced by the performance measures (RMSE and MAE) on the

testing dataset. This could be attributed to the possibility that the residuals did not contain enough non-linear patterns to be captured by the SVR model. This could be attributed to the fact that the residuals generated by the ARIMAX model had been too small and too close to zero for the SVR model to detect any significant non-linear patterns. Consequently, the model with better predictive accuracy, whether ARIMAX or the hybrid model, was selected for forecasting future road MS for each prefecture.

Table 5 The model information and performance of ARIMAX-SVR and ARIMAX alone for each prefecture

Prefectures	Four variables							Two variables						
	ARIMAX		ARIMAX		Hybrid ARIMAX-SVR		ARIMAX		ARIMAX		Hybrid ARIMAX-SVR			
	model ( $p,d,q$ )	Fitting accuracy	RMSE	MAE	RMSE	MAE	RMSE	MAE	model ( $p,d,q$ )	Fitting accuracy	RMSE	MAE	RMSE	MAE
Hokkaido	(1,2,0)	1.73	0.93	7.42	7.42	6.82	6.71	(1,1,2)	1.75	1.06	0.50	0.39	0.51	0.41
Aomori	(1,2,0)	0.29	0.14	0.91	0.89	0.95	0.92	(1,1,0)	0.30	0.14	0.35	0.28	0.37	0.31
Iwate	(1,2,1)	0.42	0.25	0.59	0.56	0.74	0.69	(1,1,1)	0.47	0.25	0.38	0.30	0.85	0.72
Miyagi	(1,2,1)	0.35	0.17	2.37	2.04	2.58	2.24	(1,1,0)	0.36	0.17	1.76	1.50	2.02	1.77
Akita	(1,2,0)	0.34	0.18	1.01	1.00	1.10	1.05	(1,1,1)	0.35	0.18	0.84	0.82	0.93	0.84
Yamagata	(1,2,0)	0.32	0.18	0.86	0.85	1.00	0.98	(1,1,1)	0.33	0.18	0.07	0.06	0.43	0.28
Fukushima	(1,2,0)	0.61	0.30	4.22	4.22	4.34	4.34	(1,1,0)	0.63	0.30	0.09	0.06	0.24	0.17
Ibaraki	(1,2,0)	0.53	0.21	0.40	0.35	0.50	0.43	(1,1,0)	0.53	0.24	0.17	0.15	0.32	0.26
Tochigi	(1,2,1)	0.41	0.25	0.80	0.71	0.79	0.66	(2,1,1)	0.42	0.26	0.68	0.59	0.63	0.54
Gumma	(0,2,1)	0.35	0.21	1.06	1.01	1.15	1.06	(0,2,3)	0.35	0.20	1.23	1.12	1.34	1.17
Saitama	(1,2,1)	0.49	0.33	0.70	0.49	0.76	0.56	(3,2,0)	0.54	0.24	1.48	1.28	1.42	1.22
Chiba	(1,2,0)	0.56	0.24	4.49	3.94	4.61	4.03	(0,2,3)	0.56	0.27	4.04	3.54	4.18	3.63
Tokyo	(1,2,1)	0.50	0.22	0.73	0.71	0.66	0.63	(0,2,3)	0.52	0.21	0.18	0.14	0.12	0.10
Kanagawa	(1,2,1)	0.40	0.16	1.27	1.19	1.28	1.20	(0,2,3)	0.40	0.16	1.18	1.09	1.18	1.08
Yamanashi	(1,2,0)	0.50	0.27	0.32	0.29	0.37	0.31	(2,1,2)	0.52	0.25	0.19	0.12	0.25	0.19
Niigata	(1,2,0)	0.27	0.13	0.14	0.12	0.29	0.23	(1,1,0)	0.27	0.15	0.09	0.08	0.24	0.20

Toyama	(1,2,0)	0.31	0.16	0.80	0.75	0.76	0.67	(1,2,1)	0.32	0.16	1.29	1.16	1.25	1.12
Ishikawa	(1,2,0)	0.29	0.14	0.42	0.41	0.46	0.46	(2,1,0)	0.29	0.15	0.11	0.10	0.25	0.19
Nagano	(1,2,1)	0.24	0.16	0.89	0.70	0.95	0.70	(1,1,1)	0.26	0.16	0.53	0.43	0.61	0.44
Fukui	(1,2,1)	0.38	0.24	3.05	3.03	3.23	3.17	(3,1,1)	0.39	0.23	1.38	1.32	1.70	1.55
Gifu	(2,2,0)	0.42	0.19	1.63	1.63	1.66	1.66	(1,1,0)	0.42	0.20	0.13	0.10	0.11	0.09
Shizuoka	(2,2,1)	3.01	1.21	3.01	2.50	3.55	3.08	(1,1,1)	3.11	1.27	4.91	4.47	3.82	3.27
Aichi	(2,2,3)	0.80	0.58	5.00	4.69	5.78	5.35	(2,2,3)	0.81	0.57	8.04	7.80	8.89	8.52
Mie	(1,2,0)	0.42	0.25	0.94	0.89	0.91	0.86	(2,1,3)	0.41	0.26	0.88	0.81	0.87	0.75
Shiga	(0,1,3)	0.26	0.18	1.22	1.20	1.11	1.06	(0,1,2)	0.31	0.23	0.29	0.27	0.52	0.45
Kyoto	(1,2,0)	0.20	0.10	0.93	0.83	0.89	0.80	(2,1,0)	0.20	0.11	0.88	0.78	0.88	0.77
Osaka	(3,2,2)	0.86	0.51	1.88	1.82	2.65	2.35	(1,1,0)	1.08	0.68	0.99	0.74	1.06	0.75
Nara	(1,2,0)	0.44	0.21	0.25	0.22	0.29	0.26	(1,2,0)	0.44	0.19	0.70	0.64	0.66	0.55
Wakayama	(3,2,1)	0.24	0.13	0.85	0.78	0.88	0.77	(1,1,2)	0.24	0.14	0.50	0.44	0.64	0.57
Hyogo	(1,2,1)	0.37	0.21	0.85	0.72	1.59	1.20	(1,1,1)	0.39	0.21	1.62	1.39	2.01	1.55
Tottori	(0,2,1)	0.10	0.04	0.19	0.17	0.23	0.19	(0,2,1)	0.10	0.04	0.26	0.22	0.31	0.26
Shimane	(2,2,0)	0.20	0.12	1.22	1.21	1.26	1.25	(2,1,1)	0.20	0.12	0.54	0.54	0.58	0.58
Okayama	(1,2,0)	0.45	0.22	0.95	0.79	1.05	0.83	(2,1,1)	0.46	0.22	1.22	1.11	1.21	1.05
Hiroshima	(1,2,2)	0.48	0.30	0.80	0.71	0.97	0.80	(1,1,1)	0.50	0.31	0.18	0.15	0.50	0.32
Yamaguchi	(1,2,0)	0.36	0.21	0.32	0.32	0.31	0.27	(0,2,2)	0.37	0.20	0.15	0.14	0.23	0.20
Tokushima	(0,2,1)	0.12	0.06	0.35	0.34	0.34	0.34	(2,1,2)	0.12	0.07	0.07	0.06	0.09	0.08
Kagawa	(0,2,1)	0.17	0.09	0.83	0.79	0.80	0.75	(2,1,0)	0.17	0.10	0.34	0.27	0.33	0.24
Ehime	(2,2,1)	0.21	0.13	0.43	0.34	0.57	0.44	(1,1,1)	0.21	0.13	0.42	0.34	0.38	0.34

Kochi	(2,2,1)	0.23	0.14	0.48	0.39	0.61	0.50	(2,1,1)	0.25	0.15	0.11	0.10	0.26	0.19
Fukuoka	(0,2,1)	0.44	0.26	0.60	0.59	0.56	0.53	(0,2,2)	0.44	0.25	0.64	0.63	0.76	0.75
Saga	(1,2,0)	0.23	0.11	0.40	0.39	0.36	0.34	(1,1,0)	0.23	0.12	0.49	0.49	0.52	0.50
Nagasaki	(0,2,1)	0.26	0.15	0.87	0.75	0.92	0.83	(2,1,0)	0.25	0.13	3.04	2.79	3.09	2.82
Kumamoto	(1,2,0)	0.26	0.12	1.61	1.49	1.69	1.55	(1,1,1)	0.26	0.13	1.09	0.98	1.15	1.05
Oita	(0,2,1)	0.22	0.11	0.83	0.81	0.78	0.74	(1,1,3)	0.19	0.12	0.12	0.10	0.21	0.19
Miyazaki	(1,1,0)	0.42	0.25	1.15	0.96	0.94	0.72	(2,1,1)	0.41	0.23	0.81	0.74	0.79	0.74
Kagoshima	(1,2,0)	0.50	0.28	1.60	1.46	1.67	1.54	(1,2,0)	0.52	0.25	4.87	4.47	4.89	4.49
Okinawa	(1,1,0)	0.53	0.31	1.81	1.63	1.89	1.76	(1,1,0)	0.28	0.12	0.06	0.05	0.06	0.05

Note: Four variables indicate population, gross regional product (GRP), passenger transportation, and cargo transportation; Two variables indicate population and GRP, which are widely considered to be the two main ultimate drivers for environmental impact.

Table 6 The model performance of MLR, SVR, ANN, and RF for each prefecture

Prefectures	MLR		SVR		ANN		RF	
	RMSE	MAE	RMSE	MAE	RMSE	MAE	RMSE	MAE
Hokkaido	14.86	12.5	14.95	12.61	6.39	5.34	8.36	6.55
Aomori	2.94	2.67	3.33	2.98	0.65	0.53	1.33	1.07
Iwate	2.12	1.68	2.15	1.66	1.16	0.97	2.29	1.78
Miyagi	3.58	2.99	3.67	2.99	2.33	1.90	1.55	1.27
Akita	1.60	1.24	1.57	1.20	0.8	0.67	1.44	1.10
Yamagata	1.61	1.41	1.80	1.48	0.73	0.61	1.24	0.96
Fukushima	2.72	2.40	2.79	2.30	1.98	1.71	3.31	2.38

Ibaraki	2.09	1.64	2.04	1.60	1.55	1.31	2.40	1.94
Tochigi	2.09	1.79	2.16	1.85	1.76	1.53	1.93	1.51
Gumma	1.41	1.14	1.48	1.23	1.11	0.95	1.81	1.41
Saitama	1.63	1.33	1.71	1.32	1.98	1.59	1.59	1.26
Chiba	3.42	3.00	3.78	3.24	2.87	2.37	1.34	1.09
Tokyo	2.71	2.29	3.86	3.00	1.24	0.98	1.31	0.98
Kanagawa	6.63	5.65	3.15	2.28	1.06	0.91	1.01	0.76
Yamanashi	5.11	4.45	5.35	4.60	1.84	1.50	2.91	2.26
Niigata	2.54	2.16	2.94	2.30	1.22	1.04	1.08	0.88
Toyama	3.96	3.25	4.29	3.26	1.65	1.38	1.07	0.85
Ishikawa	1.97	1.74	2.11	1.82	0.85	0.73	0.84	0.65
Nagano	0.78	0.63	0.77	0.62	0.71	0.58	1.20	0.89
Fukui	3.78	3.10	4.00	3.27	2.99	2.43	2.56	2.13
Gifu	2.85	2.36	3.19	2.43	2.30	1.90	1.78	1.49
Shizuoka	8.53	7.11	10.49	6.77	5.90	4.64	3.77	2.66
Aichi	2.22	1.84	2.52	1.98	2.05	1.71	2.20	1.77
Mie	2.17	1.81	2.49	1.86	2.23	1.87	1.89	1.42
Shiga	1.49	1.31	1.57	1.29	0.99	0.83	0.72	0.58
Kyoto	1.51	1.26	1.66	1.36	1.10	0.86	0.88	0.68
Osaka	1.23	0.97	1.24	0.96	1.37	1.13	1.41	1.10
Nara	3.29	2.66	3.36	2.71	2.47	2.04	2.14	1.72
Wakayama	1.86	1.46	1.89	1.48	0.64	0.55	0.70	0.56

Hyogo	0.98	0.86	1.04	0.86	0.62	0.50	0.66	0.54
Tottori	1.28	1.11	1.37	1.17	0.48	0.39	0.78	0.61
Shimane	2.82	2.34	2.87	2.01	0.80	0.65	0.89	0.73
Okayama	3.09	2.45	3.62	2.44	3.13	2.58	1.66	1.29
Hiroshima	5.65	4.89	6.68	5.15	3.79	3.14	2.31	1.81
Yamaguchi	1.66	1.36	1.67	1.36	1.05	0.88	1.23	0.93
Tokushima	1.08	0.89	1.14	0.90	0.56	0.47	0.57	0.46
Kagawa	1.40	1.20	1.61	1.24	0.92	0.77	0.65	0.52
Ehime	2.17	1.93	2.31	2.05	0.84	0.70	1.02	0.83
Kochi	1.02	0.92	1.13	0.97	0.59	0.49	0.78	0.63
Fukuoka	4.64	3.74	5.01	4.03	2.51	2.17	1.58	1.32
Saga	1.73	1.46	2.06	1.44	0.66	0.56	0.71	0.56
Nagasaki	1.72	1.41	1.91	1.42	0.70	0.58	0.91	0.73
Kumamoto	2.97	2.45	3.76	2.87	1.47	1.21	1.51	1.16
Oita	2.94	2.62	3.14	2.80	1.26	1.02	1.85	1.28
Miyazaki	2.67	2.29	2.91	2.49	1.16	0.96	0.95	0.76
Kagoshima	4.77	4.02	5.49	3.92	1.39	1.13	1.83	1.41
Okinawa	0.67	0.58	0.72	0.59	0.78	0.67	0.59	0.49

The prediction results for each prefecture under the five SSPs by 2050 were obtained using either the ARIMAX or ARIMAX-SVR model, incorporating explanatory variables such as population, GRP, and transportation data (passenger and cargo transportation). These results can be categorized into three patterns according to the growth pattern of expected road MS: 1) Starting to shrink, where MS reaches saturation and start to decline in subsequent years; 2) Staying stable or varying with scenarios, where expected road MS remains stable or exhibits dissimilarity across different SSPs; 3) Continuing to grow, where expected MS continues to increase until midcentury. Fig. 19 illustrates examples of expected road MS under each SSP scenario, with additional results for other prefectures provided in Appendix 3.

In most prefectures, SSP5 displayed the highest expected road MS, followed by SSP1, while SSP3 represented the scenario with the lowest expected MS. SSP2, as the "middle of the road" scenario, demonstrated a moderate MS value. However, conflicting results were observed in certain regions, such as Akita and Okayama, where SSP3 emerged as the most demanding scenario (Appendix 3). Despite Hokkaido having the highest road MS in Japan, the expected MS was projected to shrink in the coming years. In Aichi prefecture, expected MS increased in SSP5 but exhibited a decreasing trend in SSP3, showcasing variability across the five SSPs. Some prefectures displayed similar trends in all scenarios with insignificant differences, such as Nagano, where MS was generally stable in the following years (Appendix 3). Conversely, road MS projections for certain prefectures, including Shiga and Osaka, indicated a notable downward trend across each SSP scenario, suggesting an expected decrease in road usage in these areas given the existing road infrastructure.

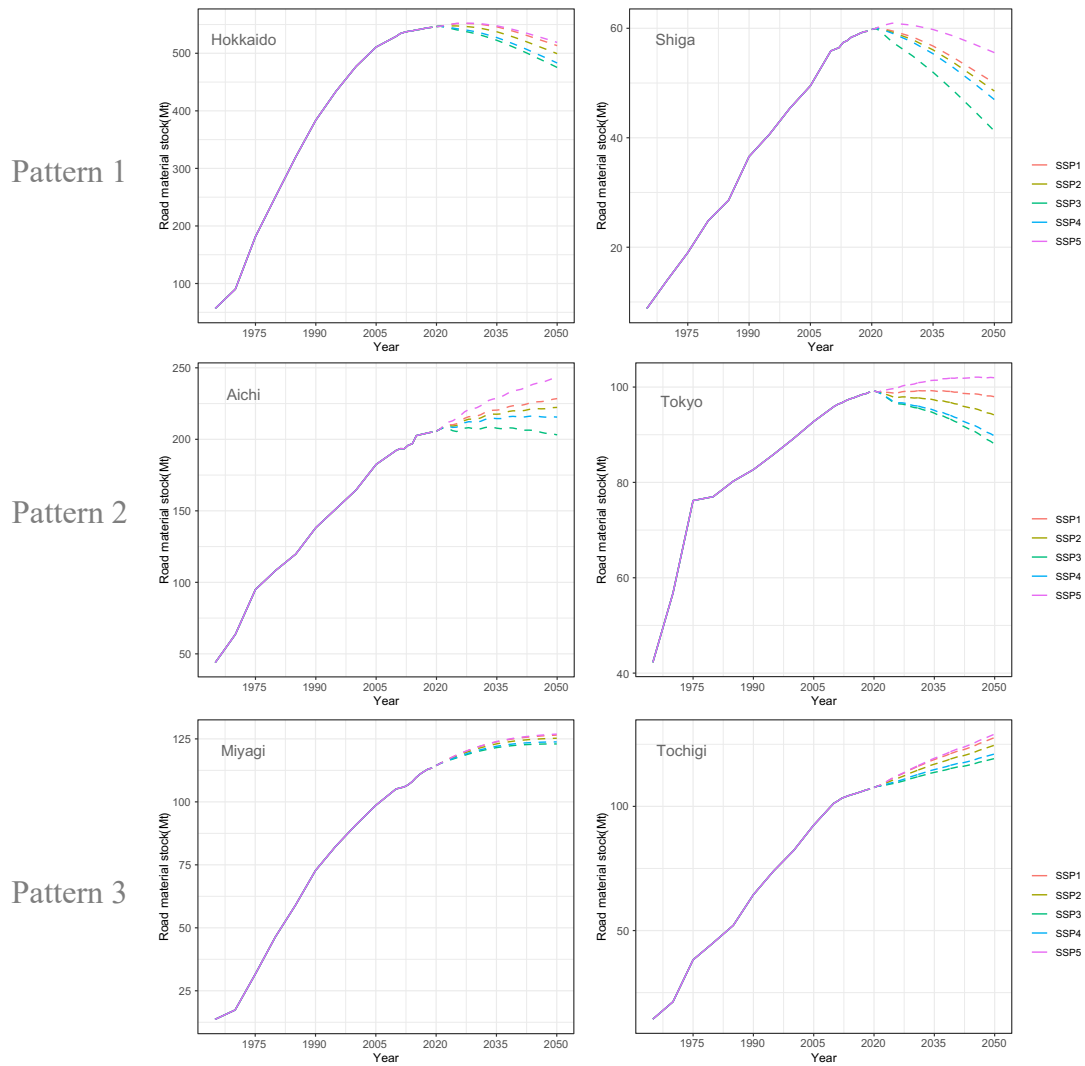


Fig. 19 Examples of expected road MS with five SSPs. Pattern 1: Starting to shrink; Pattern 2: Staying stable or varying with scenarios; Pattern 3: Continuing to grow

#### 4.2.4 Future regional differences in the magnitude of road MS discrepancies

To illustrate the anticipated future trends and regional differences in road MS for each prefecture under SSP1-5, Fig. 20 illustrates the disparities in road MS between the current state in 2020 and the projected state in 2050, providing insights into the road material composition and the magnitude of the discrepancies. The discrepancy in road MS was classified into five levels based on percentage differences: a difference within 10% is considered a slight fluctuation, an increase between 10% and 20% is categorized as moderate demand, and an increase of over 20% is deemed highly demanding. Conversely, a decrease in anticipated MS in 2050 compared to 2020 implies a reduction in road utilization, with a decrease of 10% to 20% considered a moderate reduction and a decrease of over 20% categorized as a severe reduction in utilization.

The most notable increase in road MS is observed in SSP5, where only Kyoto exhibits a severe reduction in road utilization, and Osaka shows a moderate reduction. For the remaining prefectures, projected road MS either shows slight fluctuations or further growth in the future. Conversely, SSP3 depicts the most significant decrease in road utilization, with 13 prefectures displaying a reduction trend, of which three exhibit a severe reduction in road utilization. Regarding the amount of the discrepancy and the material composition of road MS, aggregate emerges as the dominant material among the four road materials, followed by asphalt in most prefectures. However, in certain regions such as Yamanashi, Nagano, and Wakayama, the amount of concrete exhibits more variation than asphalt. This variation is primarily attributed to the relatively high proportion of concrete roads in the road types of these areas.

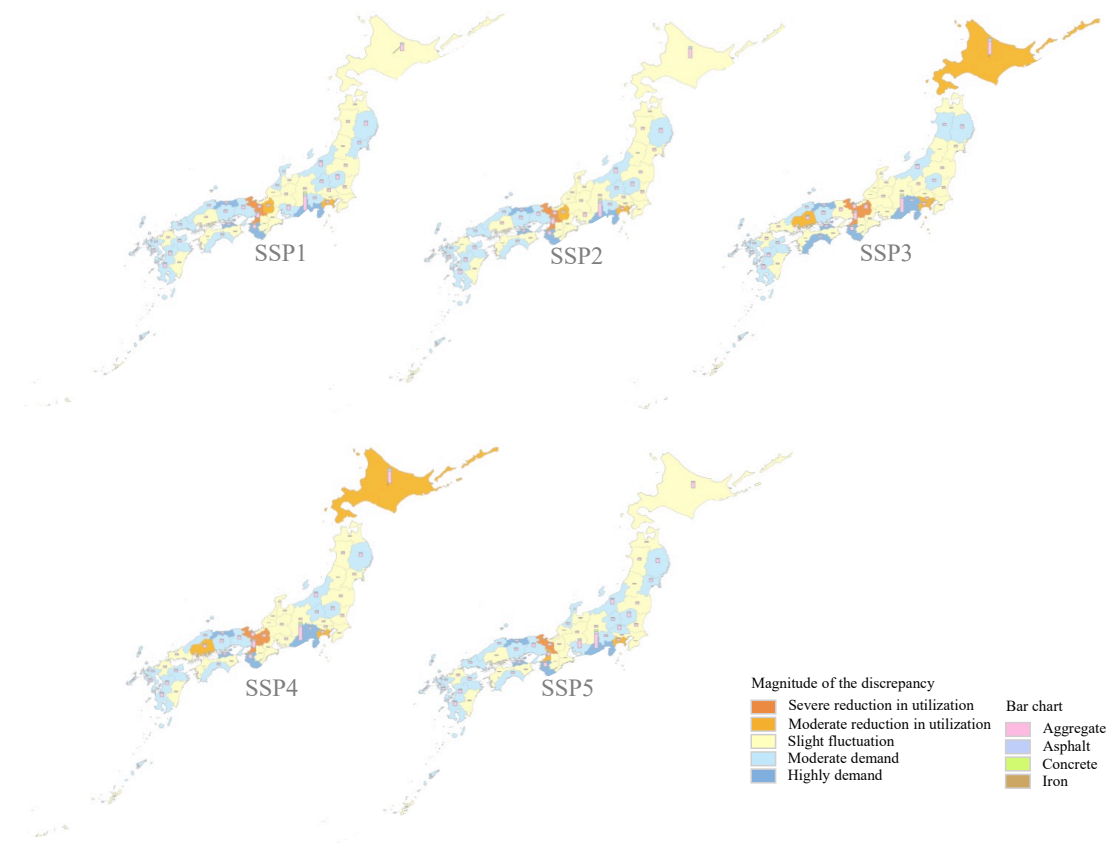


Fig. 20 Discrepancies in road material magnitude and composition between road MS in 2020 and projected road MS in 2050 under five SSPs

### 4.3 Discussion

#### 4.3.1 Identifying opportunities for material allocation under climate change

Based on the projected outcomes, the anticipated future road MS in most Japanese prefectures by 2050 continues to exhibit an upward trend compared to the current state,

as depicted in Fig. 20. This suggests a sustained demand for road materials. However, the expansion of road infrastructure comes with trade-offs, considering the evolving societal needs. Previous studies have underscored the contribution of transport infrastructure investment to economic growth (Hong et al., 2011; Sanchez and Albert, 2015; Yu et al., 2012), while simultaneously acknowledging the significant environmental impacts arising from material production in road construction and maintenance, including substantial carbon emissions (Yu et al., 2021). Moreover, given Japan's susceptibility to natural disasters and the increasing frequency of extreme weather events due to climate change, reinforcing the road network and incorporating disaster prevention features into existing facilities are crucial for ensuring the safety of aging infrastructure (MLIT, 2021).

Therefore, balancing the escalating demand for materials with environmental concerns and enhancing resilience to climate change is pivotal for developing adaptation measures in future scenarios. A potentially effective strategy involves improving resource efficiency, closely aligned with the 3R initiative (reduce, reuse, recycle) promoted by the Japanese government (ME, 2023). Policies and regulations have been implemented in Japan to manage construction waste effectively, including the establishment of waste management facilities and the mandate for waste reduction plans in construction projects. Additionally, the increased utilization of recycled materials, such as recycled asphalt, steel, and reclaimed aggregates, in road construction and maintenance emerges could be a remarkable option to minimize the need for new materials and minimize waste (dos Reis et al., 2021; Poulikakos et al., 2017). The quantification of current road MS performed in this study provides great significance in understanding potential of secondary materials that could be reused in the future. Furthermore, Japan has one of the world's most extensive public transportation systems, with an extensive network of trains, buses, and subways. Strategically harnessing public transportation resources and prioritizing future transportation requirements for public transit could represent a promising approach to mitigate the environmental impact of future road construction. Embracing technological innovation and cultivating green infrastructure are also adaptive strategies to enhance the resilience of road infrastructure against the impacts of climate change.

#### 4.3.2 Road infrastructure management in a highly urbanized and aging society

The projections for road MS in certain prefectures indicate significant downward

trends in some SSPs or even across all SSPs, as illustrated in Fig. 19. Given the prolonged lifespan of roads, this declining demand for MS may result in reduced road usage in these areas under existing infrastructure conditions. However, if zoom in on these regions, there is an uneven demand for road infrastructure within these regions. As road networks play a pivotal role in connecting people, facilitating goods and services movement, and influencing economic development and population distribution, they create opportunities for economic development while also encourage migration to urban centers to influence population distribution. Since the late 1990s, the population of non-metropolitan areas in Japan has been declining rapidly, largely due to the economic recession, and people from non-metropolitan areas have been moving to work in metropolitan areas (Lee et al., 2021). Increasing concentration of the population in metropolitan areas has led to increased traffic volume and demand for road infrastructure in these areas. Addressing this challenge necessitates improvements in road networks and transportation systems to prevent traffic congestion and longer commute times. The Japanese government has been gradually establishing policies to reduce the pressure on infrastructure in metropolitan areas. For instance, new regional development projects are being initiated in cities such as Tokyo, and evolving technologies such as intelligent transportation systems are being leveraged to address the issue (MLIT, 2021).

Despite the implementation of policies to alleviate infrastructure pressure in metropolitan areas, depopulation in non-metropolitan areas poses a potential reduction in local demand for road infrastructure. This may result in diminished road maintenance and development, potentially leading to increased safety risks and challenges in handling extreme weather conditions. Moreover, Japan's aging population, coupled with the younger demographic's tendency to migrate to urban areas, leaves the elderly as the primary residents in non-metropolitan areas, relying more on public transit than private vehicles. This dynamic may result in inefficient road use and increased emphasis on road safety. The inefficient road use and maintenance costs not justified by the demand level pose significant financial and labor challenges for policymakers. To address these challenges, local governments must engage in comprehensive transportation planning that considers evolving demographic and transportation needs, allocating resources accordingly to ensure safe and efficient transportation while optimizing road space usage.

## **5. Building MS dynamics: analyzing spatial patterns and forecasting future developments**

### 5.1 Study area

The three major metropolitan areas of Japan, namely the Greater Tokyo Area, the Kenki Metropolitan Area, and the Chukyo Metropolitan Area, represent pivotal hubs of economic, cultural, and political activity in the nation. More than half of the country's population lived in three major metropolitan areas in 2022 (Statistics Bureau of Japan, 2023). The designated areas are displayed in Fig. 21. These regions were designated due to their significant population densities, economic output, and strategic roles in both national and international contexts (MIC, 2013).

The Greater Tokyo Area, encompassing the Tokyo Metropolis along with the surrounding prefectures, stands as the preeminent urban and economic region of Japan. It is the most populous urban area in the country, with a population exceeding 36.8 million in 2022, accounting for 29.5% of Japan's total population (Statistics Bureau of Japan, 2023). This region is not only the center of Japan's economic activity, contributing significantly to the national GDP, but also a global hub for multinational corporations, financial institutions, and cutting-edge industries. In addition, the Kinki Metropolitan Area is located in the Kansai region of Japan. This area is a major economic hub with diversified industries, including manufacturing and pharmaceuticals. This metropolitan area has a combined population of approximately 18 million people in 2022, marking it as Japan's second-largest urban agglomeration (Statistics Bureau of Japan, 2023). The Chukyo Metropolitan Area, centered around Nagoya in Aichi Prefecture and extending into surrounding prefectures, boasts a population of 11 million in 2022, ranking as the third-largest metropolitan area in Japan (Statistics Bureau of Japan, 2023). This region is known for its robust industrial strength, and its strategic central location facilitates trade and connectivity within Japan and internationally.

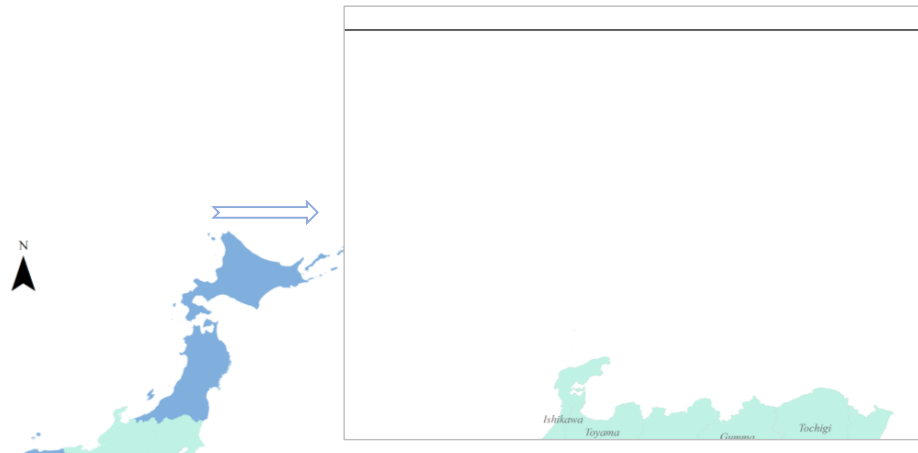


Fig. 21 Location of the three major metropolitan areas in Japan

## 5.2 Methodology

### 5.2.1 Estimation of historical spatial building MS

The estimation of historical spatial MS and its material composition of buildings in three metropolitan regions was conducted through a bottom-up methodology. This granular approach, which emphasizes the accumulation and analysis of individual data points to infer a comprehensive whole, is elaborately delineated in section 2.2.1. To create a detailed GIS database of construction MSs for study areas, data on the detailed locations and distributions of buildings is required. In this chapter, Zmap-TOWNII (2009, 2016, 2020) provided by Zenrin Co., Ltd. as the base data was utilized. Zmap-TOWNII is a residential map database, created by survey staff walking the areas. In urban areas, surveys are conducted annually, and in other districts, they are conducted every few years to update changes. Therefore, the more recent the data year, the more refined the shape of the building polygons in urban areas. By utilizing stored information such as the shape of polygons, number of floors, types of buildings, the MS for each building was calculated by multiplying the total floor area of each building and the amount of construction materials of per unit floor area (i.e., MI, material input per unit area) (Tanikawa et al., 2015; Tanikawa and Hashimoto, 2009). MS of buildings in study area in 2009, 2016, and 2020 was estimated.

### 5.2.2 Projection of serviceable building MS by 2050

To forecast the MS of buildings within the designated study area, the anticipated future spatial distribution of the population across three metropolitan areas was employed as a foundational reference, framed within five SSPs. Due to constraints in

data availability, mesh data consisting of 1 km × 1 km resolution grids detailing population distribution for the year 2015 and building floor area data for the year 2016 were utilized to establish a regression model within each mesh unit. A suite of regression techniques, including LR, polynomial regression (PR), RF, gradient boosting model (GBM), and SVR, were employed to capture the intricate relationship between population and building floor area within each mesh. LR, RF, and SVR were explained and conducted in the previous chapters. In addition to that, PR allows for capturing the non-linear relationship between variables, and can fit a wide range of data shapes, making it suitable for trend analysis and forecasting (Edwards, 2002; Ostertagová, 2012). GBM can handle complex and non-linear relationships between features and the target variable by combining multiple weak predictive models, typically decision trees, into a strong model. It is less prone to overfitting, especially with the use of regularization techniques and because it builds trees sequentially, each one correcting the errors of the previous (Bentéjac et al., 2021; Natekin and Knoll, 2013). The model demonstrating the best performance after validation processes, was subsequently adopted as the final predictive tool to forecast future building floor area under the five SSP scenarios. Given the challenges in projecting future building structure types, these five aforementioned predictive models were also leveraged to capture the intricate relationship between floor area and MS within each mesh. The model that emerged with the best fit was then used as the ultimate approach to project the MS of buildings in the future, based on the forecasted floor area under the five SSPs.

It is important to note that projections indicate a significant decline in Japan's future population, which logically infers a concomitant reduction in the demand for buildings. Nevertheless, considering the long lifespan typical of buildings, a substantial volume of existing structures is likely to become obsolete. Hence, the projected floor area, grounded on population trends, effectively represents the "functional space" - the quantum of building floor area that is not only utilized but also aligns with the needs of the residents. In the subsequent section, the projected floor area and MS of buildings were referred as "projected serviceable building floor area" and "projected MS of serviceable buildings," respectively. The term "serviceable building" is indicative of structures that are neither vacant nor obsolete, underscoring their utility and occupancy relevance in the future urban landscape.

### 5.2.3 Data sources

As previously mentioned, building data from the years 2009, 2016, and 2020 was acquired from Zenrin Co., Ltd (Zenrin Co., Ltd. 2023). Additionally, population distribution data for the year 2015 was sourced from ESRI Japan 2022 (ESRI Japan, 2022). Projections for future population distribution under the five SSPs were obtained from the A-PLAT platform (A-PLAT, 2023).

#### 5.2.4 Model fitting for relationship between floor area, population, and building MS

The performances of various regression models were evaluated through a common split of 80% for training and 20% for testing dataset, a methodological choice that aligns with standard practices in statistical model validation. The evaluation metrics employed were RMSE, and MAE and performance results of all models are presented in Table 7. For the regression predicting floor area from population, the GBM manifested superior predictive accuracy, evidenced by the lowest RMSE and MAE values, suggesting a robust capacity of this model in capturing the underlying patterns in the data. The SVR model exhibited closely comparable performance. In contrast, the LR model, while reasonable, lagged in predictive precision, as indicated by its higher metrics. For the regression predicting total MS from floor area, the PR and GBM demonstrated similar performance, with relatively high RMSE and MAE. The SVR model showed a relatively lower RMSE, indicating its potential robustness against large errors. Thus, GBM and SVR model were selected as the projection models for the future floor area and total MS of buildings under 5 SSPs until 2050 respectively.

Table 7 Performance results of LR, PR, RF, GBM, and SVR

	LR	PR	RF	GBM	SVR
	RMSE:	RMSE:	RMSE:	RMSE:	RMSE:
Floor area ~ Population	44795.87	34015.36	35671.89	32159.19	32366.98
	MAE:	MAE:	MAE:	MAE:	MAE:
	30440.27	20329.26	18924.76	17299.03	17380.96
	RMSE:	RMSE:	RMSE:	RMSE:	RMSE:
Total MS ~ Floor area	140695.9	166711.7	184446.6	163633.4	120043.8
	MAE:	MAE:	MAE:	MAE:	MAE:
	85612.84	51927.01	56515.14	51674.23	42750.6

### 5.3 Results

#### 5.3.1 Evolution and material composition of building MS

The spatial evolution and material composition of building MS in three metropolitan areas in Japan over a period spanning from 2009 to 2020 is displayed in Fig. 22. The vast majority of materials are concentrated in Japan's major urban agglomerations. From east to west, these include the Greater Tokyo Area, the Nagoya metropolitan area, and the Osaka-Kyoto-Kobe region. In the northern and central parts, several smaller MS distributions also visible, but the building MS is distributed in these areas at a lower density. A clear trend of increase is observable across all categories of materials. In 2009, the total building material stock was approximately 6.58 billion tons, with concrete being the predominant material, accounting for about 76% of the total. Gravel, steel, mortar, timber, and other materials constituted the remainder, with gravel at 8.6%, steel at 5.1%, mortar at 3.2%, timber at 3.2%, and other materials at 3.7%. By 2016, the total material stock had risen to nearly 6.95 billion tons. Concrete remained the most substantial component, though its proportion slightly decreased to around 75.9% of the total stock. The shares of other materials increased marginally. In 2020, the total building material stock further increased to approximately 7.07 billion tons. Concrete's share saw a minor decline to approximately 75.6%, whereas the shares of other materials showed a slight increase with gravel to 8.8%, steel to 5.1%. The data indicates a gradual but consistent growth in the overall building material stock, with a slight redistribution among the various material types. Despite minor fluctuations in the proportions of each material, concrete dominates the material composition through the years.

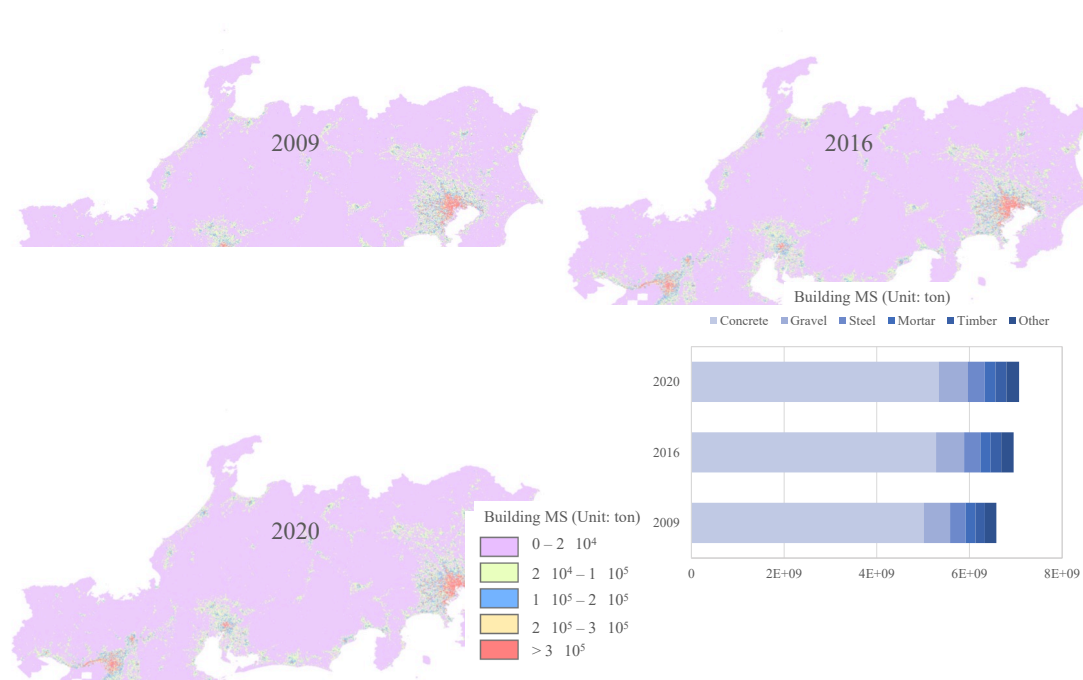


Fig. 22 The spatial evolution and material composition of building MS in three metropolitan areas in Japan in 2009, 2016, and 2020

### 5.3.2 Projections of floor area and MS of serviceable buildings under five SSPs

The projections for floor area and MS of serviceable buildings in three metropolitan areas in Japan, under five SSPs until the year 2050 is presented in Fig. 23. SSP1 to SSP5 each encapsulate distinct narratives on how socioeconomic factors might evolve over time. The trend across all SSPs shows a decline in serviceable building floor area, with SSP1 starting at approximately 3.71 billion m<sup>2</sup> in 2025 and diminishing steadily to about 3.33 billion m<sup>2</sup> by 2050. Similarly, SSP2 through SSP5 all indicate a gradual reduction, aligning with the anticipated decrease in Japan's future population and the consequent reduction in demand for buildings providing services, potentially leading to an increase in vacant properties. This contraction mirrors trends in MS, which in SSP1, for instance, is projected to fall from around 5.73 billion tons in 2025 to approximately 5.25 billion tons in 2050. The overarching implication of these projections suggests an impending surplus in built environment capacity relative to the population's needs, which could result in a significant number of unoccupied buildings, considering the long lifespan of such structures. These results underscore the need for strategic urban planning, including the repurposing or deconstruction of existing

buildings to align with the demographic shifts anticipated in the coming decades.

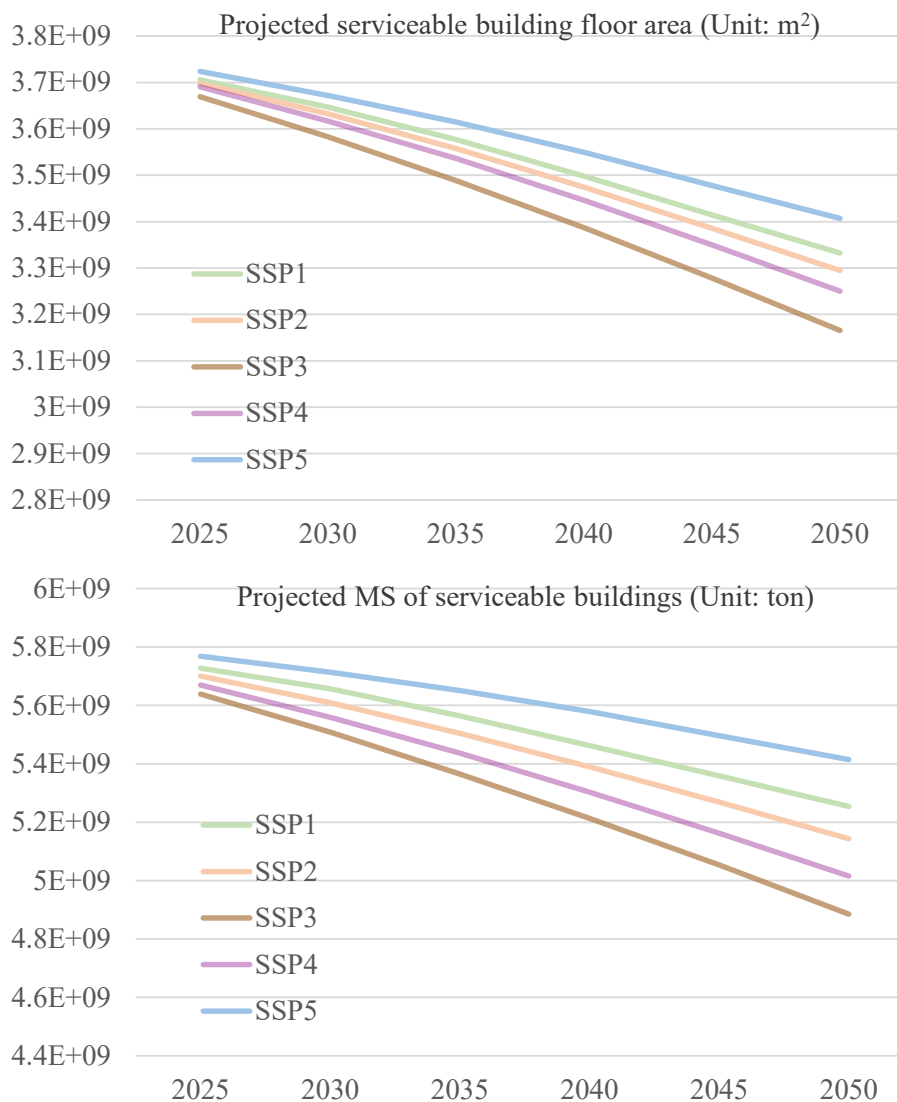


Fig. 23 The projections for serviceable building floor area and MS of serviceable buildings under five SSPs until the year 2050

#### 5.4 Discussions

Japan is experiencing a significant decrease in population. This trend is particularly evident in rural areas, where a decrease in population has led to a lower demand for serviceable buildings, thus an increase in vacant house (Kubo and Yui, 2020). In contrast, metropolitan areas are witnessing an increase in built areas due to the influx of population. The ongoing expansion in urban centers and metropolitan cities necessitates continuous material inputs for new construction. This conflicting phenomenon creates unique challenges in managing building resources.

In the context of future population decline, vacant house issue raises concerns

regarding the management of these structures and the associated demolish waste. This rise in vacant properties necessitates efficient management strategies for demolition waste to mitigate environmental impacts. A key strategy in this regard is the shift towards circular material use (Gillott et al., 2023). This approach involves recycling or repurposing materials from demolished buildings, thereby reducing the need for new material production and minimizing construction waste. The concept of urban mining emerges as a pivotal opportunity in this scenario. This involves the extraction of valuable materials from vacant buildings for reuse or recycling, reducing the demand for new building materials and minimizing construction waste. This practice significantly reduces the demand for new building materials, offering a sustainable solution to resource management (Peng et al., 2021). The implementation of urban mining not only provides environmental benefits but also holds the potential to stimulate local economies. It can create new industries focused on the recycling and repurposing of building materials, thereby contributing to economic growth and sustainability in the face of demographic changes.

On the other hand, the ongoing expansion of urban centers and metropolitan areas in Japan necessitates a continuous input of materials. Construction is a carbon intensive process stemming both from the production of building materials and their transportation to construction sites (You et al., 2011; Zhang, Y. et al., 2019). To mitigate these environmental impacts, innovative and sustainable approaches are essential. One effective strategy is the utilization of secondary materials in new construction. These materials, sourced from recycled demolition waste, not only help in reducing waste accumulation but also play a crucial role in curbing carbon emissions associated with the production of new building materials. The use of secondary materials effectively closes the loop in the building materials lifecycle, contributing to a more sustainable construction industry (Peng et al., 2021). Another approach is the renovation of existing structures. Renovating buildings can significantly reduce the demand for new construction materials and decrease the volume of construction waste generated. Moreover, renovating buildings to enhance their energy efficiency is a critical step towards reducing operational carbon emissions. This approach not only can mitigate the environmental impacts of its urban expansion while promoting sustainable urban development.

## **6. Urban infrastructure evolution: identifying driving mechanisms and assessing**

## **land use changes**

### 6.1 Methodology

#### 6.1.1 Models for LULCC simulation

There are two primary types of models for future land use simulation and prediction: spatial causal models and discrete dynamic models (Gao et al., 2022). Spatial causal models, such as the CLUE-S, predicts the future land use based on the cause-effect relationships between various factors and land use changes but doesn't fully capture the underlying processes (Verburg et al., 2002). In contrast, discrete dynamic models, notably cellular automata (CA), is adept at simulating the complex self-organizing behavior of land use by accounting for inter-patch interactions, with the foundational concept being the extraction of land-use transition rules to determine the probability of land type occurrences within each cellular unit (Tobler, 1979).

For CA-based models, two main strategies are employed for deducing transformation rules: transition analysis strategy (TAS) and pattern analysis strategy (PAS). Models that utilize TAS, such as logistic-CA and ANN-CA, analyze land use changes between two time periods but can become complex as the variety of land uses increases (Arsanjani et al., 2013; Munshi et al., 2014; Yang et al., 2016; Zeshan et al., 2021). PAS-based models, such as CA-Markov and future land use simulation (FLUS) model, use land use data from a single period to predict future land use, which simplifies calculations but may not capture specific transition rules or the dynamic nature of land-use changes (Hamad et al., 2018; Lin et al., 2020; Liu et al., 2017; Sang et al., 2011). An emergent model, known as PLUS model, proposed by Liang et al. (2021), was applied in this research for future land use simulation. PLUS model merges the strengths and resolves the limitations of both TAS and PAS, and offers an innovative approach to mining land use transition rules based on data from two periods. This CA-based model employs a strategy that generates multiple types of patches, making it more suitable for simulating actual landscapes. Moreover, PLUS can dynamically simulate the interactions between various driving factors and land use compositions. This capability is essential for understanding the complex interplay of factors that contribute to land use changes. PLUS model has been applied to various scenarios, such as urban land use simulations (Koko et al., 2023), habitat quality prediction (Zhao et al., 2022), ecological risk projection (Zhang, S. et al., 2022), and ecological service value simulation (Li et al., 2021).

### 6.1.2 Land use change simulation with PLUS model

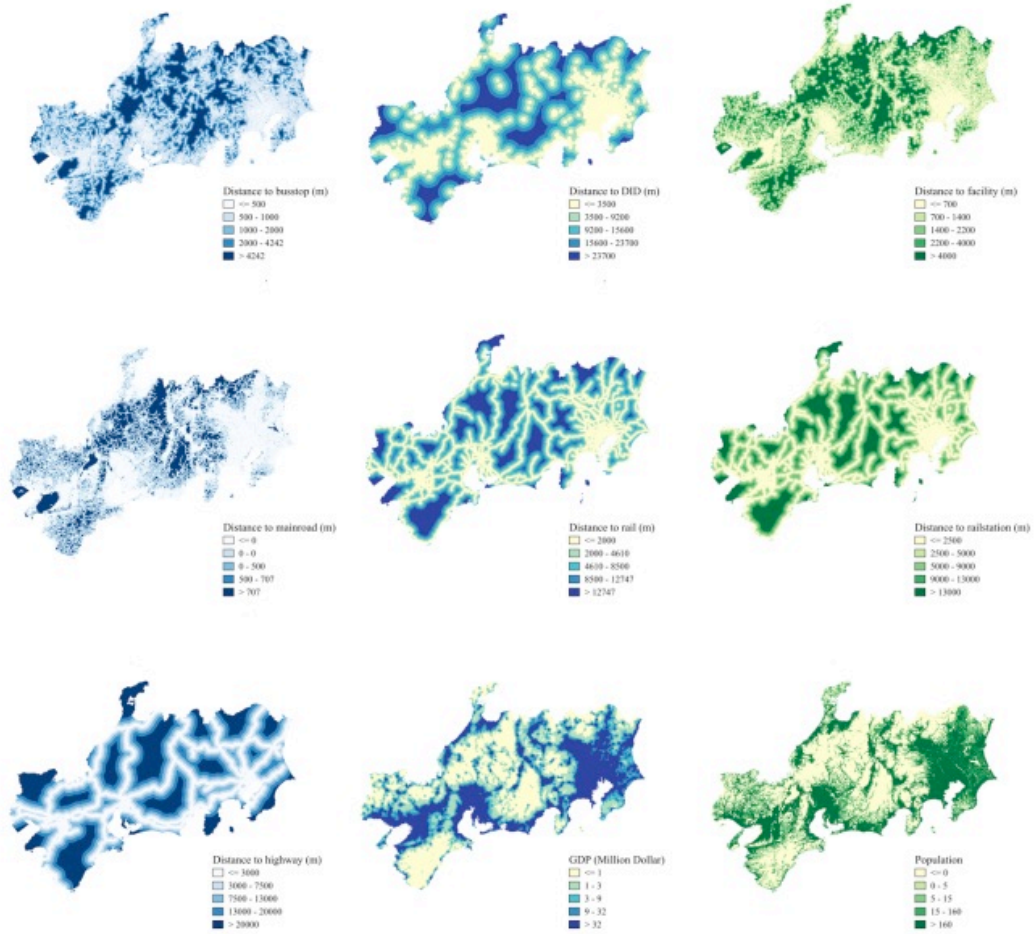
The PLUS model was utilized to simulate the evolution of land use types. PLUS model mainly consists of two parts: (1) a rule mining framework based on the land expansion analysis strategy (LEAS), which investigates potential transition rules using two land use datasets from 2009 and 2021. This transition analysis strategy involves selecting random sampling points according to the changing land use, and the RF classification (RFC) algorithm is employed to assess the interrelationships between land use compositions and several driving factors, ultimately deriving the transition rules for land use composition (Yao et al., 2017). In this research, 13 driving factors were chosen to calculate the occurrence probability of each land use type (Fig. 24), encompassing socio-economic factors as well as climatic and environmental factors. 10% of the cell units was used with uniform sampling method for training and the number of regression trees is set to 500 in this research. (2) the application of a CA-based multiple random seeds (CARS), to project land use dynamics. The CARS module is a CA model that creates land use patches using random seeds of multiple types. The CA model is a land use simulation model that is driven by scenarios and combines global land use demands with local land use competition effects (Liang et al., 2021). Open water bodies were designated as spatial constraints. The neighborhood effects were quantified using a 3×3 Moore neighborhood.

Markov chain and LR models were used to simulate future land use demands. The Markov-chain method, with its probabilistic nature, is adept at handling the inherent uncertainties in land use change predictions. It effectively captures the temporal dynamics of land use transitions, essential for short- to medium-term forecasting. The method's simplicity, coupled with its ability to capture complex temporal land use change processes, makes it a popular choice. Conversely, LR offers a quantitative framework for understanding the relationships between various driving factors, such as economic, demographic, and environmental variables, and land use changes. This method's strength lies in its data-driven insights, which are grounded in historical data and observed trends, thereby enhancing the model's predictive capabilities. Moreover, the flexibility and adaptability of linear regression models allow for continuous refinement and adjustment as more data becomes available.

Since in land use forecasting, the Markov chain model calculates the land use transition probabilities based on data from two input time points and then uses these

transition probabilities to predict future land use conditions. Therefore, Markov chain models are usually used to forecast future states over the same time intervals (Han et al., 2015). Hence, this research used the predicted land use demand results for the year 2049 as the results for 2050. This study used the changes in the total area of each land use type from 2009 to 2021 to represent the neighborhood weights of the corresponding land use types from 2021 to 2050 (Zhang, S. et al., 2022). For specific parameters setting and the simulation process, see (Liang et al., 2021).

Socioeconomic factors:



Climatic and environmental factors:

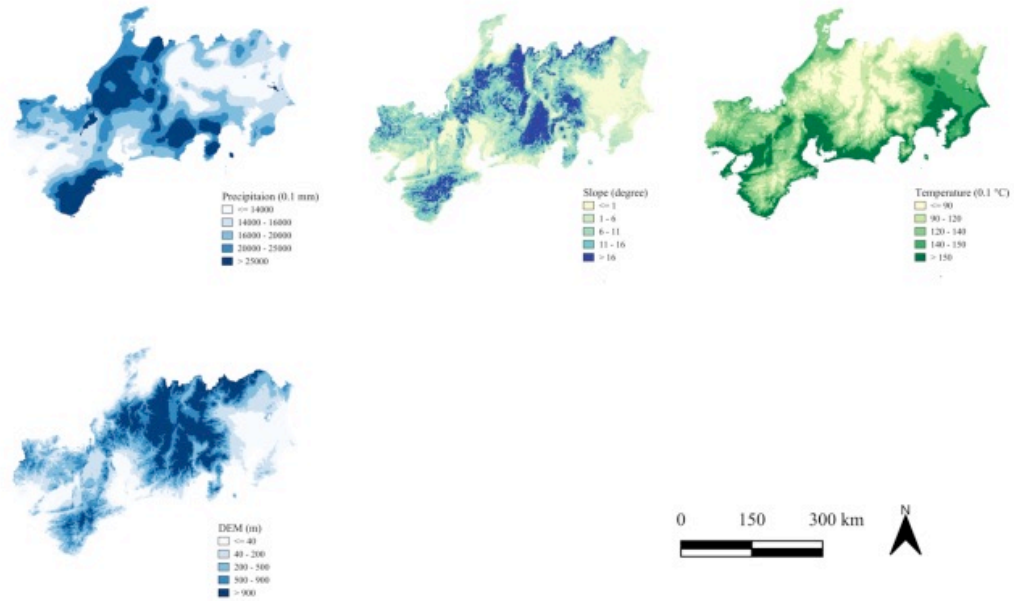


Fig. 24 Driving factors

### 6.1.3 Data sources

Land use data for the study area of the years 2009, 2014, 2016, and 2021 was obtained from the Ministry of Land, Infrastructure, Transport and Tourism of Japan, featuring a resolution of 100 meters (MLIT, 2023b). This dataset categorizes land use within each 100 m mesh, designating various types such as paddy fields, agricultural land, forests, wastelands, building areas, main transportation lands, lakes, rivers, etc. For drive factors, among socioeconomic factors, GDP distribution data were obtained from (Chen et al., 2022). The other spatial distribution data of drive factors such as public facility, bus stop, railway, etc. were obtained from the Ministry of Land, Infrastructure, Transport and Tourism of Japan (MLIT, 2023b) The patterns of distance were calculated by Euclidean distance analysis with ArcGIS software. Data of climatic and environmental factors were derived from the Ministry of Land, Infrastructure, Transport and Tourism of Japan (MLIT, 2023b).

The land use data underwent a process of spatial aggregation using ArcGIS software, transforming the resolution from 100 m to 500 m. During this transformation, the land use types were reclassified into seven categories: forest, water area, cropland, road, construction area, other land, and wasteland. The reclassification, along with the original land use type classification and definitions, is thoroughly detailed in Table 8.

Table 8 Land use type and code

Code	Land use type	Definition	Reclassification code	Reclassification land use type
0100	Cropland	Paddy field, dry field, swamp field, lotus field, and other fields classified as 'cropland'.	3	Cropland
0200	Other agricultural land	Land for cultivating wheat, rice, vegetables, grasslands, turf, apples, pears, peaches, grapes, tea, paulownia, wax tree, paper mulberry, and palm tree.	3	
0300	-	-	-	-
0400	-	-	-	-
0500	Forest	Areas densely with perennial plants.	1	Forest
0600	Wasteland	Lands identified as wasteland, cliffs, rocks,	7	Wasteland

		perennial snow, wetlands, mining areas, etc., based on former land use data.		
0700	Building site	Residential areas, urban areas, etc., where buildings are densely situated.	5	Construction area
0800	-	-	-	-
0901	Road	Roads and such, captured as areas.	4	Road
0902	Railway	Railways, marshalling yards, etc., captured as areas.	4	
1000	Other	Athletic stadiums, airports, racecourses, baseball fields, schools, port districts, vacant land in artificially reclaimed areas, etc.	6	Other
1100	River and lake	Man-made lakes, natural lakes, ponds, fish farms, etc., which always hold water at normal water levels, and riverbeds in river areas.	2	Water area
1200	-	-	-	-
1300	-	-	-	-
1400	Seashore	Beach areas consisting of sand, gravel, and rocks.	2	Water area
1500	Marine area	Hidden rocks, mudflats, sea passes are also included in the sea area.	2	
1600	Golf course	The boundaries of a golf course are the outer edges of the fairways and roughs and the border with the forest.	6	Other

#### 6.1.4 Validation of PLUS model

The Kappa coefficient was used in this research to measure the accuracy of PLUS model. The Kappa coefficient is a widely used statistical measure in land use change model validation and quantifies the degree of accuracy and reliability in a classification system, particularly in the context of comparing observed (actual) data to predicted (modeled) data. In the context of land use change models, the Kappa coefficient helps in assessing how well the model has predicted land use changes when compared to

actual observed changes. The equation for the Kappa coefficient ( $K$ ) is:

$$K = \frac{P_o - P_e}{1 - P_e} \quad (12)$$

where  $P_o$  is the observed agreement ratio, which is the proportion of instances where the model's predictions and the actual observations agree.  $p_e$  is the expected agreement ratio, which is the proportion of instances where agreement could be expected by random chance.

The value of  $K$  ranges from -1 to 1. A value of 1 indicates perfect agreement between the model predictions and the actual data. A value of 0 indicates that the strength of agreement is poor. Negative values suggest a disagreement between predictions and observations. Value ranges from 0.61 to 0.80 indicates a substantial level of agreement. This suggests that the model is quite reliable in its predictions, with a significant proportion of its classifications aligning well with the observed reality. Value ranges from 0.81 to 1.00 indicates an almost perfect level of agreement. It reflects a very high level of precision in the model's classification ability, indicating that the model is effective in capturing and reproducing the patterns and relationships present in the observed data. In this research, the  $K$  of PLUS model is 0.82 and the overall accuracy is 0.90, indicating that the model's predictions are highly accurate and closely match the actual observed data. The detailed information is showed in Table 9.

Table 9 Validation results of the PLUS model

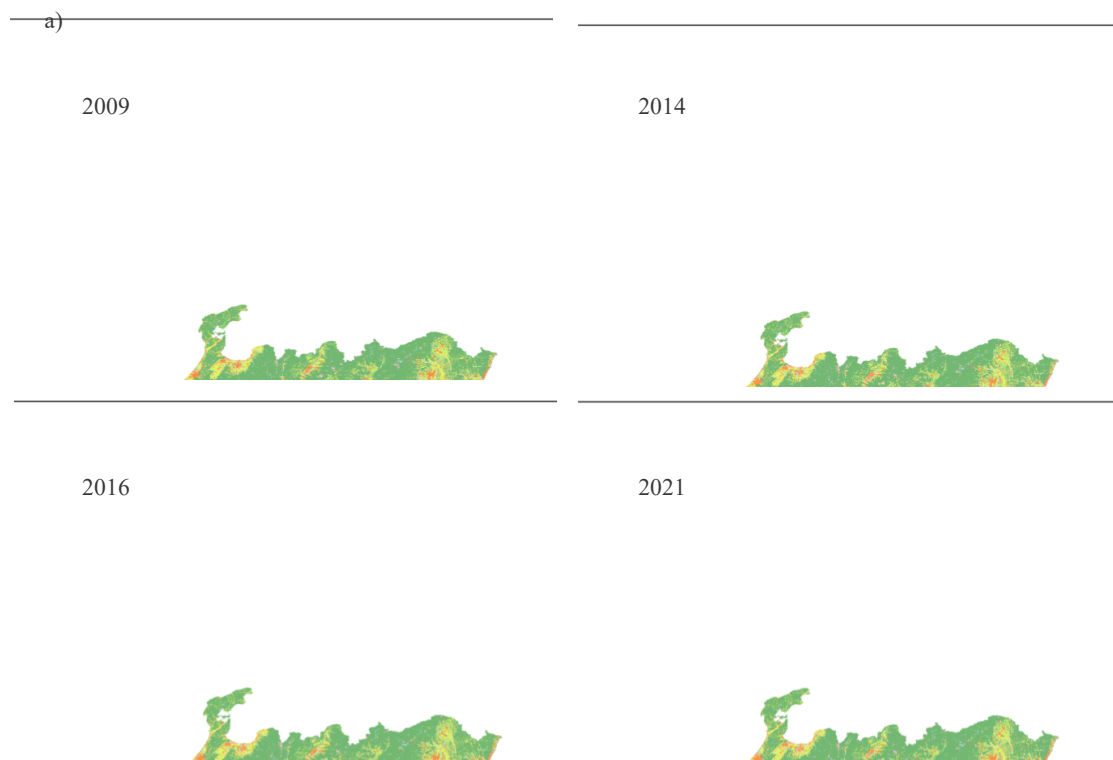
	Commission Error	Omission Error	Producer's Accuracy	User's Accuracy
Forest	0.05	0.05	0.95	0.95
Water area	0.05	0.11	0.89	0.95
Cropland	0.18	0.18	0.82	0.82
Road	0.76	0.77	0.23	0.24
Construction area	0.12	0.13	0.87	0.88
Other land	0.40	0.38	0.62	0.60
Wasteland	0.42	0.41	0.59	0.58

## 6.2 Results

### 6.2.1 Evolution of historical land use change

The evolution of land use types for the years 2009, 2014, 2016, and 2021 across

three metropolitan areas in Japan is depicted in Fig. 25 a), with area shifts in the land use spaces shown in Fig. 25 b). The expansion of urban areas, as indicated by the red tones, appears in the peripheries of urban centers, where the encroachment into natural landscapes is more pronounced. The area shifts of historical land use data for three metropolitan areas demonstrate a complex interplay between urban expansion and the preservation of natural and agricultural landscapes, with the former exhibiting a steady increase at the potential expense of cropland, underscoring the challenges of sustainable urban planning. In 2009, construction areas representing urban development decreased. This is consistent with Tanikawa et al. (2015)'s finding that Japan's building MS peaked in 2005-2008 and declined slightly thereafter. Interestingly, forested areas showed a decrease at first, but gradually began to recover. Cropland saw a significant decrease. Other land use categories such as water, other, and wasteland displayed minor variances. The road infrastructure increased from 264.5 km<sup>2</sup> to 991.75 km<sup>2</sup>, signifying improved transportation networks, potentially to support the urban growth.



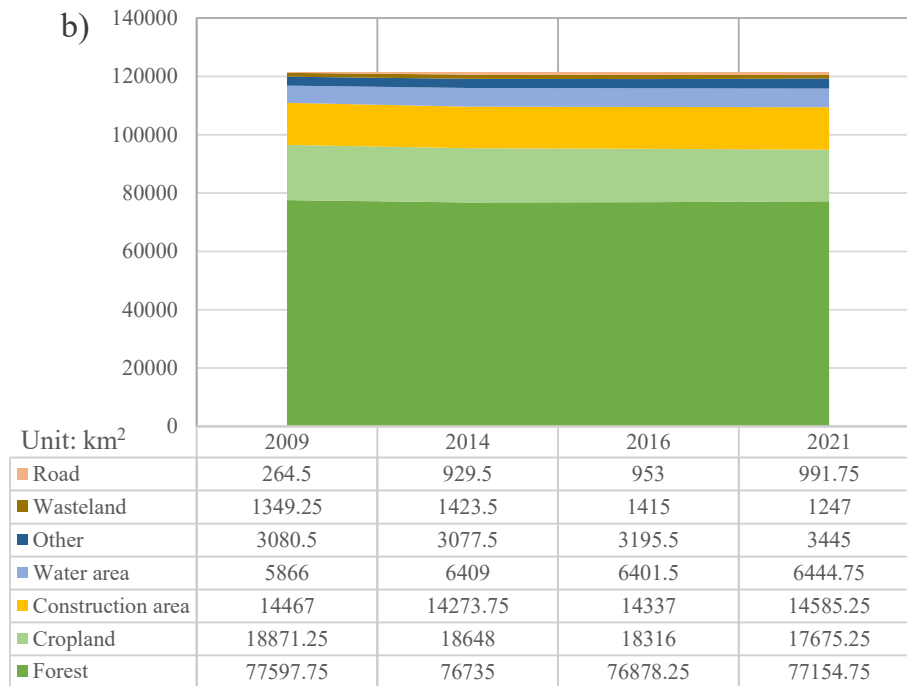


Fig. 25 Historical land use changes: a) The spatial evolution of land use types; b) Area shifts in the land use types

### 6.2.2 Identification of drive factor importance in three metropolitan areas of Japan

Understanding the contribution of driving factors to the expansion of each type of land use is crucial for supporting the development of effective and sustainable land management strategies. The contributions of various driving factors to the expansion of different land use types through RFC are illustrated in Fig. 26, with driving factors arranging in order of contribution for each land use type. The expansions of construction area and wasteland were notably contributed by population, highlighting the role of demographic distribution in urban development. Forest areas are mostly influenced by slope, which aligns with the understanding that forests are often found in steeper, less accessible regions. Road expansions are considerably influenced by their proximity to existing rail networks, which may reflect planning strategies that favor connectivity. Expansion of other land type was contributed a lot with precipitation, underlining the importance of climatic factors in their distribution.

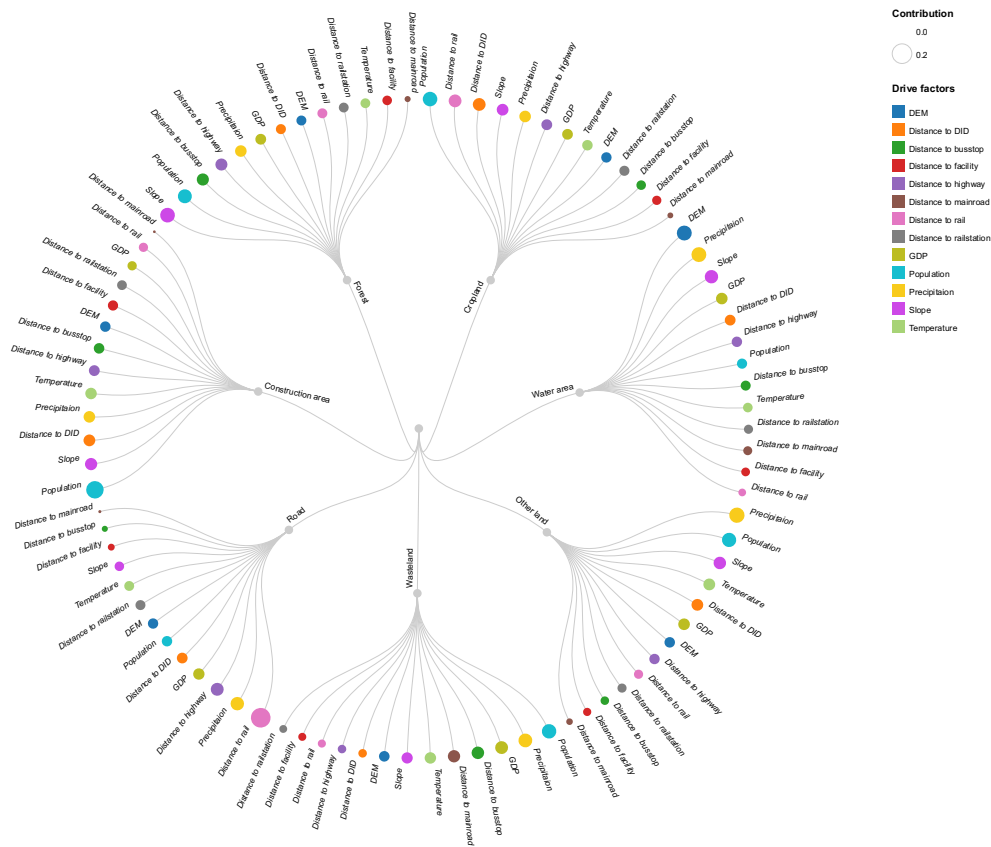


Fig. 26 Contributions of driving factors to the expansion of different land use types through RFC

### 6.2.3 Estimating future land use demands

The future land use demand was predicted by Markov chain and LR model, and the projected trends from these two models are displayed in Fig. 27. According to the LR model, there is a gradual and consistent decrease in cropland and wasteland areas over time, with cropland decreasing from 69600 cells (with resolution of 500m×500m) in 2022 to 54637 cells in 2050, and wasteland from 4768 to 1839 cells in the same period, suggesting a progressive conversion of these land types into other categories. Conversely, forest, water area, road, construction area, and 'other' land categories are projected to increase with LR model. The forest area is expected to grow modestly yet steadily, while construction area and road area show a notable increase from 56024 to 60974 cells and from 4034 to 4983 cells, reflecting ongoing urbanization trends.

On the other hand, projection results of Markov chain model indicate a similar downward trend for cropland, from 70701 cells in 2021 to 58656 cells by 2050, and a decline in wasteland from 4988 to 3932 cells over the same period. Markov chain model also suggests growth in forest area, which aligns with the LR model's predictions. Both

models predict an increase in the construction area, with the Markov chain model projecting a more pronounced growth from 58341 to 62303 cells by 2050, compared to the LR model. Roads also exhibit an upward trend in both models, with the LR model projecting an increase to 4983 cells by 2050 and the Markov chain suggesting a rise to 4748 cells by 2050.

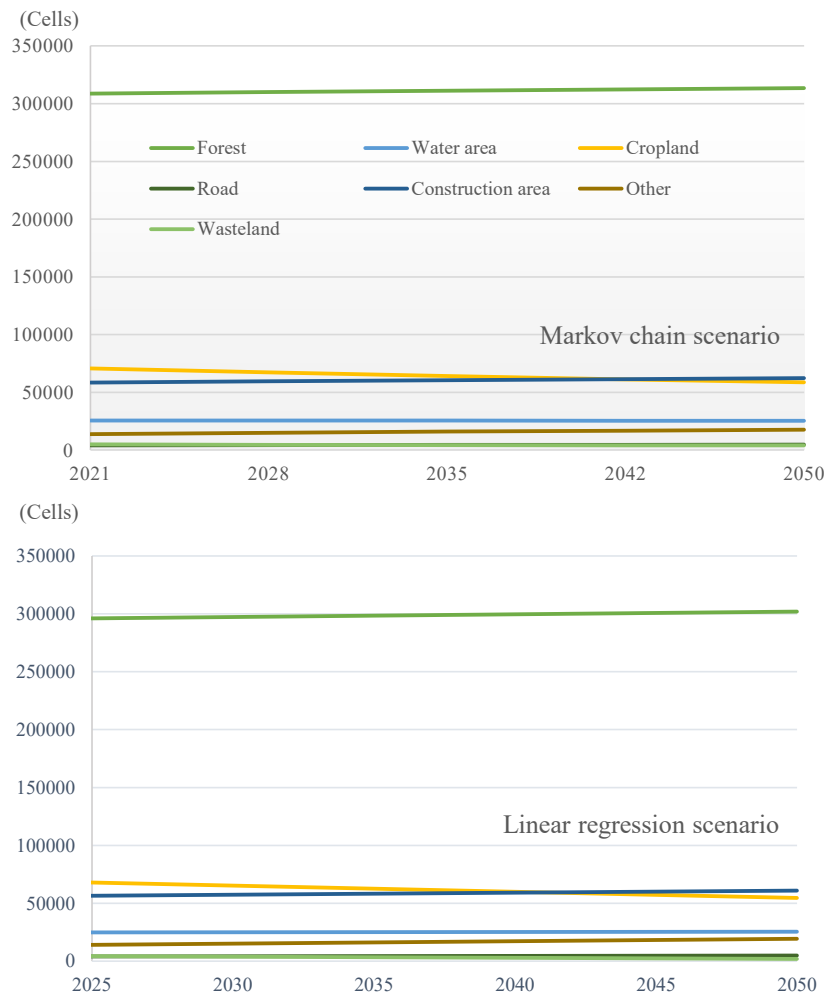


Fig. 27 Prediction of the future land use demand by Markov chain and LR models  
6.2.4 Future land use projection in 2050

After the training process of RFC in LEAS part, the development potential of each land use type on each cell was predicted by applying obtained RFCs. Finally, the PLUS model outputs seven development potential maps which will be used to simulate the future land use in CARS module. The development potential map of each land use type is presented in Fig. 28.

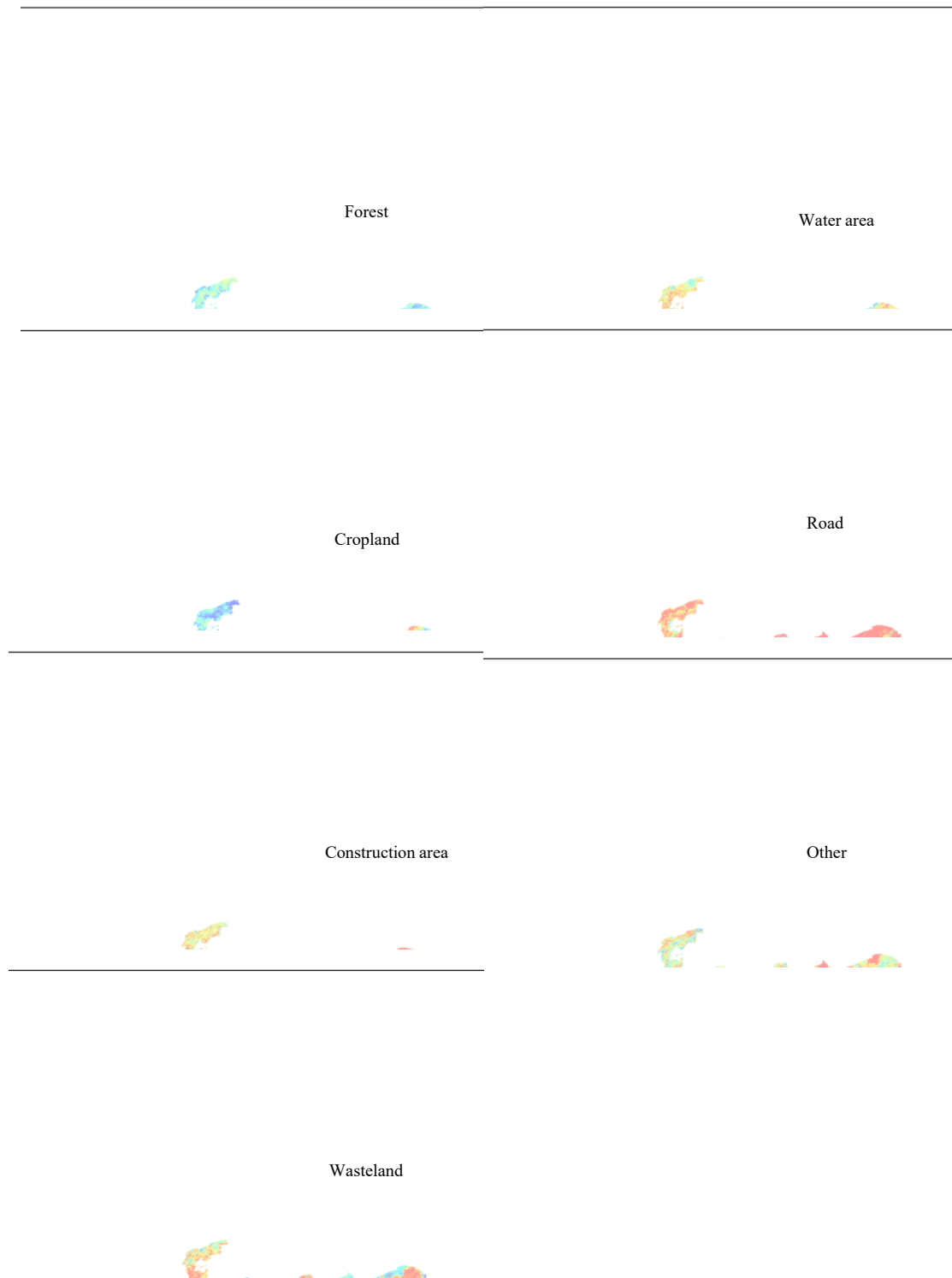


Fig. 28 The development potential maps of seven land use types

The land use simulation results for the year 2050 based on Markov chain and LR scenarios are illustrated in Fig. 29. It is important to note that the final area of each land use category will be close to, but not necessarily equal to, the land use demand. This discrepancy is because the land use area is determined not only by the "top-down" land use demand but also by the "bottom-up" local geographic conditions. The final land use

area is a result of the interplay between these top-down and bottom-up influences. Despite slight differences in specific land category projections, a notable difference observed is that the distribution of wasteland is more concentrated in the LR scenario. Both models clearly indicate ongoing urban expansion and a reduction in cropland and wasteland areas, reflecting trends of urbanization and consequences of population decline.

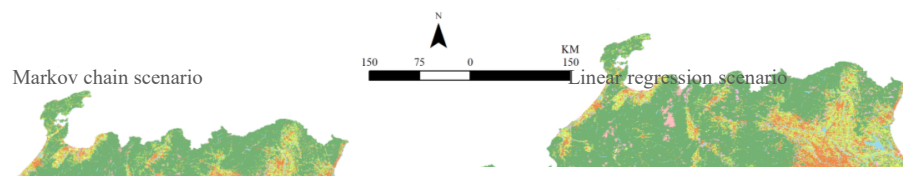


Fig. 29 Future land use simulation under Markov chain and LR scenarios

### 6.3 Discussion

This chapter employed a LULCC model to simulate the evolving landscape of three metropolitan areas in Japan to the year 2050. The simulation results indicate an increase in roads and construction areas, parallel with a decline in cropland and an increase in forest cover. This trend aligns with the broader demographic shifts in Japan, characterized by a decreasing population and an urban migration trend among the younger population (Iwasaki, 2021). These demographic changes have profound impacts on land use. As the living standards continue to improve in the future, there is a potential rise of demand for green infrastructure and public green areas in urban settings. The increasing population density in urban areas not only leads to increased demand for urban infrastructure but also emphasizes the necessity for expanding public facilities such as green spaces and parks. This expansion is not only essential for enhancing urban livability but also aligns with the goals of sustainable development, necessitating future land use simulation studies to measure these aspects accurately and comprehensively. As urban areas evolve, the material composition and usage in public infrastructure such as parks, recreational areas, and green spaces also become increasingly significant. Therefore, a comprehensive evaluation of MS in public

facilities in the future work will provide a more holistic view of urban sustainability, enabling the creation of urban spaces that are not only green and livable but also resource-efficient and environmentally responsible. On the other hand, the depopulation of rural areas, particularly the outflow of younger people, contributes to the decline in agricultural activities, as evident in the decreasing cropland. This phenomenon potentially leads to underutilized rural landscapes, which may gradually transition into forested areas, either through natural succession or reforestation initiatives (Tsunoda and Enari, 2020).

The expansion of green areas, such as forests, is beneficial for ecology such as the increased carbon absorption and sequestration, as forests act as carbon sinks, absorbing CO<sub>2</sub> from the atmosphere, which is a crucial process in mitigating climate change (Nunes et al., 2020). However, the increasing built-up areas, particularly roads and construction, are associated with higher carbon emissions through the whole life cycle of urban infrastructure (Huo et al., 2020; Zhang, Y. et al., 2019), thus presenting a challenging trade-off in urban planning and environmental sustainability. While urban expansion continues to accommodate the shifting population, it is imperative to take adaptation measures which integrates urban development with environmental conservation such as incorporating green infrastructure, promoting urban green spaces that not only enhance urban livability but also contribute to carbon absorption (Liao et al., 2020). Moreover, sustainable urban design, including energy-efficient buildings and eco-friendly transportation systems, can also mitigate the carbon footprint of urban expansion.

## **7 Conclusions**

### **7.1 Summary of the findings**

This research identifies how various building attributes influence MI and investigates the spatiotemporal evolution and patterns of MS within buildings and road networks. Future MS of anticipated road and serviceable buildings under Japanese SSPs is projected. A LULCC model is employed to explore and simulate the spatiotemporal changes in various land use types, encompassing roadways and construction area.

The MI plays a crucial role in the field of IE, particularly in the accounting of MS. MI, essentially a measure of the amount of material used per unit of construction, is a key indicator for understanding the material demand and environmental impact of

infrastructure projects. To explore the impacts of building attributes on building's MI, a raw MI database with Chinese building samples was utilized. This was done to measure the importance of four building attributes using an innovative RF methodology. The importance of each variable was normalized to establish an overarching hierarchy of MI. The influence of each building attribute on MI was examined through partial dependence. Findings revealed that building structure and construction periods hold greater importance compared to use type and region for buildings in China. PD plots uncover the disparity of MI between structures, construction periods, utilization purpose, and regions. Subsequently, a full hierarchical MI dataset of six selected building materials were predicted by the RF model. This hierarchical MI dataset allows researchers to choose and adjust complete RF-based MIs according to the building feature(s) available in their physical quantity data.

As another major component of infrastructure, road networks have profound impacts on economic growth, social dynamics, and environmental sustainability. Thus, a comprehensive approach involving material flow analysis and MS analysis was utilized to delve into the historical evolution and development patterns of Japan's road network from 1965 to 2020. Results indicated that over 55 years, the total road MS in Japan increased by 5.5 times, rising from 758.39 Mt in 1965 to 4917.92 Mt in 2020, with significant growth observed in the eastern, central, and southern regions in each period. This MS growth was primarily dominated by the aggregate of four key materials constituting the road MS. Through a detailed examination of the road MS time series data, the study projected the anticipated road MS in each Japanese prefecture by the year 2050. This projection was based on national SSPs of Japan and included a range of explanatory variables such as population dynamics, economic indicators, passenger and cargo transportation. To achieve this, an array of forecasting models including ARIMAX, ARIMAX-SVR, MLR, SVR, ANN, and RF were compared and analyzed for their effectiveness. The projections of expected road MS under the five SSPs by 2050 revealed diverse trends across prefectures. Some regions exhibited varying trends depending on the SSP scenario, while others demonstrated more consistent patterns of increase or decrease.

Next, this study selected Japan's three major metropolitan areas as a research region to gain a spatial understanding of the evolution and distribution patterns of building MS. Within these areas, the study analyzed the evolution of building MS and

the composition of MS materials. Findings indicated a gradual growth in the overall building material stock, with a slight redistribution among the various material types. Additionally, floor area and MS of serviceable buildings up to 2050 under the SSPs in Japan were forecasted, considering the scenario of a significant population decrease. The trends across all SSPs showed a decline in both serviceable building floor area and MS.

Subsequently, this research explored the underlying mechanisms driving infrastructure development by analyzing the contributions of various driving factors within three metropolitan areas. Furthermore, this research conducted an analysis of the historical changes in land use types within these areas, followed by a projection of the future distribution and changes of different land use types using PLUS model by 2050. RFC approach was employed to identify and quantify the contribution of various driving factors behind the expansion of each land use type. Both scenarios clearly indicated ongoing urban expansion and a reduction in cropland and wasteland areas, reflecting trends of urbanization and consequences of population decline in three metropolitan areas of Japan.

## 7.2 Research implications

Infrastructure has historically served as the essential framework for human societies, forging a vital and unbreakable connection between socioeconomic progress, social welfare, and the built environment. Analyzing the spatiotemporal evolution and patterns of infrastructure's MS, we can identify opportunities for material recycling and reuse, thus providing insights for minimizing the carbon footprint of infrastructure development while ensuring its efficiency and resilience. MI is a key indicator in accounting the MS of infrastructure using bottom-up approach. However, the process of acquiring accurate MI data and relevant building information poses a substantial challenge in this domain. Gathering detailed and precise data about the materials used in construction requires comprehensive and often complex data collection methods. This difficulty is compounded in regions with a rich history of construction, where buildings may have been constructed over various periods and with differing techniques and materials. Moreover, the lack of standardized methods for collecting and reporting such data further complicates the process. Consequently, researchers and practitioners in the field often face hurdles in obtaining reliable and consistent MI data, which is essential for accurate material stock accounting and subsequent ecological analysis.

Given these complexities, there is a growing need for systematic approaches to harmonize MI categorization across different regions and develop robust methodologies for the collection and analysis of MI data. Addressing these challenges is critical for advancing the field of IE, particularly in improving the accuracy of material stock accounting and enhancing our understanding of the environmental implications of built environments. This research provides a valuable insight into identifying the most influential factors for MI of buildings. The RF-based hierarchical MI dataset enables researchers to select and adjust MIs based on the available hierarchical physical inventory, therefore not only contributing to the development of China's future built environment stock studies, but also enhancing the comparability of MI research across different regions. Furthermore, the establishment of a hierarchical MI is of great importance for comprehending the potential of urban mining. It plays a key role in advancing societal goals such as the circular economy and urban sustainability.

By closely examining the historical and forecasted MS, the study identifies areas where the demand for road infrastructure is likely to continue and regions where it may decline, potentially due to factors such as demographic shifts. This nuanced understanding is pivotal for a comprehensive assessment of the future evolution of road MS across Japan's diverse prefectures. Such insights are invaluable for guiding resource allocation and shaping policy decisions in the realm of road infrastructure management. This approach not only contributes to a more informed planning process but also aids in the strategic development of road infrastructure that aligns with future societal and economic needs.

Combining the analysis of MS in buildings with land use change dynamics. By forecasting the future needs for serviceable buildings and understanding the evolving patterns of land use, the study provides insights into urban development and infrastructure planning. This is particularly relevant in the context of Japan's expected demographic shifts, as it helps in strategizing resource allocation and urban planning to accommodate future societal needs. Furthermore, the identification of key drivers behind land use changes through RFC offers a nuanced understanding of urban expansion and its environmental impacts. This knowledge is crucial for developing sustainable urban development strategies, particularly in the context of promoting a circular economy and reducing the ecological footprint of urban growth.

### 7.3 Limitations of research and future work

Although this research provides insights into advancing goals such as circular economy and urban sustainable development, there are still some limitations. The first is from the aspect of data availability. MIs are influenced by multiple variables such as local construction preferences, regulations, climate, historical and economic factors, and urban and rural locations, which may influence MI but were not included in this study due to data limitations. Therefore, more variables should be considered as further data is collected. A more extensive collection of representative data and granular data also needs to be carried out in the future. Furthermore, although RF model is known for its robustness and versatility, like any algorithm, it has its limitations. Its 'black box' nature, especially when handling a large number of trees, limits the interpretability of the model's decision-making process. While Random Forest can manage a substantial number of features, its performance may not be optimal in cases of extremely high-dimensional data, leading to a more complex model that demands significant computational resources. Additionally, there is a risk of overfitting in noisy datasets if the model is not properly tuned, and the algorithm shows inherent bias in calculating variable importance, favoring variables with more categories or those that are continuous over binary variables.

Moreover, the timely updating of data is important. For instance, the population distribution data used in this study for both current and future projections are based on 2015 estimates. However, due to various factors, the actual population changes may diverge from these past projections, potentially impacting the accuracy of simulation results that rely on this input data. Therefore, it becomes crucial to regularly update and revise the data in accordance with realistic developments to ensure the reliability and relevance of the study's outcomes.

In addition, while this research employed the PLUS model to simulate future land use types, it primarily focused on the driving mechanisms behind the expansion of land use types. For future work, it is essential to integrate scenarios based on comprehensive urban planning knowledge and social demands. This integration would provide a more holistic understanding of land use dynamics, factoring in not only the statistical and probabilistic aspects of land use change but also the practical implications of urban planning policies and societal trends. Such an approach would allow for a more nuanced interpretation of how future land use changes align with, or diverge from, planned urban

development trajectories and social needs. This is particularly relevant in the context of a country like Japan, where demographic shifts are reshaping urban landscapes. Incorporating these aspects into land use simulations would enhance the practical relevance of forecasts, providing valuable insights for sustainable urban development.

At last, the impact of several uncertain factors such as the COVID-19 pandemic, the rise of shared services, and the development of autonomous driving technologies were not considered in this research. For instance, the COVID-19 pandemic has caused significant changes in travel patterns. The rise of telework and virtual meetings might permanently reshape business travel and private vehicle usage, with the degree of these changes influencing long-term transportation and road demand. This issue is closely linked to another limitation: the precision of projections is heavily reliant on the quality and accessibility of input data. To address this, it's crucial to conduct future research that utilizes additional data sources and encourages collaboration with experts across various fields, including economy, transportation, and environment. Incorporating a broader range of factors, such as technological progress and more dynamic socioeconomic data, could enhance the accuracy of forecasts.

## Acknowledgements

First and foremost, I would like to extend my deepest and most sincere gratitude to Professor Hiroki Tanikawa, my supervisor, who offered me the priceless opportunity to be a part of this wonderful laboratory. Prof. Tanikawa guided me through the realm of material flow and stock and industrial ecology and supervised my PhD work. Beyond the academic sphere, Prof. Tanikawa provided me boundless support and encouragement throughout my three years in Japan, making this chapter of my academic and personal life truly joyful and memorable.

I also want to express my deep gratitude to those who have supported me along this journey. Jing Guo, during my doctoral studies, provided me with countless guidance and assistance in my research, all while being a cherished friend. The days spent together in Nagoya were the most vibrant and memorable moments of my early days in Japan. Naho Yamashita, not only offer valuable research assistance as a teacher, but your presence as a friend also brought a sense of relaxation and joy to my time in the lab.

I am deeply grateful to every member of this lab. Interacting with all of you has consistently brought a genuine sense of joy. The encounters with each of you have enriched my life, making it more colorful and fulfilling. I am also very thankful to the other teachers in the lab for providing research guidance and help to our students. Big thanks to Marie Hatada for consistently providing us with the most timely and effective assistance. Your support has contributed significantly to the positive atmosphere within the lab.

I extend my deep gratitude to my parents, who have consistently provided unconditional support, and to my friends in China who have always been a source of encouragement to me. Despite the geographical separation, our hearts remain intimately connected. A special thanks to Yanni, Enya, and HOYO-MiX; your music has accompanied me through countless quiet nights, always giving comfort to my spirit and peace to my mind. Finally, I would like to express my appreciation to the China Scholarship Council of the Ministry of Education for the financial support provided during my time in Japan.

## Figure list

Fig. 1 Three phases of MS analysis in the evolutionary process .....	13
Fig. 2 Size and composition of building samples .....	23
Fig. 3 Computation test of the number of trees ( <i>ntree</i> ).....	26
Fig. 4 The overall framework of building MI analysis using RF model .....	29
Fig. 5 Correlation analysis: Cramer’s V test results of categorical variables .....	30
Fig. 6 Correlation analysis: Pearson’s correlation test results of building materials .....	31
Fig. 7 Building feature importance: Means of variable importance measures over 50 permutations with RMSE as the loss-function for the RF model .....	32
Fig. 8 Building feature importance: Means of variable importance measures over 50 permutations with RMSE as the loss-function for the RF model after removing one of the variables.....	33
Fig. 9 Normalized variable importance for the RF model .....	34
Fig. 10 Effects of building attributes on MI: partial dependence plots.....	36
Fig. 11 RF-based MI for cement (Unit: ton/100 m <sup>2</sup> ) .....	38
Fig. 12 Difference between RF-based MI and mean values of MI.....	39
Fig. 13 Overview and research methodology .....	49
Fig. 14 The material and regional composition .....	53
Fig. 15 The material composition with values in each prefecture for different period (Unit: Mt) .....	54
Fig. 16 The change in the percentage of each road material from 1965 to 2020..	55
Fig. 17 Trends in road MS over the past half century: a) The amount of road MS growth for each prefecture (Unit: Mt); b) The average annual growth rate for each prefecture .....	57
Fig. 18 The evolution of the total road MS in 1965, 1980, 1995, 2010, and 2020 .....	58
Fig. 19 Examples of expected road MS with five SSPs. Pattern 1: Starting to shrink; Pattern 2: Staying stable or varying with scenarios; Pattern 3: Continuing to grow .....	66
Fig. 20 Discrepancies in road material magnitude and composition between road MS in 2020 and projected road MS in 2050 under five SSPs .....	67
Fig. 21 Location of the three major metropolitan areas in Japan.....	71
Fig. 22 The spatial evolution and material composition of building MS in three metropolitan areas in Japan in 2009, 2016, and 2020.....	75
Fig. 23 The projections for serviceable building floor area and MS of serviceable buildings under five SSPs until the year 2050 .....	76
Fig. 24 Driving factors .....	82
Fig. 25 Historical land use changes: a) The spatial evolution of land use types; b) Area shifts in the land use types .....	86
Fig. 26 Contributions of driving factors to the expansion of different land use types through RFC.....	87
Fig. 27 Prediction of the future land use demand by Markov chain and LR models .....	88
Fig. 28 The development potential maps of seven land use types.....	89
Fig. 29 Future land use simulation under Markov chain and LR scenarios .....	90

## Table list

Table 1 Test results of <i>mtry</i> parameter .....	26
Table 2 Estimated MI with construction year and use type information (Unit: ton/100 m <sup>2</sup> ).....	41
Table 3 R-square and significance of linear regressions for each prefecture in Japan between the number of passenger vehicles and GRP .....	48
Table 4 Information and parameters for MLR, SVR, ANN, and RF models on Weka platform.....	51
Table 5 The model information and performance of ARIMAX-SVR and ARIMAX alone for each prefecture.....	60
Table 6 The model performance of MLR, SVR, ANN, and RF for each prefecture .....	62
Table 7 Performance results of LR, PR, RF, GBM, and SVR .....	73
Table 8 Land use type and code .....	82
Table 9 Validation results of the PLUS model.....	84

## References

- AIRIA, 2023. Automobile Inspection and Registration Information Association of Japan. Available at: <https://www.airia.or.jp/publish/statistics/number.html>.
- Anderberg, S., 1998. Industrial metabolism and the linkages between economics, ethics and the environment. *Ecological Economics* 24(2-3), 311-320.
- A-PLAT, 2022. Climate Change Adaptation Information Platform of Japan. Available at: <https://adaptation-platform.nies.go.jp/en/>.
- A-PLAT, 2023. Climate Change Adaptation Information Platform of Japan. Available at: <https://adaptation-platform.nies.go.jp/socioeconomic/population.html>
- Arceo, A., Tham, M., Guven, G., MacLean, H.L., Saxe, S., 2021. Capturing variability in material intensity of single-family dwellings: A case study of Toronto, Canada. *Resources Conservation and Recycling* 175.
- Arehart, J.H., Pomponi, F., D'Amico, B., Srubar, W.V., 2022. Structural material demand and associated embodied carbon emissions of the United States building stock: 2020-2100. *Resources Conservation and Recycling* 186.
- Arora, M., Raspall, F., Cheah, L., Silva, A., 2019. Residential building material stocks and component-level circularity: The case of Singapore. *Journal of Cleaner Production* 216, 239-248.
- Arsanjani, J.J., Helbich, M., Kainz, W., Boloorani, A.D., 2013. Integration of logistic regression, Markov chain and cellular automata models to simulate urban expansion. *International Journal of Applied Earth Observation and Geoinformation* 21, 265-275.
- Augiseau, V., Barles, S., 2017. Studying construction materials flows and stock: A review. *Resources, Conservation and Recycling* 123, 153-164.
- Awad, M., Khanna, R., 2015. Support Vector Regression, Efficient Learning Machines: Theories, Concepts, and Applications for Engineers and System Designers. Apress, Berkeley, CA, pp. 67-80.
- Bauer, N., Calvin, K., Emmerling, J., Fricko, O., Fujimori, S., Hilaire, J., Eom, J., Krey, V., Kriegler, E., Mouratiadou, I., 2017. Shared socio-economic pathways of the energy sector—quantifying the narratives. *Global Environmental Change* 42, 316-330.
- Bentéjac, C., Csörgő, A., Martínez-Muñoz, G., 2021. A comparative analysis of gradient boosting algorithms. *Artificial Intelligence Review* 54, 1937-1967.
- Berberoglu, S., Akın, A., Clarke, K.C., 2016. Cellular automata modeling approaches to forecast urban growth for adana, Turkey: A comparative approach. *Landscape and urban planning* 153, 11-27.
- Bergsma, W., 2013. A bias-correction for Cramer's V and Tschuprow's T. *Journal of the Korean Statistical Society* 42(3), 323-328.
- Berrill, P., Hertwich, E.G., 2021. Material flows and GHG emissions from housing stock evolution in US counties, 2020–60. *Buildings and Cities* 2(1).
- Biecek, P., Burzykowski, T., 2021. Explanatory model analysis: explore, explain, and examine predictive models. CRC Press.
- Bolanle, A., Oluwadare, A., 2017. ARIMA and ARIMAX Stochastic models for fertility in Nigeria. *International Journal of Mathematics and Computer Application Research* 7(5), 1-20.
- Breiman, L., 2001. Random forests. *Machine learning* 45(1), 5-32.
- Broto, V.C., Allen, A., Rapoport, E., 2012. Interdisciplinary Perspectives on Urban Metabolism. *Journal of Industrial Ecology* 16(6), 851-861.
- Burghardt, K., Uhl, J.H., Lerman, K., Leyk, S., 2022. Road network evolution in the

- urban and rural United States since 1900. *Computers, Environment and Urban Systems* 95, 101803.
- Cao, Z., Shen, L., Zhong, S., Liu, L., Kong, H., Sun, Y., 2018. A Probabilistic Dynamic Material Flow Analysis Model for Chinese Urban Housing Stock. *Journal of Industrial Ecology* 22(2), 377-391.
- Che, J.X., Wang, J.Z., 2010. Short-term electricity prices forecasting based on support vector regression and Auto-regressive integrated moving average modeling. *Energy Conversion and Management* 51(10), 1911-1917.
- Chen, H., Matsushashi, K., Takahashi, K., Fujimori, S., Honjo, K., Gomi, K., 2020. Adapting global shared socio-economic pathways for national scenarios in Japan. *Sustainability Science* 15(3), 985-1000.
- Chen, J., Gao, M., Cheng, S., Hou, W., Song, M., Liu, X., Liu, Y., 2022. Global 1 km×1 km gridded revised real gross domestic product and electricity consumption during 1992–2019 based on calibrated nighttime light data. *Scientific Data* 9(1), 202.
- Chinowsky, P.S., Price, J.C., Neumann, J.E., 2013. Assessment of climate change adaptation costs for the US road network. *Global Environmental Change-Human and Policy Dimensions* 23(4), 764-773.
- Clarke, K.C., 2008. Mapping and modelling land use change: an application of the SLEUTH model. *Landscape analysis and visualisation: Spatial models for natural resource management and planning*, 353-366.
- COGA, 2022. Cabinet Office, Government of Japan. Available at: [https://www.esri.cao.go.jp/jp/sna/sonota/kenmin/kenmin\\_top.html](https://www.esri.cao.go.jp/jp/sna/sonota/kenmin/kenmin_top.html).
- Cutler, A., Cutler, D.R., Stevens, J.R., 2012. Random forests. *Ensemble machine learning: Methods and applications*, 157-175.
- Dai, T.J., Yue, Z.C., 2023. The evolution and decoupling of in-use stocks in Beijing. *Ecological Economics* 203, 10.
- Dash, R.K., Nguyen, T.N., Cengiz, K., Sharma, A., 2021. Fine-tuned support vector regression model for stock predictions. *Neural Computing and Applications*, 1-15.
- Daxbeck, H., Buschmann, H., Neumayer, S., Brandt, B., 2009. Methodology for mapping of physical stocks. Deliverable 2.3. Resource Management Agency (RMA). 77p.
- de Abreu, V.H.S., Santos, A.S., Monteiro, T.G.M., 2022. Climate Change Impacts on the Road Transport Infrastructure: A Systematic Review on Adaptation Measures. *Sustainability* 14(14), 8864.
- De Wolf, C., Hoxha, E., Hollberg, A., Fivet, C., Ochsendorf, J., 2020. Database of Embodied Quantity Outputs: Lowering Material Impacts Through Engineering. *Journal of Architectural Engineering* 26(3).
- De Wolf, C., Yang, F., Cox, D., Charlson, A., Hattan, A.S., Ochsendorf, J., 2016. Material quantities and embodied carbon dioxide in structures. *Proceedings of the Institution of Civil Engineers-Engineering Sustainability* 169(4), 150-161.
- Deetman, S., Marinova, S., van der Voet, E., van Vuuren, D.P., Edelenbosch, O., Heijungs, R., 2020. Modelling global material stocks and flows for residential and service sector buildings towards 2050. *Journal of Cleaner Production* 245.
- dos Reis, G.S., Quattrone, M., Ambros, W.M., Cazacliu, B.G., Sampaio, C.H., 2021. Current Applications of Recycled Aggregates from Construction and Demolition: A Review. *Materials* 14(7).
- Dou, J., Yunus, A.P., Dieu Tien, B., Merghadi, A., Sahana, M., Zhu, Z., Chen, C.-W., Khosravi, K., Yang, Y., Binh Thai, P., 2019. Assessment of advanced random forest and decision tree algorithms for modeling rainfall-induced landslide susceptibility

- in the Izu-Oshima Volcanic Island, Japan. *Science of the Total Environment* 662, 332-346.
- Edwards, J.R., 2002. Alternatives to difference scores: Polynomial regression and response surface methodology. *Advances in measurement and data analysis*, 350-400.
- Ehrlich, P.R., Holdren, J.P., 1971. IMPACT OF POPULATION GROWTH. *Science* 171(3977), 1212-&.
- Eibe, F., Hall, M.A., Witten, I.H., 2016. The WEKA workbench. Online appendix for data mining: practical machine learning tools and techniques, Morgan Kaufmann. Morgan Kaufmann Publishers San Francisco, California.
- Eisenack, K., Stecker, R., Reckien, D., Hoffmann, E., 2012. Adaptation to climate change in the transport sector: a review of actions and actors. *Mitigation and Adaptation Strategies for Global Change* 17(5), 451-469.
- Erkman, S., 1997. Industrial ecology: an historical view. *Journal of cleaner production* 5(1-2), 1-10.
- ESRI Japan, 2022. Available at: <https://www.esri.com/products/data-content-starter/>.
- e-Stat, 2022. Available at: <https://www.e-stat.go.jp/en>.
- Fan, G.-F., Yu, M., Dong, S.-Q., Yeh, Y.-H., Hong, W.-C., 2021. Forecasting short-term electricity load using hybrid support vector regression with grey catastrophe and random forest modeling. *Utilities Policy* 73, 101294.
- Fishman, T., Heeren, N., Pauliuk, S., Berrill, P., Tu, Q.S., Wolfram, P., Hertwich, E.G., 2021. A comprehensive set of global scenarios of housing, mobility, and material efficiency for material cycles and energy systems modeling. *Journal of Industrial Ecology* 25(2), 321-332.
- Fishman, T., Schandl, H., Tanikawa, H., 2016. Stochastic Analysis and Forecasts of the Patterns of Speed, Acceleration, and Levels of Material Stock Accumulation in Society. *Environmental Science & Technology* 50(7), 3729-3737.
- Frame, B., Lawrence, J., Ausseil, A.-G., Reisinger, A., Daigneault, A., 2018. Adapting global shared socio-economic pathways for national and local scenarios. *Climate Risk Management* 21, 39-51.
- Friedman, J.H., 2001. Greedy function approximation: A gradient boosting machine. *Annals of Statistics* 29(5), 1189-1232.
- Fu, C., Zhang, Y., Deng, T., Daigo, I., 2021. The evolution of material stock research: From exploring to rising to hot studies. *Journal of Industrial Ecology*.
- Gao, L., Tao, F., Liu, R., Wang, Z., Leng, H., Zhou, T., 2022. Multi-scenario simulation and ecological risk analysis of land use based on the PLUS model: A case study of Nanjing. *Sustainable Cities and Society* 85, 104055.
- Gassner, A., Lederer, J., Fellner, J., 2020. Material stock development of the transport sector in the city of Vienna. *Journal of Industrial Ecology* 24(6), 1364-1378.
- Gassner, A., Lederer, J., Kovacic, G., Mollay, U., Schremmer, C., Fellner, J., 2021. Projection of material flows and stocks in the urban transport sector until 2050-A scenario-based analysis for the city of Vienna. *Journal of Cleaner Production* 311, 13.
- Gillott, C., Mihkelson, W., Lanau, M., Cheshire, D., Tingley, D.D., 2023. Developing regenerate: A circular economy engagement tool for the assessment of new and existing buildings. *Journal of Industrial Ecology* 27(2), 423-435.
- Gonti, P., Nageli, C., Rosado, L., Kalmykova, Y., Osterbring, M., 2018. Material-intensity database of residential buildings: A case-study of Sweden in the international context. *Resources Conservation and Recycling* 130, 228-239.
- Graedel, T.E., 2019. Material Flow Analysis from Origin to Evolution. *Environmental*

- Science & Technology 53(21), 12188-12196.
- Gregorutti, B., Michel, B., Saint-Pierre, P., 2017. Correlation and variable importance in random forests. *Statistics and Computing* 27(3), 659-678.
- Gu, L., 2009. *Studies on the Environmental Impact of the Building Industry in China Based on the Life Cycle Assessment* [In Chinese]. Tsinghua University.
- Guo, J., Miatto, A., Shi, F., Tanikawa, H., 2019. Spatially explicit material stock analysis of buildings in Eastern China metropolises. *Resources Conservation and Recycling* 146, 45-54.
- Guo, Z., Hu, D., Zhang, F., Huang, G., Xiao, Q., 2014. An integrated material metabolism model for stocks of urban road system in Beijing, China. *Science of the Total Environment* 470, 883-894.
- Göswein, V., Krones, J., Celentano, G., Fernández, J.E., Habert, G., 2018. Embodied GHGs in a Fast Growing City: Looking at the Evolution of a Dwelling Stock using Structural Element Breakdown and Policy Scenarios. *Journal of Industrial Ecology* 22(6), 1339-1351.
- Haberl, H., Wiedenhofer, D., Schug, F., Frantz, D., Virag, D., Plutzer, C., Gruhler, K., Lederer, J., Schiller, G., Fishman, T., Lanau, M., Gattringer, A., Kemper, T., Liu, G., Tanikawa, H., van der Linden, S., Hostert, P., 2021. High-Resolution Maps of Material Stocks in Buildings and Infrastructures in Austria and Germany. *Environmental Science & Technology* 55(5), 3368-3379.
- Hall, M., Frank, E., Holmes, G., Pfahringer, B., Reutemann, P., Witten, I.H., 2009. The WEKA data mining software: an update. *ACM SIGKDD explorations newsletter* 11(1), 10-18.
- Hamad, R., Balzter, H., Kolo, K., 2018. Predicting land use/land cover changes using a CA-Markov model under two different scenarios. *Sustainability* 10(10), 3421.
- Han, H., Yang, C., Song, J., 2015. Scenario simulation and the prediction of land use and land cover change in Beijing, China. *Sustainability* 7(4), 4260-4279.
- Han, J., Chen, W.-Q., Zhang, L., Liu, G., 2018. Uncovering the Spatiotemporal Dynamics of Urban Infrastructure Development: A High Spatial Resolution Material Stock and Flow Analysis. *Environmental Science & Technology* 52(21), 12122-12132.
- Han, J., Xiang, W.-N., 2013. Analysis of material stock accumulation in China's infrastructure and its regional disparity. *Sustainability Science* 8(4), 553-564.
- Heeren, N., Fishman, T., 2019. A database seed for a community-driven material intensity research platform. *Scientific Data* 6.
- Heeren, N., Jakob, M., Martius, G., Gross, N., Wallbaum, H., 2013. A component based bottom-up building stock model for comprehensive environmental impact assessment and target control. *Renewable & Sustainable Energy Reviews* 20, 45-56.
- Hirvonen, J., Heljo, J., Jokisalo, J., Kurvinen, A., Saari, A., Niemelä, T., Sankelo, P., Kosonen, R., 2021. Emissions and power demand in optimal energy retrofit scenarios of the Finnish building stock by 2050. *Sustainable Cities and Society* 70.
- Hong, J.J., Chu, Z.F., Wang, Q., 2011. Transport infrastructure and regional economic growth: evidence from China. *Transportation* 38(5), 737-752.
- Hong, L., Zhou, N., Feng, W., Khanna, N., Fridley, D., Zhao, Y., Sandholt, K., 2016. Building stock dynamics and its impacts on materials and energy demand in China. *Energy Policy* 94, 47-55.
- Honjo, K., Gomi, K., Kanamori, Y., Takahashi, K., Matsushashi, K., 2021. Long-term projections of economic growth in the 47 prefectures of Japan: An application of Japan shared socioeconomic pathways. *Heliyon* 7(3), 13.

- Hossain, M.S., Ahmed, S., Uddin, M.J., 2021. Impact of weather on COVID-19 transmission in south Asian countries: An application of the ARIMAX model. *Science of the Total Environment* 761, 9.
- Hu, D., You, F., Zhao, Y., Yuan, Y., Liu, T., Cao, A., Wang, Z., Zhang, J., 2010. Input, stocks and output flows of urban residential building system in Beijing city, China from 1949 to 2008. *Resources Conservation and Recycling* 54(12), 1177-1188.
- Hu, M., Pauliuk, S., Wang, T., Huppel, G., van der Voet, E., Muller, D.B., 2010. Iron and steel in Chinese residential buildings: A dynamic analysis. *Resources Conservation and Recycling* 54(9), 591-600.
- Huang, C., Han, J., Chen, W.-Q., 2017. Changing patterns and determinants of infrastructures' material stocks in Chinese cities. *Resources Conservation and Recycling* 123, 47-53.
- Huang, T., Shi, F., Tanikawa, H., Fei, J., Han, J., 2013. Materials demand and environmental impact of buildings construction and demolition in China based on dynamic material flow analysis. *Resources Conservation and Recycling* 72, 91-101.
- Huo, T., Li, X., Cai, W., Zuo, J., Jia, F., Wei, H., 2020. Exploring the impact of urbanization on urban building carbon emissions in China: Evidence from a provincial panel data model. *Sustainable Cities and Society* 56, 102068.
- Hyndman, R.J., Athanasopoulos, G., 2018. *Forecasting: principles and practice*. OTexts.
- Hyndman, R.J., Khandakar, Y., 2008. Automatic time series forecasting: the forecast package for R. *Journal of statistical software* 27, 1-22.
- IEA, 2019. Transport sector CO<sub>2</sub> emissions by mode in the Sustainable Development Scenario, 2000-2030. Available at: <https://www.iea.org/data-and-statistics/charts/transport-sector-co2-emissions-by-mode-in-the-sustainable-development-scenario-2000-2030>.
- Iwasaki, Y., 2021. Shrinkage of regional cities in Japan: Analysis of changes in densely inhabited districts. *Cities* 113, 103168.
- Jantz, C.A., Goetz, S.J., Shelley, M.K., 2004. Using the SLEUTH urban growth model to simulate the impacts of future policy scenarios on urban land use in the Baltimore-Washington metropolitan area. *Environment and Planning B: Planning and Design* 31(2), 251-271.
- Jonker, G., Harmsen, J., 2012. *Engineering for sustainability: a practical guide for sustainable design*. Elsevier.
- Jullien, A., Dauvergne, M., Cerezo, V., 2014. Environmental assessment of road construction and maintenance policies using LCA. *Transportation Research Part D-Transport and Environment* 29, 56-65.
- Kasraian, D., Maat, K., Stead, D., van Wee, B., 2016. Long-term impacts of transport infrastructure networks on land-use change: an international review of empirical studies. *Transport Reviews* 36(6), 772-792.
- Kavgic, M., Mavrogianni, A., Mumovic, D., Summerfield, A., Stevanovic, Z., Djurovic-Petrovic, M., 2010. A review of bottom-up building stock models for energy consumption in the residential sector. *Building and Environment* 45(7), 1683-1697.
- Kleemann, F., Lederer, J., Aschenbrenner, P., Rechberger, H., Fellner, J., 2016. A method for determining buildings' material composition prior to demolition. *Building Research and Information* 44(1), 51-62.
- Kleemann, F., Lederer, J., Rechberger, H., Fellner, J., 2017. GIS-based Analysis of Vienna's Material Stock in Buildings. *Journal of Industrial Ecology* 21(2), 368-380.

- Koetse, M.J., Rietveld, P., 2009. The impact of climate change and weather on transport: An overview of empirical findings. *Transportation Research Part D: Transport and Environment* 14(3), 205-221.
- Koko, A.F., Han, Z., Wu, Y., Zhang, S., Ding, N., Luo, J., 2023. Spatiotemporal Analysis and Prediction of Urban Land Use/Land Cover Changes Using a Cellular Automata and Novel Patch-Generating Land Use Simulation Model: A Study of Zhejiang Province, China. *Land* 12(8), 1525.
- Krausmann, F., Wiedenhofer, D., Lauk, C., Haas, W., Tanikawa, H., Fishman, T., Miatto, A., Schandl, H., Haberl, H., 2017. Global socioeconomic material stocks rise 23-fold over the 20th century and require half of annual resource use. *Proceedings of the National Academy of Sciences of the United States of America* 114(8), 1880-1885.
- Krogh, A., 2008. What are artificial neural networks? *Nature biotechnology* 26(2), 195-197.
- Kubo, T., Yui, Y., 2020. *The rise in vacant housing in post-growth Japan*. Springer.
- Kuhn, M., 2015. *Caret: classification and regression training*. Astrophysics Source Code Library, ascl: 1505.1003.
- Lanau, M., Liu, G., 2020. Developing an urban resource cadaster for circular economy: A case of Odense, Denmark. *Environmental science & technology* 54(7), 4675-4685.
- Lanau, M., Liu, G., Kral, U., Wiedenhofer, D., Keijzer, E., Yu, C., Ehlert, C., 2019. Taking stock of built environment stock studies: Progress and prospects. *Environmental science & technology* 53(15), 8499-8515.
- Laurance, W.F., Clements, G.R., Sloan, S., O'connell, C.S., Mueller, N.D., Goosem, M., Venter, O., Edwards, D.P., Phalan, B., Balmford, A., 2014. A global strategy for road building. *Nature* 513(7517), 229-232.
- Le Boulzec, H., Mathy, S., Verzier, F., Andrieu, B., Monfort-Climent, D., Vidal, O., 2023. Material requirements and impacts of the building sector in the shared socioeconomic pathways. *Journal of Cleaner Production* 428, 139117.
- Lederer, J., Gassner, A., Fellner, J., Mollay, U., Schremmer, C., 2021. Raw materials consumption and demolition waste generation of the urban building sector 2016-2050: A scenario-based material flow analysis of Vienna. *Journal of Cleaner Production* 288, 12.
- Lederer, J., Gassner, A., Kleemann, F., Fellner, J., 2020. Potentials for a circular economy of mineral construction materials and demolition waste in urban areas: a case study from Vienna. *Resources Conservation and Recycling* 161.
- Lee, W., Ebi, K.L., Kim, Y., Hashizume, M., Honda, Y., Hideki, H., Choi, H.M., Choi, M., Kim, H., 2021. Heat-mortality risk and the population concentration of metropolitan areas in Japan: a nationwide time-series study. *International Journal of Epidemiology* 50(2), 602-612.
- Li, C., Wu, Y., Gao, B., Zheng, K., Wu, Y., Li, C., 2021. Multi-scenario simulation of ecosystem service value for optimization of land use in the Sichuan-Yunnan ecological barrier, China. *Ecological Indicators* 132, 108328.
- Li, S.P., Wang, Z., Zhang, T.A., Yue, Q., 2022. Quantification and spatial distribution of aluminum in-use stocks in Henan Province, China. *Resources Conservation and Recycling* 186, 10.
- Liang, H., Dong, L., Tanikawa, H., Zhang, N., Gao, Z., Luo, X., 2017. Feasibility of a new-generation nighttime light data for estimating in-use steel stock of buildings and civil engineering infrastructures. *Resources Conservation and Recycling* 123, 11-23.

- Liang, X., Guan, Q., Clarke, K.C., Liu, S., Wang, B., Yao, Y., 2021. Understanding the drivers of sustainable land expansion using a patch-generating land use simulation (PLUS) model: A case study in Wuhan, China. *Computers, Environment and Urban Systems* 85, 101569.
- Liao, Q., Wang, Z., Huang, C., 2020. Green infrastructure offset the negative ecological effects of urbanization and storing water in the three gorges reservoir area, China. *International Journal of Environmental Research and Public Health* 17(21), 8077.
- Lin, J., He, X., Lu, S., Liu, D., He, P., 2021a. Investigating the influence of three-dimensional building configuration on urban pluvial flooding using random forest algorithm. *Environmental Research* 196.
- Lin, J., Lu, S., He, X., Wang, F., 2021b. Analyzing the impact of three-dimensional building structure on CO2 emissions based on random forest regression. *Energy* 236.
- Lin, W., Sun, Y., Nijhuis, S., Wang, Z., 2020. Scenario-based flood risk assessment for urbanizing deltas using future land-use simulation (FLUS): Guangzhou Metropolitan Area as a case study. *Science of the Total Environment* 739, 139899.
- Liu, T., Hu, D., 2006. Environmental impact of residential building construction in Beijing: 1949-2003-Assessing the construction materials' environmental impact by LCA [In Chinese]. *J. Grad. Sch. Chin. Acad. Sci.*, 12, pp. 231-241.
- Liu, X., Liang, X., Li, X., Xu, X., Ou, J., Chen, Y., Li, S., Wang, S., Pei, F., 2017. A future land use simulation model (FLUS) for simulating multiple land use scenarios by coupling human and natural effects. *Landscape and Urban Planning* 168, 94-116.
- Luo, W., Mineo, K., Matsushita, K., Kanzaki, M., 2018. Consumer willingness to pay for modern wooden structures: A comparison between China and Japan. *Forest Policy and Economics* 91, 84-93.
- Ma, J., Xia, D., Guo, H., Wang, Y., Niu, X., Liu, Z., Jiang, S., 2022. Metaheuristic-based support vector regression for landslide displacement prediction: A comparative study. *Landslides* 19(10), 2489-2511.
- Maksymiuk, S., Gosiewska, A., Biecek, P., 2020. Landscape of R packages for eXplainable Artificial Intelligence. *arXiv preprint arXiv:2009.13248*.
- Marcellus-Zamora, K.A., Gallagher, P.M., Spataro, S., Tanikawa, H., 2016. Estimating Materials Stocked by Land-Use Type in Historic Urban Buildings Using Spatio-Temporal Analytical Tools. *Journal of Industrial Ecology* 20(5), 1025-1037.
- Marinova, S., Deetman, S., van der Voet, E., Daioglou, V., 2020. Global construction materials database and stock analysis of residential buildings between 1970-2050. *Journal of Cleaner Production* 247.
- Markolf, S.A., Hoehne, C., Fraser, A., Chester, M.V., Underwood, B.S., 2019. Transportation resilience to climate change and extreme weather events—Beyond risk and robustness. *Transport policy* 74, 174-186.
- ME, 2023. Ministry of the Environment of Japan. Available at: <https://www.env.go.jp/recycle/3r/initiative/en/index.html>.
- Mechelli, A., Viera, S., 2019. *Machine learning: methods and applications to brain disorders*. Academic Press.
- Meijer, J.R., Huijbregts, M.A.J., Schotten, K., Schipper, A.M., 2018. Global patterns of current and future road infrastructure. *Environmental Research Letters* 13(6), 10.
- Mesta, C., Kahhat, R., Santa-Cruz, S., 2019. Geospatial Characterization of Material Stock in the Residential Sector of a Latin-American City. *Journal of Industrial Ecology* 23(1), 280-291.
- MIC, 2013 Ministry of Internal Affairs and Communications of Japan

- [https://www.soumu.go.jp/main\\_content/000354244.pdf](https://www.soumu.go.jp/main_content/000354244.pdf).
- Miatto, A., Dawson, D., Nguyen, P.D., Kanaoka, K.S., Tanikawa, H., 2021. The urbanisation-environment conflict: Insights from material stock and productivity of transport infrastructure in Hanoi, Vietnam. *Journal of Environmental Management* 294, 12.
- Miatto, A., Schandl, H., Forlin, L., Ronzani, F., Borin, P., Giordano, A., Tanikawa, H., 2019. A spatial analysis of material stock accumulation and demolition waste potential of buildings: A case study of Padua. *Resources Conservation and Recycling* 142, 245-256.
- Miatto, A., Schandl, H., Tanikawa, H., 2017a. How important are realistic building lifespan assumptions for material stock and demolition waste accounts? *Resources Conservation and Recycling* 122, 143-154.
- Miatto, A., Schandl, H., Wiedenhofer, D., Krausmann, F., Tanikawa, H., 2017b. Modeling material flows and stocks of the road network in the United States 1905-2015. *Resources Conservation and Recycling* 127, 168-178.
- MLIT, 2021. Ministry of Land, Infrastructure, Transport and Tourism of Japan. 2021 Roads in Japan. Available at: [https://www.mlit.go.jp/road/road\\_e/pdf/ROAD2021web.pdf](https://www.mlit.go.jp/road/road_e/pdf/ROAD2021web.pdf).
- MLIT, 2022. Ministry of Land, Infrastructure, Transport and Tourism of Japan. Available at: <https://www.mlit.go.jp/road/ir/ir-data/tokei-nen/index.html>.
- MLIT, 2023a. Ministry of Land, Infrastructure, Transport and Tourism of Japan. Available at: <https://www.mlit.go.jp/k-toukei/saishintoukeihyou.html>.
- MLIT, 2023b. Ministry of Land, Infrastructure, Transport and Tourism of Japan. Available at: <https://nlftp.mlit.go.jp/ksj/index.html>
- Moody, J., Farr, E., Papagelis, M., Keith, D.R., 2021. The value of car ownership and use in the United States. *Nature Sustainability* 4(9), 769-+.
- Munshi, T., Zuidgeest, M., Brussel, M., van Maarseveen, M., 2014. Logistic regression and cellular automata-based modelling of retail, commercial and residential development in the city of Ahmedabad, India. *Cities* 39, 68-86.
- Nageli, C., Jakob, M., Catenazzi, G., Ostermeyer, Y., 2020. Towards agent-based building stock modeling: Bottom-up modeling of long-term stock dynamics affecting the energy and climate impact of building stocks. *Energy and Buildings* 211.
- Natekin, A., Knoll, A., 2013. Gradient boosting machines, a tutorial. *Frontiers in neuroinformatics* 7, 21.
- National Institute of Population and Social Security Research, 2023. Available at: [https://www.ipss.go.jp/pp-zenkoku/j/zenkoku2023/pp\\_zenkoku2023.asp](https://www.ipss.go.jp/pp-zenkoku/j/zenkoku2023/pp_zenkoku2023.asp).
- Nguyen, C., Wang, Y., Nguyen, H.N., 2013. Random forest classifier combined with feature selection for breast cancer diagnosis and prognostic.
- Nguyen, T.C., Fishman, T., Miatto, A., Tanikawa, H., 2019. Estimating the Material Stock of Roads: The Vietnamese Case Study. *Journal of Industrial Ecology* 23(3), 663-673.
- Nunes, L.J., Meireles, C.I., Pinto Gomes, C.J., Almeida Ribeiro, N.M., 2020. Forest contribution to climate change mitigation: Management oriented to carbon capture and storage. *Climate* 8(2), 21.
- O'Neill, B.C., Kriegler, E., Ebi, K.L., Kemp-Benedict, E., Riahi, K., Rothman, D.S., van Ruijven, B.J., van Vuuren, D.P., Birkmann, J., Kok, K., Levy, M., Solecki, W., 2017. The roads ahead: Narratives for shared socioeconomic pathways describing world futures in the 21st century. *Global Environmental Change-Human and Policy Dimensions* 42, 169-180.

- Ostertagová, E., 2012. Modelling using polynomial regression. *Procedia Engineering* 48, 500-506.
- Peng, Z., Lu, W., Webster, C.J., 2021. Quantifying the embodied carbon saving potential of recycling construction and demolition waste in the Greater Bay Area, China: Status quo and future scenarios. *Science of the Total Environment* 792.
- Pongratz, J., Schwingshackl, C., Bultan, S., Obermeier, W., Havermann, F., Guo, S., 2021. Land use effects on climate: current state, recent progress, and emerging topics. *Current Climate Change Reports*, 1-22.
- Popp, A., Calvin, K., Fujimori, S., Havlik, P., Humpenöder, F., Stehfest, E., Bodirsky, B.L., Dietrich, J.P., Doelmann, J.C., Gusti, M., 2017. Land-use futures in the shared socio-economic pathways. *Global Environmental Change* 42, 331-345.
- Poulikakos, L.D., Papadaskalopoulou, C., Hofko, B., Gschosser, F., Falchetto, A.C., Bueno, M., Arraigada, M., Sousa, J., Ruiz, R., Petit, C., Loizidou, M., Partl, M.N., 2017. Harvesting the unexplored potential of European waste materials for road construction. *Resources Conservation and Recycling* 116, 32-44.
- Reyna, J.L., Chester, M.V., 2015. The Growth of Urban Building Stock Unintended Lock-in and Embedded Environmental Effects. *Journal of Industrial Ecology* 19(4), 524-537.
- Riahi, K., van Vuuren, D.P., Kriegler, E., Edmonds, J., O'Neill, B.C., Fujimori, S., Bauer, N., Calvin, K., Dellink, R., Fricko, O., Lutz, W., Popp, A., Cuaresma, J.C., Samir, K.C., Leimbach, M., Jiang, L.W., Kram, T., Rao, S., Emmerling, J., Ebi, K., Hasegawa, T., Havlik, P., Humpenoder, F., da Silva, L.A., Smith, S., Stehfest, E., Bosetti, V., Eom, J., Gernaat, D., Masui, T., Rogelj, J., Strefler, J., Drouet, L., Krey, V., Luderer, G., Harmsen, M., Takahashi, K., Baumstark, L., Doelman, J.C., Kainuma, M., Klimont, Z., Marangoni, G., Lotze-Campen, H., Obersteiner, M., Tabeau, A., Tavoni, M., 2017. The Shared Socioeconomic Pathways and their energy, land use, and greenhouse gas emissions implications: An overview. *Global Environmental Change-Human and Policy Dimensions* 42, 153-168.
- Saavedra, Y.M.B., Iritani, D.R., Pavan, A.L.R., Ometto, A.R., 2018. Theoretical contribution of industrial ecology to circular economy. *Journal of Cleaner Production* 170, 1514-1522.
- Sanchez, P.C., Albert, M.G., 2015. TRANSPORT INFRASTRUCTURES, CO2 EMISSIONS AND ECONOMIC GROWTH: NEW EVIDENCE FROM OECD COUNTRIES. *International Journal of Transport Economics* 42(2), 251-268.
- Sang, L., Zhang, C., Yang, J., Zhu, D., Yun, W., 2011. Simulation of land use spatial pattern of towns and villages based on CA-Markov model. *Mathematical and Computer Modelling* 54(3-4), 938-943.
- Schandl, H., Lu, Y., Che, N., Newth, D., West, J., Frank, S., Obersteiner, M., Rendall, A., Hatfield-Dodds, S., 2020. Shared socio-economic pathways and their implications for global materials use. *Resources, Conservation and Recycling* 160, 104866.
- Schandl, H., Marcos-Martinez, R., Baynes, T., Yu, Z.F., Miatto, A., Tanikawa, H., 2020. A spatiotemporal urban metabolism model for the Canberra suburb of Braddon in Australia. *Journal of Cleaner Production* 265.
- Schebek, L., Schnitzer, B., Blesinger, D., Koehn, A., Miekley, B., Linke, H.J., Lohmann, A., Motzko, C., Seemann, A., 2017. Material stocks of the non-residential building sector: the case of the Rhine-Main area. *Resources Conservation and Recycling* 123, 24-36.
- Schiller, G., Miatto, A., Gruhler, K., Ortlepp, R., Deilmann, C., Tanikawa, H., 2019. Transferability of Material Composition Indicators for Residential Buildings: A

- Conceptual Approach Based on a German-Japanese Comparison. *Journal of Industrial Ecology* 23(4), 796-807.
- Schiller, G., Mueller, F., Ortlepp, R., 2017. Mapping the anthropogenic stock in Germany: Metabolic evidence for a circular economy. *Resources Conservation and Recycling* 123, 93-107.
- Shaik, M.E., Islam, M.M., Hossain, Q.S., 2021. A review on neural network techniques for the prediction of road traffic accident severity. *Asian Transport Studies* 7, 100040.
- Shi, F., Huang, T., Tanikawa, H., Han, J., Hashimoto, S., Moriguchi, Y., 2012. Toward a Low Carbon-Dematerialization Society Measuring the Materials Demand and CO<sub>2</sub> Emissions of Building and Transport Infrastructure Construction in China. *Journal of Industrial Ecology* 16(4), 493-505.
- Smola, A.J., Schölkopf, B., 2004. A tutorial on support vector regression. *Statistics and computing* 14, 199-222.
- Sohail, A., Cheema, M.A., Ali, M.E., Toosi, A.N., Rakha, H.A., 2023. Data-driven approaches for road safety: a comprehensive systematic literature review. *Safety science* 158, 105949.
- Sohl, T.L., Claggett, P.R., 2013. Clarity versus complexity: Land-use modeling as a practical tool for decision-makers. *Journal of Environmental Management* 129, 235-243.
- Sprecher, B., Verhagen, T.J., Sauer, M.L., Baars, M., Heintz, J., Fishman, T., 2022. Material intensity database for the Dutch building stock: Towards Big Data in material stock analysis. *Journal of Industrial Ecology* 26(1), 272-280.
- Staffini, A., 2022. Stock Price Forecasting by a Deep Convolutional Generative Adversarial Network. *Frontiers in Artificial Intelligence* 5, 16.
- Statistics Bureau of Japan, 2023 Available at: <https://www.stat.go.jp/data/jinsui/2022np/pdf/2022np.pdf>
- Stephan, A., Athanassiadis, A., 2018. Towards a more circular construction sector: Estimating and spatialising current and future non-structural material replacement flows to maintain urban building stocks. *Resources Conservation and Recycling* 129, 248-262.
- Strobl, C., Boulesteix, A.-L., Zeileis, A., Hothorn, T., 2007. Bias in random forest variable importance measures: Illustrations, sources and a solution. *BMC Bioinformatics* 8(1), 25.
- Sun, H.W., Gui, D.W., Yan, B.W., Liu, Y., Liao, W.H., Zhu, Y., Lu, C.W., Zhao, N., 2016. Assessing the potential of random forest method for estimating solar radiation using air pollution index. *Energy Conversion and Management* 119, 121-129.
- Tang, J., Zheng, L., Han, C., Yin, W., Zhang, Y., Zou, Y., Huang, H., 2020. Statistical and machine-learning methods for clearance time prediction of road incidents: A methodology review. *Analytic Methods in Accident Research* 27, 100123.
- Tanikawa, H., Fishman, T., Okuoka, K., Sugimoto, K., 2015. The Weight of Society Over Time and Space: A Comprehensive Account of the Construction Material Stock of Japan, 1945-2010. *Journal of Industrial Ecology* 19(5), 778-791.
- Tanikawa, H., Hashimoto, S., 2009. Urban stock over time: spatial material stock analysis using 4d-GIS. *Building Research & Information* 37(5-6), 483-502.
- Tobler, W.R., 1979. Cellular geography. *Philosophy in geography*, 379-386.
- Tolosi, L., Lengauer, T., 2011. Classification with correlated features: unreliability of feature ranking and solutions. *Bioinformatics* 27(14), 1986-1994.
- Tsunoda, H., Enari, H., 2020. A strategy for wildlife management in depopulating rural

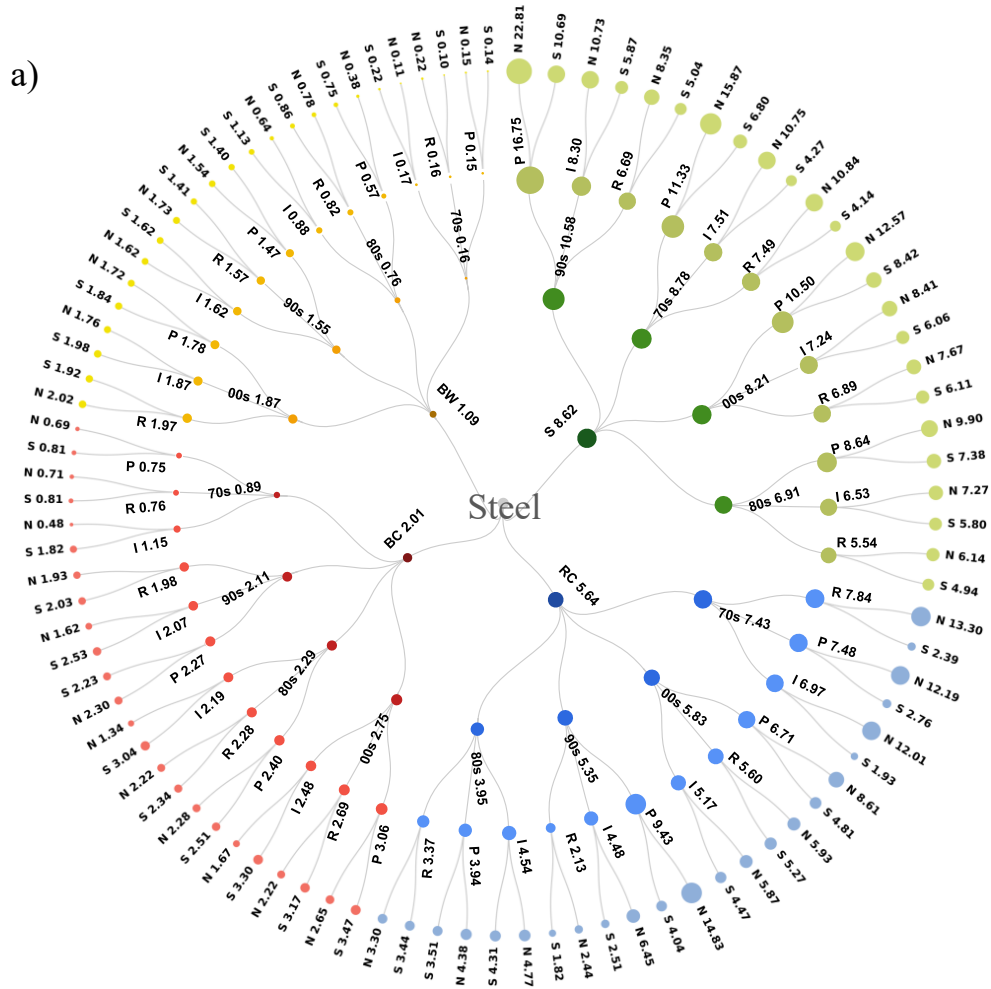
- areas of Japan. *Conservation Biology* 34(4), 819-828.
- UNEP, 2021. New report reveals how infrastructure defines our climate. Available at: <https://www.unep.org/news-and-stories/press-release/new-report-reveals-how-infrastructure-defines-our-climate>.
- UNEP, 2022. 2022 Global Status Report for Buildings and Construction. Available at: <https://www.unep.org/resources/publication/2022-global-status-report-buildings-and-construction>.
- Verburg, P.H., Soepboer, W., Veldkamp, A., Limpiada, R., Espaldon, V., Mastura, S.S., 2002. Modeling the spatial dynamics of regional land use: the CLUE-S model. *Environmental management* 30, 391-405.
- Vilaysouk, X., Saypadith, S., Hashimoto, S., 2022. Semisupervised machine learning classification framework for material intensity parameters of residential buildings. *Journal of Industrial Ecology* 26(1), 72-87.
- Wang, H.Y., Chen, D.J., Duan, H.B., Yin, F.F., Niu, Y.N., 2019. Characterizing urban building metabolism with a 4D-GIS model: A case study in China. *Journal of Cleaner Production* 228, 1446-1454.
- Wang, J.Y., Bretz, M., Dewan, M.A.A., Delavar, M.A., 2022. Machine learning in modelling land-use and land cover-change (LULCC): Current status, challenges and prospects. *Science of the Total Environment* 822.
- Wang, T., Tian, X., Hashimoto, S., Tanikawa, H., 2015. Concrete transformation of buildings in China and implications for the steel cycle. *Resources Conservation and Recycling* 103, 205-215.
- Wang, Z.Y., Wang, Y.R., Zeng, R.C., Srinivasan, R.S., Ahrentzen, S., 2018. Random Forest based hourly building energy prediction. *Energy and Buildings* 171, 11-25.
- Wiedenhofer, D., Steinberger, J.K., Eisenmenger, N., Haas, W., 2015. Maintenance and Expansion Modeling Material Stocks and Flows for Residential Buildings and Transportation Networks in the EU25. *Journal of Industrial Ecology* 19(4), 538-551.
- Wiedmann, T., Lenzen, M., Keysser, L.T., Steinberger, J.K., 2020. Scientists' warning on affluence. *Nature Communications* 11(1), 10.
- Wu, M., Yu, L., Zhang, J., 2023. Road expansion, allocative efficiency, and pro-competitive effect of transport infrastructure: Evidence from China. *Journal of Development Economics*, 103050.
- Wu, T., Zhao, H.M., Ou, X.M., 2014. Vehicle Ownership Analysis Based on GDP per Capita in China: 1963-2050. *Sustainability* 6(8), 4877-4899.
- Wudad, A., Naser, S., Lameso, L., 2021. The impact of improved road networks on marketing of vegetables and households' income in Dedo district, Oromia regional state, Ethiopia. *Heliyon* 7(10), 8.
- Xu, D.H., Zhang, Q., Ding, Y., Huang, H.P., 2020. Application of a Hybrid ARIMA-SVR Model Based on the SPI for the Forecast of Drought-A Case Study in Henan Province, China. *Journal of Applied Meteorology and Climatology* 59(7), 1239-1259.
- Xu, D.H., Zhang, Q., Ding, Y., Zhang, D., 2022. Application of a hybrid ARIMA-LSTM model based on the SPEI for drought forecasting. *Environmental Science and Pollution Research* 29(3), 4128-4144.
- Yan, L., Wang, H., Zhang, X., Li, M.-Y., He, J., 2017. Impact of meteorological factors on the incidence of bacillary dysentery in Beijing, China: a time series analysis (1970-2012). *PLoS One* 12(8), e0182937.
- Yang, D., Guo, J., Sun, L., Shi, F., Liu, J., Tanikawa, H., 2020. Urban buildings material intensity in China from 1949 to 2015. *Resources, Conservation and Recycling* 159,

- 104824.
- Yang, D., Shi, F., Liu, J., Guo, J., Tanikawa, H., 2019. China's building material intensity coefficient dataset (1949-2015). Available at: <https://doi.org/10.5281/ZENODO.2704917>.
- Yang, X., Chen, R., Zheng, X., 2016. Simulating land use change by integrating ANN-CA model and landscape pattern indices. *Geomatics, Natural Hazards and Risk* 7(3), 918-932.
- Yang, Y., Zhang, D., Nan, Y., Liu, Z., Zheng, W., 2019. Modeling urban expansion in the transnational area of Changbai Mountain: a scenario analysis based on the zoned Land Use Scenario Dynamics-urban model. *Sustainable Cities and Society* 50, 101622.
- Yang, Z.S., Jia, P., Liu, W.D., Yin, H.C., 2017. Car ownership and urban development in Chinese cities: A panel data analysis. *Journal of Transport Geography* 58, 127-134.
- Yao, Y., Liu, X., Li, X., Liu, P., Hong, Y., Zhang, Y., Mai, K., 2017. Simulating urban land-use changes at a large scale by integrating dynamic land parcel subdivision and vector-based cellular automata. *International Journal of Geographical Information Science* 31(12), 2452-2479.
- Yegnanarayana, B., 2009. Artificial neural networks. PHI Learning Pvt. Ltd.
- Yokoi, R., Watari, T., Motoshita, M., 2022. Future greenhouse gas emissions from metal production: gaps and opportunities towards climate goals. *Energy & Environmental Science* 15(1), 146-157.
- You, F., Hu, D., Zhang, H.T., Guo, Z., Zhao, Y.H., Wang, B.N., Yuan, Y., 2011. Carbon emissions in the life cycle of urban building system in China-A case study of residential buildings. *Ecological Complexity* 8(2), 201-212.
- Yu, B., Li, L., Tian, X., Yu, Q.N., Liu, J.Z., Wang, Q., 2021. Material stock quantification and environmental impact analysis of urban road systems. *Transportation Research Part D-Transport and Environment* 93, 17.
- Yu, H., Li, G., 1999. Construction Project Investment Estimation Handbook [In Chinese]. China Architecture & Building Press, Beijing, China.
- Yu, N.N., De Jong, M., Storm, S., Mi, J.N., 2012. The growth impact of transport infrastructure investment: A regional analysis for China (1978-2008). *Policy and Society* 31(1), 25-38.
- Yuan, F., Xu, Y., Li, Q., Mostafavi, A., 2022. Spatio-temporal graph convolutional networks for road network inundation status prediction during urban flooding. *Computers, Environment and Urban Systems* 97, 101870.
- Zenrin Co., Ltd. 2023. Available at: <https://www.zenrin.co.jp/product/category/gis/basemap/zmaptown/index.html>
- Zeshan, M.T., Mustafa, M.R.U., Baig, M.F., 2021. Monitoring land use changes and their future prospects using GIS and ANN-CA for Perak River Basin, Malaysia. *Water* 13(16), 2286.
- Zhang, D., Huang, Q., He, C., Wu, J., 2017. Impacts of urban expansion on ecosystem services in the Beijing-Tianjin-Hebei urban agglomeration, China: A scenario analysis based on the Shared Socioeconomic Pathways. *Resources, Conservation and Recycling* 125, 115-130.
- Zhang, L., Lu, Q.Q., Yuan, Z.W., Jiang, S.Y., Wu, H.J., 2023. A bottom-up modeling of metabolism of the residential building system in China toward 2050. *Journal of Industrial Ecology* 27(2), 587-600.
- Zhang, R., Guo, J., Yang, D., Shirakawa, H., Shi, F., Tanikawa, H., 2022. What matters most to the material intensity coefficient of buildings? Random forest-based

- evidence from China. *Journal of Industrial Ecology* 26(5), 1809-1823.
- Zhang, S., Zhong, Q., Cheng, D., Xu, C., Chang, Y., Lin, Y., Li, B., 2022. Landscape ecological risk projection based on the PLUS model under the localized shared socioeconomic pathways in the Fujian Delta region. *Ecological Indicators* 136, 108642.
- Zhang, Y., Yan, D., Hu, S., Guo, S., 2019. Modelling of energy consumption and carbon emission from the building construction sector in China, a process-based LCA approach. *Energy Policy* 134, 110949.
- Zhang, Y.M., Luo, L., Yang, J.C., Liu, D.H., Kong, R.X., Feng, Y.B., 2019. A hybrid ARIMA-SVR approach for forecasting emergency patient flow. *Journal of Ambient Intelligence and Humanized Computing* 10(8), 3315-3323.
- Zhang, Y.P., Zhao, H.T., Yu, Y.D., Wang, T., Zhou, W.J., Jinag, J., Chen, D.J., Zhu, B., 2019. Copper in-use stocks accounting at the sub-national level in China. *Resources Conservation and Recycling* 147, 49-60.
- Zhao, B., Li, S., Liu, Z., 2022. Multi-Scenario Simulation and Prediction of Regional Habitat Quality Based on a System Dynamic and Patch-Generating Land-Use Simulation Coupling Model—A Case Study of Jilin Province. *Sustainability* 14(9), 5303.
- Zhong, H., Wang, J., Jia, H., Mu, Y., Lv, S., 2019. Vector field-based support vector regression for building energy consumption prediction. *Applied Energy* 242, 403-414.

## Appendices

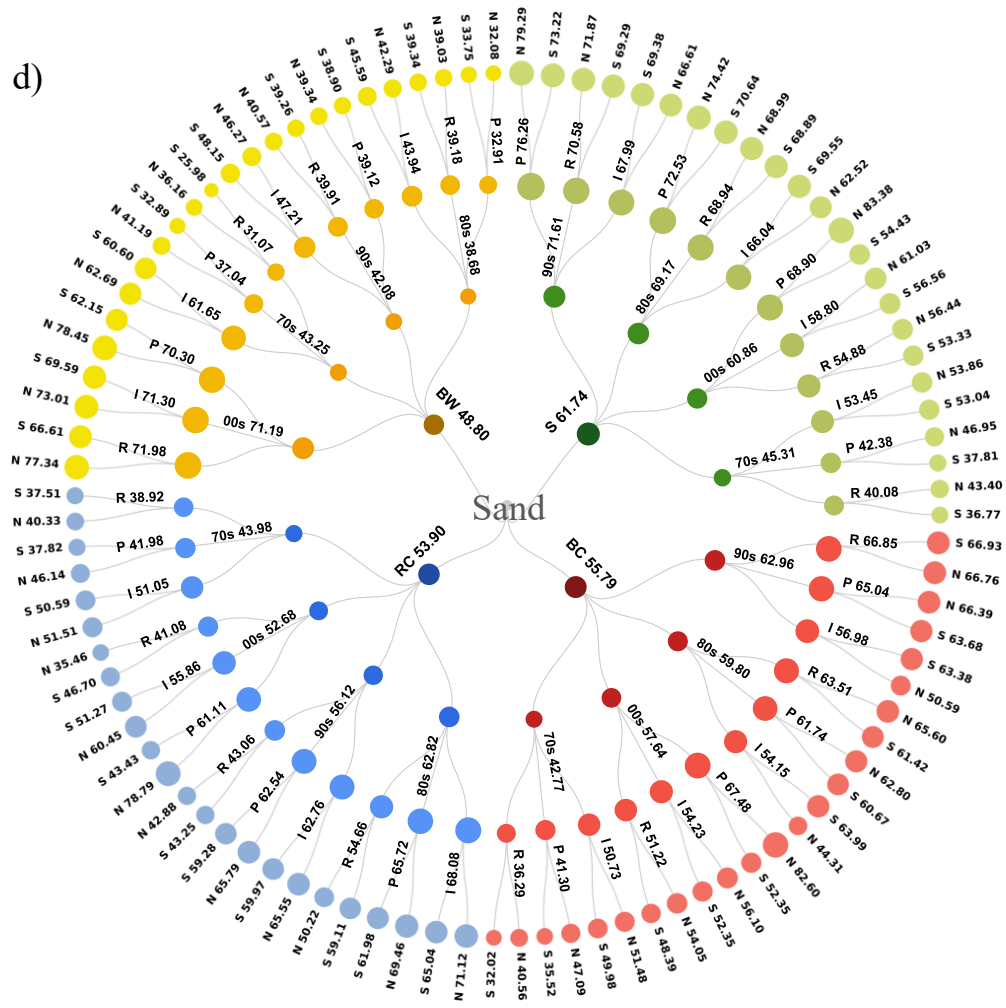
Appendix 1. RF-based MI for a) steel; b) brick; c) wood; d) sand; e) gravel (Unit: ton/100 m<sup>2</sup>)







d)





Appendix 2. RF-based MI dataset for all materials (Unit: ton/100 m<sup>2</sup>)

Structure	Construction year	Use type	Region	RF-based MI					
				Steel	Cement	Brick	Wood	Sand	Gravel
Brick-wood	00s	I	Northern	1.76	10.36	52.50	4.33	73.01	28.44
Brick-wood	70s	I	Northern	0.11	8.85	84.10	8.59	62.69	36.78
Brick-wood	80s	I	Northern	0.64	5.04	101.89	4.43	42.29	29.55
Brick-wood	90s	I	Northern	1.62	7.71	93.17	4.29	46.27	30.70
Brick-concrete	00s	I	Northern	1.67	11.08	53.95	2.27	56.10	28.82
Brick-concrete	70s	I	Northern	0.48	14.37	75.02	7.46	51.48	26.59
Brick-concrete	80s	I	Northern	1.34	10.60	76.31	1.49	44.31	37.75
Brick-concrete	90s	I	Northern	1.62	6.57	76.16	1.73	50.59	35.47
Steel-concrete	00s	I	Northern	5.87	15.94	27.30	2.64	60.45	31.94
Steel-concrete	70s	I	Northern	12.01	15.32	79.23	5.14	51.51	37.91
Steel-concrete	80s	I	Northern	4.77	19.24	52.43	3.45	71.12	62.77
Steel-concrete	90s	I	Northern	6.45	2.85	49.11	2.39	65.55	55.78
Steel	00s	I	Northern	8.41	8.87	28.21	2.36	61.03	71.87
Steel	70s	I	Northern	10.75	12.83	78.41	5.78	53.86	72.50
Steel	80s	I	Northern	7.27	8.08	49.93	2.43	62.52	96.16
Steel	90s	I	Northern	10.73	2.04	42.78	1.93	66.61	100.91
Brick-wood	00s	R	Northern	2.02	10.74	46.92	4.45	77.34	21.06
Brick-wood	70s	R	Northern	0.22	9.26	73.95	9.57	36.16	36.62
Brick-wood	80s	R	Northern	0.78	4.80	102.20	4.53	39.03	29.71
Brick-wood	90s	R	Northern	1.73	9.94	90.82	4.40	40.57	28.01
Brick-concrete	00s	R	Northern	2.22	14.81	54.48	1.55	54.05	36.50
Brick-concrete	70s	R	Northern	0.71	14.64	72.13	5.75	40.56	27.31
Brick-concrete	80s	R	Northern	2.22	14.40	85.61	1.60	65.60	45.44
Brick-concrete	90s	R	Northern	1.93	15.16	84.75	1.78	66.76	37.77
Steel-concrete	00s	R	Northern	5.93	21.69	14.68	1.77	35.46	46.55

Steel-concrete	70s	R	Northern	13.30	30.78	95.96	6.99	40.33	75.02
Steel-concrete	80s	R	Northern	3.30	18.55	33.28	2.25	50.22	54.43
Steel-concrete	90s	R	Northern	2.44	15.81	13.32	1.73	42.88	45.04
Steel	00s	R	Northern	7.67	19.08	17.06	1.93	56.44	80.13
Steel	70s	R	Northern	10.84	24.08	93.24	6.17	43.40	92.80
Steel	80s	R	Northern	6.14	19.12	33.33	2.24	68.99	93.89
Steel	90s	R	Northern	8.35	22.33	15.59	2.03	71.87	94.54
Brick-wood	00s	P	Northern	1.72	10.54	49.26	3.68	78.45	29.40
Brick-wood	70s	P	Northern	0.15	8.48	84.43	8.19	41.19	48.22
Brick-wood	80s	P	Northern	0.38	4.01	109.88	3.72	32.08	23.38
Brick-wood	90s	P	Northern	1.54	9.74	95.48	3.64	39.34	39.97
Brick-concrete	00s	P	Northern	2.65	15.41	46.41	2.54	82.60	17.79
Brick-concrete	70s	P	Northern	0.69	13.04	75.66	4.89	47.09	32.88
Brick-concrete	80s	P	Northern	2.28	14.48	85.80	1.68	62.80	45.07
Brick-concrete	90s	P	Northern	2.30	15.82	76.24	1.61	66.39	42.11
Steel-concrete	00s	P	Northern	8.61	31.86	18.68	2.88	78.79	35.25
Steel-concrete	70s	P	Northern	12.19	27.72	91.92	3.81	46.14	61.82
Steel-concrete	80s	P	Northern	4.38	19.19	57.49	1.95	69.46	54.84
Steel-concrete	90s	P	Northern	14.83	31.51	44.95	2.89	65.79	78.20
Steel	00s	P	Northern	12.57	23.60	19.99	2.97	83.38	79.54
Steel	70s	P	Northern	15.87	22.77	88.09	4.14	46.95	91.17
Steel	80s	P	Northern	9.90	21.73	49.83	2.35	74.42	102.71
Steel	90s	P	Northern	22.81	33.84	34.75	3.09	79.29	119.19
Brick-wood	00s	I	Southern	1.98	10.20	57.00	3.41	69.59	35.96
Brick-wood	70s	I	Southern	0.22	2.13	82.79	3.78	60.60	30.62
Brick-wood	80s	I	Southern	1.13	4.97	96.72	3.37	45.59	45.83
Brick-wood	90s	I	Southern	1.62	7.19	86.04	3.43	48.15	39.44
Brick-concrete	00s	I	Southern	3.30	15.76	58.41	2.08	52.35	33.58
Brick-concrete	70s	I	Southern	1.82	10.03	80.35	1.14	49.98	17.25
Brick-concrete	80s	I	Southern	3.04	16.30	87.73	2.29	63.99	64.33

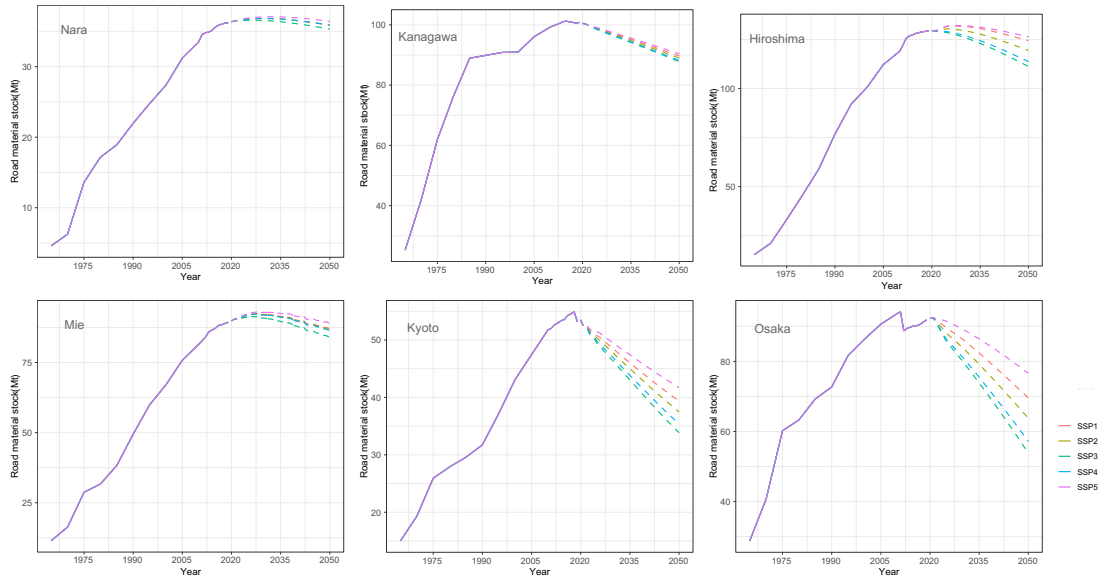
Brick-concrete	90s	I	Southern	2.53	9.76	76.99	1.96	63.38	44.54
Steel-concrete	00s	I	Southern	4.47	15.82	25.69	1.85	51.27	28.56
Steel-concrete	70s	I	Southern	1.93	9.64	65.35	0.93	50.59	13.37
Steel-concrete	80s	I	Southern	4.31	18.31	46.31	1.71	65.04	58.68
Steel-concrete	90s	I	Southern	2.51	6.26	46.18	2.28	59.97	50.80
Steel	00s	I	Southern	6.06	11.45	26.87	1.94	56.56	68.41
Steel	70s	I	Southern	4.27	8.23	65.70	1.25	53.04	57.60
Steel	80s	I	Southern	5.80	10.49	46.17	1.93	69.55	97.36
Steel	90s	I	Southern	5.87	3.85	42.38	2.19	69.38	97.53
Brick-wood	00s	R	Southern	1.92	9.72	48.44	4.29	66.61	26.01
Brick-wood	70s	R	Southern	0.10	0.92	58.99	5.19	25.98	23.88
Brick-wood	80s	R	Southern	0.86	3.36	85.79	4.29	39.34	33.41
Brick-wood	90s	R	Southern	1.41	8.20	76.30	4.39	39.26	31.80
Brick-concrete	00s	R	Southern	3.17	18.31	55.19	1.80	48.39	31.58
Brick-concrete	70s	R	Southern	0.81	6.38	60.81	0.68	32.02	6.68
Brick-concrete	80s	R	Southern	2.34	14.55	80.30	2.14	61.42	44.84
Brick-concrete	90s	R	Southern	2.03	15.94	80.97	1.58	66.93	39.20
Steel-concrete	00s	R	Southern	5.27	21.02	9.97	2.01	46.70	42.95
Steel-concrete	70s	R	Southern	2.39	17.28	79.49	2.23	37.51	42.53
Steel-concrete	80s	R	Southern	3.44	18.25	40.52	1.90	59.11	55.11
Steel-concrete	90s	R	Southern	1.82	13.28	9.61	3.04	43.25	46.19
Steel	00s	R	Southern	6.11	19.89	12.42	2.06	53.33	74.91
Steel	70s	R	Southern	4.14	12.85	77.66	1.44	36.77	70.80
Steel	80s	R	Southern	4.94	18.34	40.55	2.11	68.89	90.37
Steel	90s	R	Southern	5.04	19.90	11.98	2.65	69.29	91.39
Brick-wood	00s	P	Southern	1.84	9.78	52.69	3.95	62.15	37.89
Brick-wood	70s	P	Southern	0.14	1.24	78.46	4.69	32.89	50.10
Brick-wood	80s	P	Southern	0.75	3.07	92.54	3.96	33.75	32.48
Brick-wood	90s	P	Southern	1.40	8.29	79.16	3.99	38.90	42.66
Brick-concrete	00s	P	Southern	3.47	19.04	52.49	2.66	52.35	26.88

Brick-concrete	70s	P	Southern	0.81	5.35	81.29	3.63	35.52	29.50
Brick-concrete	80s	P	Southern	2.51	16.03	77.84	2.60	60.67	47.67
Brick-concrete	90s	P	Southern	2.23	15.19	66.97	2.12	63.68	40.41
Steel-concrete	00s	P	Southern	4.81	20.96	17.35	2.36	43.43	35.95
Steel-concrete	70s	P	Southern	2.76	15.61	75.07	2.65	37.82	46.76
Steel-concrete	80s	P	Southern	3.51	16.84	45.51	2.07	61.98	61.35
Steel-concrete	90s	P	Southern	4.04	20.20	39.80	2.87	59.28	67.27
Steel	00s	P	Southern	8.42	21.24	18.54	2.60	54.43	77.30
Steel	70s	P	Southern	6.80	12.34	73.09	3.12	37.81	80.09
Steel	80s	P	Southern	7.38	19.97	42.94	2.40	70.64	101.23
Steel	90s	P	Southern	10.69	26.17	33.75	2.82	73.22	111.64

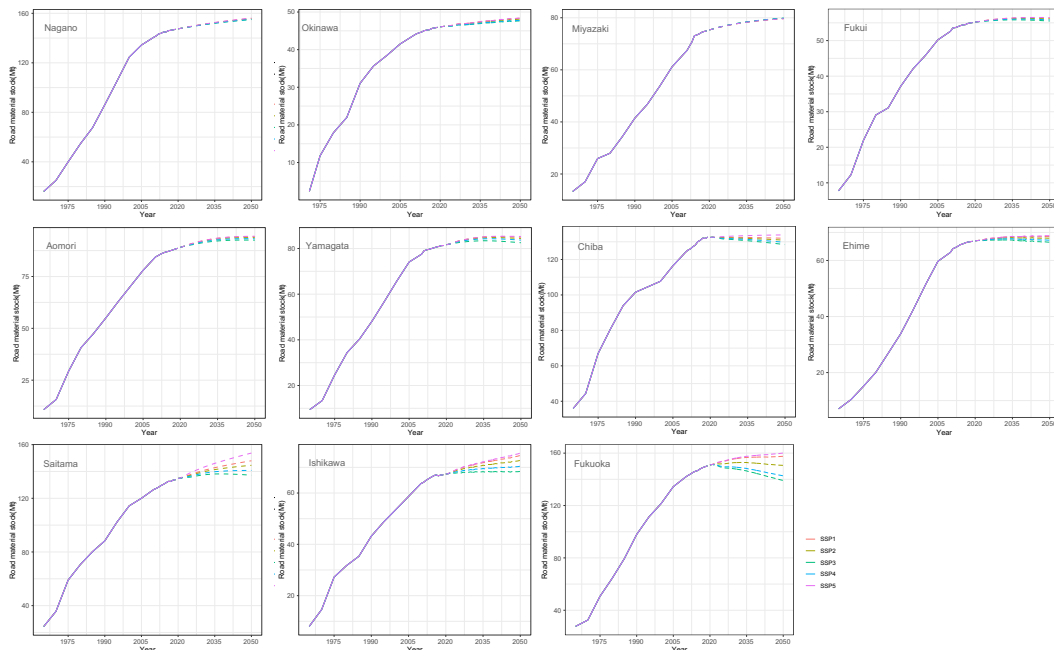
Note: 70s: 1970s and before; 80s: 1980s; 90s: 1990s; 00s: 2000s and after; I: industrial; P: public; R: residential; S: southern; N: northern

## Appendix 3. Results of expected demand for road MS with each SSP scenario for the remaining prefectures

### Pattern 1: Starting to shrink



### Pattern 2: Staying stable or varying with scenarios



### Pattern 3: Continuing to grow

